Some studies in the disintegration of laminar liquid jets in immiscible binary liquid systems

Thesis

SOME STUDIES IN THE DISINTEGRATION OF LAMINAR LIQUID JETS IN IMMISCIBLE BINARY LIQUID SYSTEMS

A thesis presented in partial fulfilment of the requirements of the C.N.A.A for the Degree of Master of Philosophy

By

SHUAIB AHMAD KHAN

Collaborating Establishments:

Engineering Mechanics
The Open University
Walton Hall
Milton Keynes.

Peel Jones Copper Product Limited
Saltburn by the Sea
Cleveland

Sponsoring Establishment :

Department of Chem. Engg.
Teesside Polytechnic
Middlesbrough
Cleveland.

OCTOBER 1984.

DEDICATION

This work is dedicated in praise of my dearest SHABOO JI.

SOME STUDIES IN THE DISINTEGRATION OF LAMINAR LIQUID JETS IN IMMISCIBLE BINARY LIQUID SYSTEMS.

by

SHUAIB AHMAD KHAN

October 1984.

ACKNOWLEDGEMENTS

I wish to express my sincere gratitude to Dr M M Anwar, who directed this research programme and offered continuous guidance and encouragement during the course of the work. I would also like to thank Dr D W Pritchard for his interest and help in this project.

I wish to express my sincere thanks to Mr A Bright for his support, interest and cooperation during the experimental work of the project at the Open University.

I am grateful to Dr J R Walls, Head of Chemical Engineering Department for providing laboratory facilities for the experimental work at the Teesside Polytechnic.

My thanks also due to members of the staff, technicians and my colleagues for their cooperation.

Finally I would like to thank Siraj Bhai for providing an accomodation for the period of this work.

October 1984.

S A Khan

CONTENTS

Cont.

Title : Some Studies In The Disintegration of Laminar Liquid Jets In Immiscible Binary Liquid Systems.

Author : Shuaib Ahmad Khan.

ABSTRACT

The breakup of a liquid jet in an immiscible liquid has been investigated. The variation in the jet break-up length was studied to determine the influence of various parameters e.g. amplitude and frequency of the applied vibrations.

To generate experimental data a rig was designed and constructed. To maintain a constant flow of the dispersed phase through the nozzle, a number of techniques were tried, A compressed air system was found to be the most suitable to develop a constant head for the flow and no variation in the flow of a dispersed phase was observed after 12 hours.

Initially experiments were conducted at a high flow rate of the dispersed phase and the variation in the jet length was measured under the influence of externally applied vibrations. It was found that amplitude and frequency of the applied vibration influenced the jet break-up length. Rayleigh's equation was applied to correlate the experimental data. It was found that the applied frequency does not effect the growth rate but it does influence the jet break-up length. Hence Rayleigh's equation was modified to allow for this variation. The error between experimental and predicted results was found to be not more than the difference in the dropsizes. To eliminate this error, measurement technique previously employed (still photography) was supplemented with a

video technique and the jet length measurements were only taken when monosized droplets were produced.

At low flow rates it was found easier to produce monosized droplets, hence subsequent measurements were taken in this flow region. To correlate experimental data Rayleigh's equation was further modified to take into account the influence of a natural and an applied vibration. Theoretical and experimental results agree well within the range of error $\pm$ 0.30 mm

It was found that the number of monosized droplets produced were equal to the applied frequency. Any change in the frequency altered the dropsize because the flow rate was constant.

1.0 INTRODUCTION

A knowledge of dropsize and dropsize distribution is of fundamental importance for an understanding of the heat and mass transfer characteristics in liquid-liquid systems. The heat and mass transfer rates are directly proportional to the interfacial area created in liquid-liquid contactors. A number of techniques (stirrer in tank, jet disintegration in columns etc.) have been used in these contactors to bring the two phases together. For an optimum design of any contactor it is desirable to have a knowledge of the effect of various parameters on the interfacial area created.

In the present work a study of the disintegration of laminar liquid jets in immiscible liquid systems has been carried out to understand the effect of various parameters (e.g. nozzle diameter, nozzle velocity and physical properties of the systems) on the resultant dropsizes

When one liquid is injected into a second immiscible liquid a jet is formed which attains a length, depending upon the nozzle diameter, nozzle velocity and physical properties of the system.

Rayleigh(3) suggested that when the length of a liquid jet exceeds the circumference of the nozzle , it becomes unstable and a standing wave is formed at the surface of the jet. The amplitude of the wave grows exponentially and when it becomes equal to or greater than the radius of the jet, the jet breaks-up into droplets. He

correlated the jet length with nozzle velocity and nozzle diameter as ;

$$L = \frac{U_n}{B} \ln \frac{a}{\partial_o} \qquad [1]$$

A number of previous workers(16,17) have developed correlations to predict drop diameter as a function of the jet diameter. In their correlations they assumed that the jet diameter is equal to the nozzle diameter.

Das(17) and Anwar et al(25) reported that the jet diameter is a function of the jet length and cannot always be taken as equal to the nozzle diameter. They concluded that depending upon physical properties of the systems and nozzle diameter, the jet could either expand or contract and variation in the jet diameter could be expected along the jet length. In order to calculate drop size and interfacial area created by the disintegration of liquid jet it is essential to have a knowledge of jet break-up length.

The work of Anwar et al (25) was extended and an experimental programme was devised to obtain data, to enhance understanding of the effect of various parameters on the jet break-up length. Emphasis was given to the effect of amplitude and frequency of applied vibrations on the jet break-up length. The still photography and videographic techniques were applied to determine the jet break-up length, jet diameter and drop diameter.

The Rayleigh equation was modified to correlate experimental data assuming that a composite wave was generated from natural and applied vibrations. The amplitude of the composite wave was related to the amplitude of the applied vibration. It was found easier to correlate data obtain at low flowrates than at higher flowrates.

2.0 LITERATURE SURVEY :

2.1 Jet Instability and break-up

The instability of a laminar liquid jet has been a subject of investigation over the last two centuries, but over the last two decades the interest has markedly increased and this has been reflected in the vast increase of the number of publications.

In reviewing the historical evolution of the understanding of the subject , the work of Savart (1) was the first identifiable contribution. He studied the vertical liquid jet produced from an orifice into air and found that the length of liquid jet was directly proportional to the square root of the head of the liquid in the reservoir and to the orifice diameter. He also suggested that the break-up of the liquid jet was caused by the waves on the jet surface and concluded that the wavelength of these waves increased as the diameter of the orifice increased.

The first theoretical treatment into jet instability was presented by Plateau(2) in 1873. He showed that a cylinder of liquid jet was unstable when its length exceeded its circumference. When the length of liquid jet exceeds its circumference , it can be divided into two spheres of equal volume with an accompanying decrease in surface area. He hypothesised that a disturbance that causes the jet to break-up would have a wave length equal to its circumference.

Rayleigh(3) observed that Plateau's theory although it predicted the observed dependence of the wavelengh on the jet diameter, the predicted values of the wave length were generally low. Rayleigh(3) showed by considering the effect of radii of curvature on the pressure in a cylinder of liquid, that if two nodes on the surface are further apart than the circumference of the cylinder , then the pressure will be greater at the nodes than between the nodes and the wave will amplify . But if the nodes are less than circumferential distance apart , the pressure will be greater between the nodes than at the nodes and the wave will diminish.

Rayleigh(3) contributed the first quantitative description of the stability mechanism , based on the small perturbation theory . This outlines the analytical description of the transformation undergone by the cylindrical liquid column when infinitesimally displaced from its equilibrium position . From potential energy considerations he showed that the cylinder of liquid in vacuum and under the influence of surface tension forces alone is stable with respect to all classes of small disturbances and the equilibrium configuration is always unstable for a symmetrical disturbance . The equation of the surface of the jet was expressed by the Fourier series :

$$r = a + \sum_{o}^{\infty} \partial \cos(n\theta) \cos(kz) \qquad [1]$$

Where r-Radial Distance , ∂-Amplitude of disturbance ,n-cirumferential wave number,θ-Angular Distance, k-Wavenumber of a jet surface disturbance and z-Axial distance from the nozzle tip.

He compared the surface energy of the disturbed surface of the liquid jet with that of an undisturbed jet and developed the following equation for the calculation of the potential energy of the disturbed suface of the jet as :

$$Po = (-\frac{2\pi\sigma}{4a})[k^2a^2 + n^2 - 1]\,\partial^2 \qquad [2]$$

Where $n > 0$

This equation indicates that the product of disturbance period and the jet radius(ka) is always greater than zero and at the condition when $n \geqslant 1$ which is the case of non-symmetric disturbances , equation (2) shows that potential energy (Po)is always positive and hence the system is stable and the jet will not break . However if this is equal to zero , which is the case of symmetric disturbances the potential energy will be negative [for $(ka) < 1$]. The disturbance will grow and result in the disintegration of the jet into droplets .

Rayleigh(3,4) later showed that the rate of increase of the amplitude of the disturbance on the surface of liquid jet is proportional to e^{Bt} and an expression for the growth rate of symmetric disturbance is :

$$B^2 = \frac{\sigma}{\rho_d a^3}\,\frac{I_1(ka)}{I_0(ka)}\,[ka\,(1-k^2a^2)] \qquad [3]$$

Where B-is growth rate , and $I_0(ka)$ and $I_1(ka)$ are the modified Bessel function of the first kind . The wave which has the maximum growth rate can be identified by maximizing B with respect to (ka) in equation 3

B takes the maximum value for $0 < ka < 1$:

$$B_{(max)} = 0.97\sqrt{\left[\frac{\sigma}{d_j^3 \rho_d}\right]} \qquad [4]$$

$\lambda_{(max)}$ corresponding to $B_{(max)}$:

$$\lambda_{(max)} = 4.508 d_j \qquad [5]$$

and

$$(ka)_{(max)} = 0.696$$

The maximum wavelength calculated by Rayleigh was 50% greater than the value predicted by Plateau and agrees with his data for water injected into air . For the case where the viscosity of the liquid in the jet was very large compared with the inertia , he(3) produced the following equation :

$$B^2 = \frac{\sigma}{\mu_d a^3}\left[1-k^2a^2\right]\frac{I_1(ka)}{I_0(Ka)} \qquad [6]$$

Where μ_d-viscosity of the jetting liquid . He(3) also suggested a modification for the calculation of the growth rate of the disturbance on the surface of an air jet injected into a non-viscous liquid where the viscosity and the density of the jetting liquid could be considered equal to zero as :

$$B^2 = \frac{\sigma}{\rho_c a^3}\,[1-k^2a^2](ka)\,\frac{K_1(ka)}{K_0(ka)} \qquad [7]$$

Where ρ_c is the density of the continuous phase and $K_1(ka)$ and $K_0(ka)$ are modified Bessel functions of the second kind . The wave length which maximises the above equation is given by :

$$\lambda_{(max)} = 6.48 d_j$$

or

$$ka_{(max)} = 0.485$$

Weber(7) in 1931 used the same basis as Rayleigh for wave growth and by neglecting the inertial terms in the equation of motion , obtained the equation :

$$B^2 + \left(\frac{3\mu_d k^2 a^2}{\rho_d a^3}\right) B = \frac{\sigma}{2\rho_d a^3}[\,1-k^2a^2]k^2a^2 \qquad [8]$$

and

$$\lambda_{(max)} = 2.83\,\pi\, a\sqrt{\left[\,1+\frac{3\mu_d}{\sqrt{2\rho_d\sigma a}}\,\right]} \qquad [9]$$

Where σ and a are the surface tension and the radius of the jet respectively. Solving equation (9) for the inviscid jet $\lambda_{(max)}$ = 8.88a , for a very viscous liquid the wave length approaches infinity. These limiting results agree reasonably with Rayleigh's analysis.

In 1935 Tomotika(8), as a result of a detailed study presented an equation for the break-up of a liquid jet injected into a second liquid . The equation was based on the Navier Stokes Equation for small motion in each phase , neglecting the inertial terms. He highlighted the effect of viscosity ratio of the two phases on the jet break-up and neglected the effect of the velocity of the jet . In his development of the mathematical model , he took the same basis as Rayleigh for the growth rate of small disturbances ($B \alpha e^{Bt}$)

A general equation for the motion which is symmetrical about the axis can be written as ;

$$\left[\frac{\partial}{\partial t} + \frac{1}{r}\frac{\partial \Psi}{\partial z}\frac{\partial}{\partial r} - \frac{1}{r}\frac{\partial \Psi}{\partial r}\frac{\partial}{\partial z} - \frac{2}{r^2}\frac{\partial \Psi}{\partial z}\right] D\,\Psi = v.DD.\Psi \qquad [10]$$

Where v-Kinematic viscosity, Ψ- Stokes Stream Function

and

$$D = \frac{\partial^2}{\partial r^2} - \frac{1}{r}\frac{\partial}{\partial r} + \frac{\partial^2}{\partial z^2}$$ is the differential operator

Equation (10) can be simplified as

$$\left[D - \frac{1}{v}\frac{\partial}{\partial t} \right] D \psi = 0 \qquad [11]$$

Since $(D - \frac{1}{v}\frac{\partial}{\partial t})$ and D are commutative operators , the function ,ψ, can be divided into two parts. Since he assumed that the disturbance are proportional to $e^{Bt.}$ and e^{ikz}, the Stream Function ,ψ, in equation (11) can be written as ;

$$\psi_1 = \phi_1 e^{Bt + ikz.}$$

and

$$\psi_2 = \phi_2 e^{Bt + ikz.}$$

Where k was related to the wavelength of the disturbance and is equal to $2\pi / \lambda$ The solution of the equation (11) was obtained by adding ψ_1 and ψ_2 as ;

$$\begin{aligned} \psi &= \psi_1 + \psi_2 \\ &= [(A_1 r I_1(kr) + B_1 r K_1(kr)) \\ &\quad + (A_2 r I_1(k_1 r) + B_2 r K_1(k_1 r))] e^{Bt+ikz} \end{aligned} \qquad [12]$$

Where A_1, A_2, B_1, and B_2 are the arbitarary constants which are determined by physical condition at the boundary of the two phases.

The boundary conditions which can be used to evaluate constants are ;

[1] There is no slip at the surface of the jet

[2] The tangential stress parallel to the surface is continuous at the surface of the jet.

[3] The difference in the normal stress between the inside and the outside of the jet is due to interfacial tension.

On the basis of these three boundary conditions the resultant equation for the constants was suggested as ;

$$A_1 \left[i\frac{\mu_d}{\mu_c} k^2 I_1'(ka) - \frac{B\rho_d}{i\mu_c} I_0(ka) + \frac{\sigma(k^2a^2-1)}{a^2} \frac{ik}{B\mu_c} I_1(ka) \right]$$

$$+ A_2 \left[2i\frac{\mu_d}{\mu_c} k\, k_1\, I_1'(k_1a) + \frac{\sigma(k^2a^2-1)}{a^2} \frac{ik}{B\mu_c} I_1(k_1a) \right]$$

$$+ B_1 \left[2ik^2 K_1'(ka) + \frac{B\rho_c}{i\mu_c} K_0(ka) \right] - B_2 \left[2i\, kk_1' K_1'(k_1'a) \right]$$

$$= 0 \qquad [13]$$

Where $I_1'(x)$ and $K_1'(x)$ are the first derivative of the $I_1(x)$ and $K_1(x)$ respectively.

These constants were evaluated by writing equation (12) in the determinant form as ;

$$\begin{matrix} I_1(ka) & I_1(k_1a) & K_1(ka) & K_1(k_1'a) \\ kaI_0(ka) & k_1aI_0(k_1a) & -kaK_0(ka) & -k_1aK_0(k_1'a) \\ 2\frac{\mu_d}{\mu_c}-k^2I_1(ka) & \frac{\mu_d}{\mu_c}(k^2-k_1^2)I_1(k_1a) & 2k^2K_1(ka) & (k^2+k_1'^2)I_1k_1'a \\ F1 & F2 & F3 & F4 \end{matrix} = 0 \qquad [14]$$

Where :

$$F1 = 2\frac{\mu_d}{\mu_c}-k^2I_1'(ka)+\frac{B\rho_d}{i\mu_d}I_0(ka)+\frac{\sigma(k^2a^2-1)}{a^2} \quad \frac{ikI_1(ka)}{B\mu_c}$$

$$F2 = 2\frac{\mu_d}{\mu_c}-k\,k_1\,I_1(k_1a)+\frac{\sigma(k^2a^2-1)}{a^2}\,\frac{ik}{B\mu_c}-I_1(k_1a)$$

$$F3 = 2k^2 K_1'(ka) - \frac{B}{i}\frac{\mu_c}{\mu_d} K_0(ka)$$

$$F4 = 2\,k\,k_1\,' K_1'(k_1 a)$$

A more convenient form of the equation (13) was suggested to recognise the importance of the individual terms, by expansion of the determinant and with considerable rearrangement.

$$\rho_d B^2 \frac{I_0(ka)}{I_1(ka)} \left[\frac{K_0(k_1'a)}{K_1(k_1'a)} K_1' \frac{\mu_d}{\mu_c}(k^2 + k_1^2) - k^2 + \frac{I_0(k_1'a)}{I_1(k_1'a)} K_1(k_1'^2 - k^2) + \frac{K_0(ka)}{K_1(ka)} K \left\{ k^2 + K_1'^2 \frac{\mu_d}{\mu_c} (k^2 + k_1^2) \right\} \right]$$

$$+ \rho_c B^2 \frac{K_0(ka)}{K_1(ka)} \left[\frac{K_o(k_1'a)}{K_1(k_1'a)} K_1' \frac{\mu_d}{\mu_c}(k_1^2 - k^2) + \frac{I_o(k_1^2 a)}{I_1(k_1^2 a)} K_1(k^2 + K_1'^2 - \frac{2\mu_d}{\mu_c} k^2) + \frac{I_0(ka)}{I_1(ka)} k \left\{ \frac{\mu_d}{\mu_c}(k^2 + k_1^2) - (k^2 + k_1'^2) \right\} \right]$$

$$+ 2\mu_d k^2 B \frac{I_1'(k_1'a)}{I_1(k_1'a)} \left[\frac{K_0(k_1'a)}{K_1(k_1'a)} k_1 \left\{ -\frac{\mu_d}{\mu_c}(k^2 - k_1^2) - 2k^2 \right\} + \frac{I_0(k_1'a)}{I_1(k_1'a)} K_1(k_1'^2 - k^2) + \frac{K_0(ka)}{K_1(ka)} k \left\{ k^2 + k_1'^2 - \frac{\mu_d}{\mu_c}(k^2 + k_1^2) \right\} \right]$$

$$+ 2\mu_d k.k_1 B \frac{I_1'(k_1'a)}{I_1(k_1'a)} \left[\frac{K_0(k_1'a)}{K_1(k_1'a)} K_1' \left\{ 2k^2 - 2\frac{\mu_d}{\mu_c} k^2 \right\} + \frac{I_0(ka)}{I_1(ka)} k(k^2 - k_1'^2) + \frac{K_0(ka)}{K_1(ka)} k \left\{ \frac{2\mu_d}{\mu_c} - k^2 - (k^2 + K_1'^2) \right\} \right]$$

$$+ 2\mu_c k^2 B \frac{K_1'(ka)}{K_1(ka)} \left[\frac{K_0(k_1'a)}{K_1(k_1'a)} K_1 \frac{\mu_d}{\mu_c}(k^2 - k_1^2) + \frac{I_0(ka)}{I_1(ka)} K_1 \left\{ \frac{2\mu_d}{\mu_c} k^2 - (k^2 + K_1') \right\} + \frac{I_0(ka)}{I_1(ka)} k \left\{ (k^2 + K_1'^2) - \frac{\mu_d}{\mu_c}(k^2 + K_1^2) \right\} \right]$$

$$+ 2\mu_c k K_1' B \frac{K_1'(k_1'a)}{K_1(k_1'a)} \left[\frac{K_0(ka)}{K_1(ka)} k \frac{\mu_d}{\mu_c}(k_1^2 - k^2) + \frac{I_0(k_1'a)}{I_1(k_1'a)} K_1 (1 - \frac{\mu_d}{\mu_c}) 2k + \frac{I_0(ka)}{I_1(ka)} k \left\{ \frac{\mu_d}{\mu_c}(k^2 + k_1^2) - 2k^2 \right\} \right]$$

$$= \frac{\sigma(1 - k^2 a^2)}{a^3} ka \left[\frac{\mu_d}{\mu_c}(k_1^2 - k^2) \left\{ \frac{K_0(k_1'a)}{K_1(k_1'a)} K_1 - \frac{K_0(ka)}{K_1(ka)} k \right\} + (K_1'^2 - k^2) \left\{ \frac{I_0(k_1'a)}{I_1(k_1'a)} K_1 - \frac{I_0(ka)}{I_1(ka)} k \right\} \right] \qquad [15]$$

Equation (15) is a general equation for the instability of a liquid jet of vicosity (μ_d) and density (ρ_d) injected into a continuous phase of viscosity (μ_c) and density (ρ_c) , at low velocity and subject to a small symmetrical disturbance amplified by the interfacial tension.

From equation (14) it was possible to deduce all classical limiting cases. For example:

CASE 1.

Low viscosity jet in gaseous media :

The continuous phase viscosity and density terms can be neglected in equation (14). For a low viscosity jet it can further be assumed that

$$B\frac{\rho_d}{\mu_d} \gg k^2$$

Hence equation (14) simplifies to ;

$$B^2 = \frac{\sigma}{\rho_d a^3} \frac{(1-k^2a^2)ka}{I_0(ka)/I_1(ka)} \qquad [16]$$

This equation is identical to equation (7) derived by Rayleigh and the wavelength for the maximum growth rate corresponds to the dimensionless wave number $ka_{(max)} = 0.696$

CASE 2.

High viscosity liquid jet in gas :

Here viscosity and density terms of the continuous phase can be neglected and it is assumed that when $\mu_d / \mu_c \gg 1$, $ka_{(max)}$ becomes small and Bessel function in the equation (14) can be approximated as ;

$$\frac{I_1'(k_1a)}{I_1(k_1a)} \simeq \frac{1}{k_1a}$$

$$\frac{I_1'(ka)}{I_1(ka)} \simeq \frac{1}{ka}$$

and

$$\frac{I_o(ka)}{I_1(ka)} \simeq \frac{2}{ka}$$

Upon substituting these values in the equation (14) , the resultant equation becomes ;

$$B^2 = \frac{3\mu_d k^2 B}{\rho_d} = \frac{\sigma (1-k^2a^2)k^2a^2}{2\rho_d a^3} \qquad [17]$$

This equation is identical to Weber's equation (8) for viscous liquid in gases.

Christiansen(9) derived an equation for the stability of a non-viscous liquid jet in a second non-viscous liquid, where both phases have finite densities . By treating the velocity potential equation of both dispersed and continuous phases simultaneously , and assuming the velocity continuity at the interface , an equation for the growth rate was given as ;

$$B^2 = \frac{\sigma}{a^3} \cdot \frac{ka(1-k^2a^2)}{\left[\rho_d \frac{I_0(ka)}{I_1(ka)} + \rho_c \frac{K_0(ka)}{K_1(ka)}\right]} \qquad [18]$$

This equation is more suitable for liquid-liquid systems as compared to the equations of Rayleigh and Weber , because the effect of the densities of both the phases are not ignored in the derivation for the calculation of growth rate of disturbance on the surface of the jet.

The wave length that maximises ,B, is a function of (ρ_d / ρ_c). A plot of $ka_{(max)}$ against (ρ_d / ρ_c) is presented in Figure (1). Which is emphasized in the treatment of the result in the present work. In the development of his model Christiansen tried to

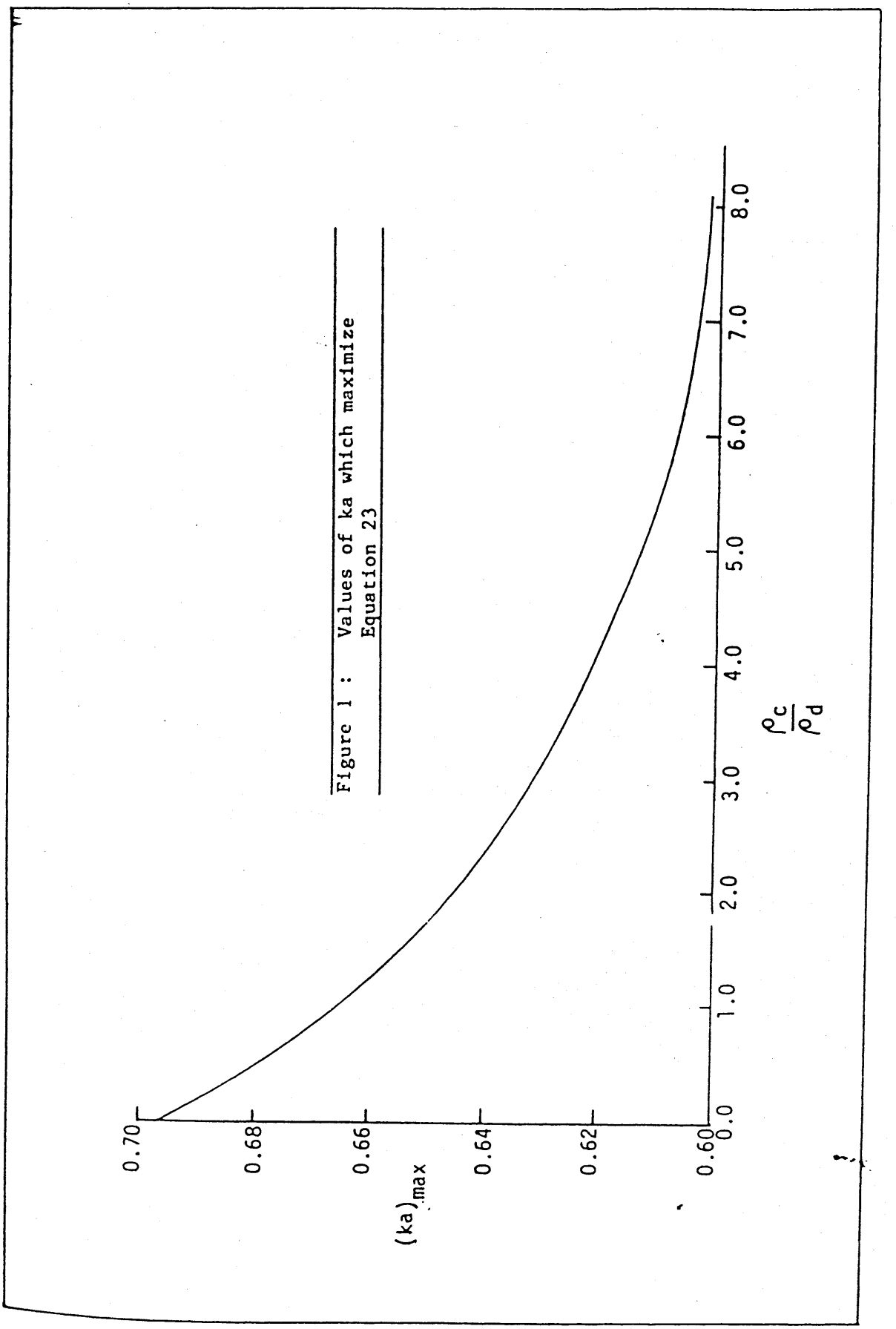

Figure 1 : Values of ka which maximize Equation 23

eliminate the simplifing assumptions made by Tomotika(8). Tomotika's analysis can not be applied to a liquid jet but only to the break-up of a stagnant thread , because the inertial terms of the Navier Stokes Equation were neglected

Middleman(10) worked on the stability of viscoelastic liquid jets in air and tried to analyse Weber's treatment . He reported that the jet break-up length for a viscoelastic fluid is slightly less than that of a Newtonian fluid. He indicated that although the wave number of a viscoelastic jetting fluid was the same as that of a Newtonian jetting fluid, the growth of disturbance was much higher .

Goren(11) suggested an approach which can be employed to predict the change in the dimensions of the wave as it grows on the surface of the jet . His derivation involves two hypotheses.Firstly the volume of the liquid between two nodes is constant and secondly, the maximum surface area is achieved at all stages of disturbance growth . On the basis of these assumptions, he explained the formation of cylindrical links between two primary waves. A comparison of the theoretical wave shape and experimental results showed good agreement.

Taylor(12) was the first worker to investigate the effect of the relative velocities of the two phases on the instability of a liquid jet. He considered the symmetric disturbances and the momentum balance and obtained an equation for the wave length and

growth rate of the maximum disturbance. In his treatment he reported that the growth rate of the disturbance is also a function of the continuous phase(gas) velocity. He neglected the effect of viscosities of the phases on the instability of a liquid jet.

Ranz and Dreier(13) modified Taylor's analysis of the instability to include the effect of viscosities of the two phases. It was assumed all the initial disturbances were of the same magnitude and an equation was derived , to relate the wave length of the fastest growing disturbance in terms of viscocity ratio , density ratio and dimensionless viscosity number.

Levich(14) studied a viscous jet injected into a gas . The continuous phase was treated as a perfect fluid having an average gross velocity (Ug) , far from the jet surface. He obtained the following equation for the disturbance growth rate as a function of velocity (Ug);

$$B^2 + 2\mu_d k^2 B = \frac{\sigma k^2 (1-k^2a^2)}{2\rho_d a} + \frac{\rho_c a^2 k^4 Ug^2}{2\rho_d}\left[\ln\frac{ka}{2}\right] \qquad [19]$$

Where :

$$\frac{K_0(ka)}{K_1(ka)} \simeq ka \ln\frac{ka}{2}$$

He also related the velocity (Ug) with the nozzle velocity by the equation as ;

$$U_n = U_g \ln \frac{a_n}{\partial_o} \qquad [20]$$

Where a_n is the nozzle radius.

It is clear from the above equation that both growth rate (B) and wavenumber (ka) increase with the nozzle velocity. It is also evident that at a very high velocity when ka is greater than unity, the instability on the jet surface will be produced. This was confirmed by experiments which support the velocity terms introduced in the equation.

Debye and Daen(15) considered the relative velocities of the phases and suggested an equation for the instability of an inviscid liquid jet in another inviscid liquid . But their derivation is for assymmetric disturbances on the surface of the jet whose amplitude is given by ;

$$\partial = \partial_o \cos \theta \, e^{Bt + ikz} \qquad [21]$$

Further they assumed that the viscosity of both phases is negligible and their equation for the growth rate is :

$$\rho_d (B - ikU_n)^2 \frac{I_0(ka)}{I_1(ka)} + \rho_c B^2 \frac{K_0(ka)}{K_1(ka)} = - k^3 \sigma \qquad [22]$$

Meister and Scheele(16) applied Tomotika's analysis to calculate the growth rate of a disturbance on a cylindrical jet and produced solutions for various limiting cases ;

CASE 1.

Low viscosity liquid jet in low viscosity liquid :

The viscosity terms of both the liquids in the equation (15) were neglected and the equation was simplified by assuming that $k \ll k'$ and $k \ll k_1$

Hence

$$B^2 = \frac{\sigma (1-k^2a^2)ka}{\rho_d a^3 \left[\frac{I_0(ka)}{I_1(ka)} + \frac{\rho_c}{\rho_d} \frac{K_0(ka)}{K_1(ka)} \right]} \qquad [23]$$

This equation is identical to the equation derived by Christiansen(9) for non-viscous liquids. The most unstable wave length was presented as a function of the density ratio.Their results are shown in Figure (1)

CASE 2.

High viscosity liquid jet in a gas :

The viscosity and density terms of the continuous phase were neglected. The viscosity of a liquid jet is much greater than the gas .

Thus ;

$\mu_d / \mu_c >> 1$ and the Bessel functions were approximated as follows ;

$$\frac{I_1'(k_1 a)}{I_1(k_1 a)} \simeq -\frac{1}{k_1 a} \qquad [24]$$

$$\frac{I_1'(ka)}{I_1(ka)} \simeq -\frac{1}{ka} \qquad [25]$$

and

$$\frac{I_0(ka)}{I_1(ka)} \simeq -\frac{2}{ka} \qquad [26]$$

These simplifications gives the equation (15)

$$B^2 + \frac{3\mu_d k^2 B}{\rho_d} = \frac{\sigma(1-k^2a^2)k^2a^2}{2\rho_d a^3} \qquad [27]$$

Equation (27) is identical to equation (8) suggested by Weber.

CASE 3.

High viscosity liquid jet in a high viscosity liquid :

This solution was also studied by Tomotika. Here it was assumed that ;

$$\frac{B\rho_c}{\mu_c} << k^2 \qquad [28]$$

and

$$\frac{B\rho_d}{\mu_d} << k^2 \qquad [29]$$

Applying these two assumptions in equation (15) , the results obtained by Tomotika can be expressed as ;

$$B = \frac{\sigma}{2a\mu_c}(1-k^2a^2)\,\phi(ka) \qquad [30]$$

Where $\phi(ka)$ is a complicated function of μ_d/μ_c and the various Bessel functions. Since $\phi(ka)$ is a function of viscosity ratio and the wave number (ka) is a function of viscosity ratio of the two phases. A plot of $(ka)_{max}$ against viscosity ratio is plotted

in Figure (2) and thus the controlling wavelength can be calculated and the growth rate of a fastest growing disturbance can be written as ;

$$B_{(max)} = \frac{\sigma}{2a\mu_c}(1-k^2a^2)\ \phi_{(max)} \qquad [31]$$

Further, Meister and Scheele also predicted the dimensionless wave number for the most unstable disturbance for all liquid -liquid systems.[a summary is given in Table (1)]

Das(17) applied this treatment in his theoretical analysis of the jet diameter and break-up length.

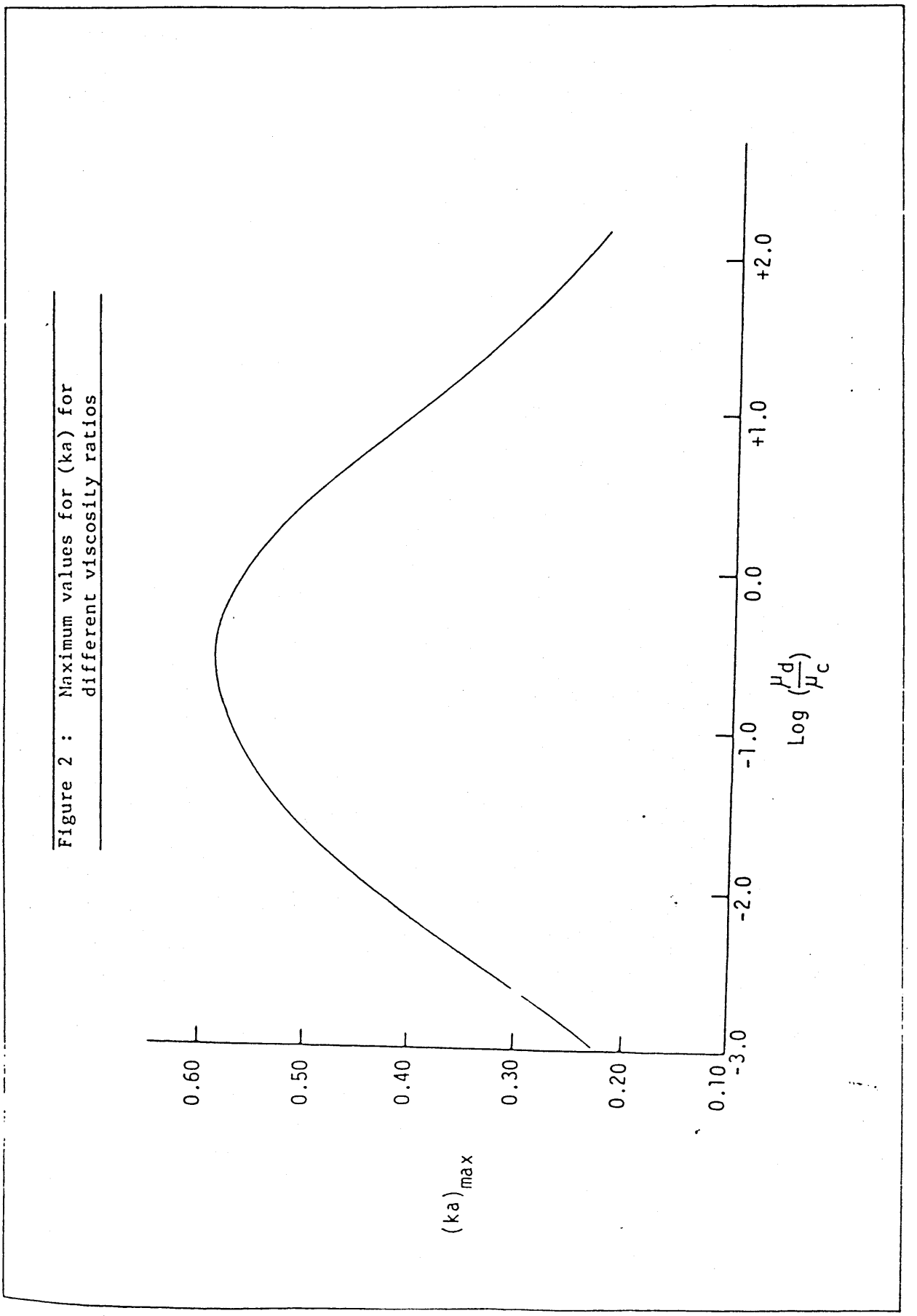

Figure 2 : Maximum values for (ka) for different viscosity ratios

TABLE - 1

Type of system		Prediction of wave number	Limitation of viscosities when a critical value of interfacial tension, nozzle diameter and density for each phase are used
Dispersed phase	Continuous phase		
Non-viscous liquid	Gas	$(ka)_{max} = 0.696$	$\mu_d < 10.0$ C.P.
Gas	Non-viscous liquid	$(ka)_{max} = 0.485$	$\mu_c < 6.0$ C.P.
Non-viscous liquid	Non-viscous liquid	Fig. 2	$\mu_d < 2.0$ C.P. $\mu_c < 2.0$ C.P.
Very viscous liquid	Gas	Approach to zero	$\mu_d > 250.0$ C.P.
Very viscous liquid	Very viscous liquid	Fig. 4	$\mu_d > 300.0$ C.P. $\mu_c > 500.0$ C.P.

2.2 LIQUID JET BREAK-UP LENGTH

The disintegration of a laminar liquid jet into droplets was studied by Lord Rayleigh (3,4) ,who presented an analytical treatment of the phenomenon. He showed that a jet is always stable except when the disturbance was assymmetric and had a wave length greater than the circumference of the jet. He further showed that the most unstable mode occured when the wave length of the disturbance was 1.435 times the circumference of the jet.

In 1917 Smith and Moss (18) investigated the jetting of various liquids into air and also a mercury jet into various aqueous solutions. Their results are shown in Figure (3).In all cases , after a jet is formed , its length increases with a small increase in the velocity (A-B in Figure 3). After the lower critical velocity point (point B) , the jet length increases linearly with the velocity (B-C). After the upper critical velocity point (point C) , the jet length falls very rapidly (C-D) , and with further increase in the velocity , it was reported that the rate of decrease of the jet length was slow .

They applied Rayleigh's instability theory to predict the variation of the jet length with the jet velocity in the laminar region (B-C) . In their analysis they assumed the velocity of the jet and the jet diameter were equal to the nozzle velocity and the nozzle diameter . They related the jet break-up length to the nozzle radius as ;

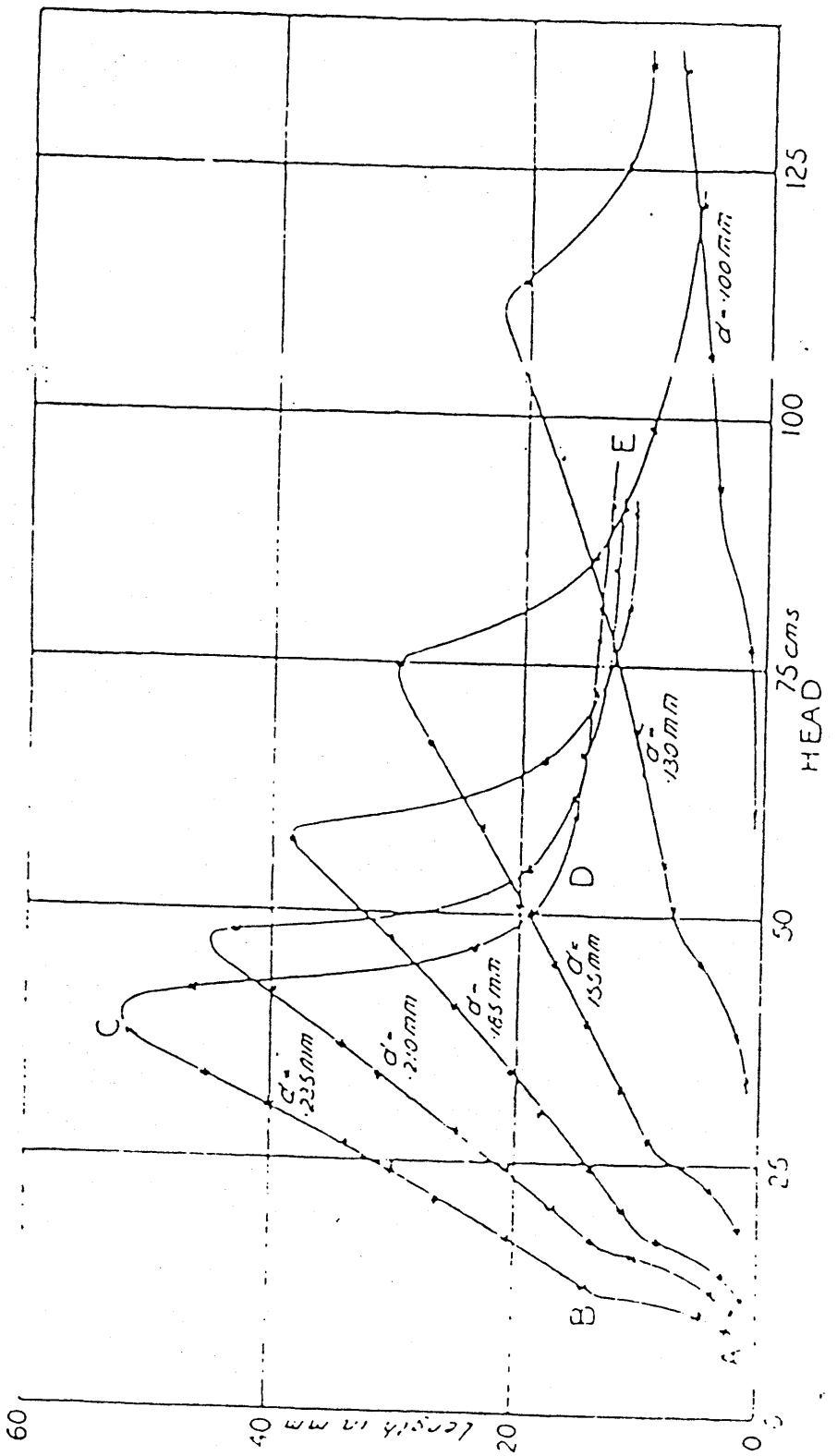

Figure 3 : Jet Instability curves presented by Smith and Moss (18)

$$L = \frac{U_n}{B} \ln \frac{a_n}{\partial_o} \qquad [32]$$

Where :

U_n- Nozzle velocity, a_n- Nozzle radius, B - Growth rate and ∂_o- initial amplitude of the disturbance.

The equation is based on the assumption that the disturbance grows exponentially with time and at break-up point , the amplitude of the disturbance is equal to the jet radius.

By substituting the values of growth rate (B) from equation (4) ;

$$\frac{L}{D_n} = K_L U_n \sqrt{\left[\frac{\rho_d D_n}{\sigma}\right]} \qquad [33]$$

Where ;

D_n - Nozzle diameter , ρ_d - Density of the dispersed phase , σ - Surface tension and K_L- is a constant , in their analysis they fixed the value as 13.

Tyler and Richardson (19) obtained experimental data for the jet break-up length in the laminar region (B-C in Figure 3). They correlated their data using the equation of Smith and Moss . They

found the value of K_L as 16 which compares with a value of 13 used by the original authors.

They suggested that this variation was due to the variation of the initial level of disturbance which is a function of the individual nozzle.

They also produced a correlation for predicting the critical value for the jet length and the jet velocity.This correlation is ;

$$U_m \sqrt{\left[\frac{\rho_d D_n}{\sigma}\right]} = 3.5 + 730 \frac{\mu_d}{\sqrt{[\sigma \rho_d D_n]}} \qquad [34]$$

De Juhasz et al (20) studied the effect of the nozzle diameter on the jet break-up length, and reported that more random break-up occured for small diameter nozzles, and employed Rayleigh's instability theory , to correlate their data.

Tyler and Watkin(21) studied the jetting of liquids into gases and in liquid media. For the case of the liquid jet in the air, they employed equation (33) to predict the jet length.They found that the value of the constant K_L. depended on the viscosity of the dispersed phase and varies from 11 to 15.

They modified the equation to include the effect of the viscosity of the jetting liquid to predict the jet length as ;

$$\frac{L}{D_n} = 10.6\ U_n \sqrt{\left[\frac{\rho_d D_n}{\sigma}\right]} \left[1 + \frac{1}{4095}\left[\frac{\sqrt{(\sigma \rho_d D_n)}}{\mu_d}\right]^{3/2}\right] \qquad [35]$$

They were the first workers to observe that the continuous phase viscosity has a significant effect on the jet length and reported that if the injected liquid is more viscous than the continuous phase , the jet is longer than the reversed case. They suggested that this effect was due to the more viscous liquid at the nozzle exit causing a smaller initial disturbance.

They also correlated the critical velocity of the jet at which the jet length is maximum as ;

$$U_m \sqrt{\left[\frac{\rho_d D_n}{\sigma}\right]} = 3.0 + 1.6 \left[\frac{\sqrt{\sigma \rho_c D_n}}{\mu_c}\right]^{1/5} \qquad [36]$$

Ohnesorge (22) reported liquid jet break-up in air and plotted results in a similar fashion to Smith and Moss . He identified each region with the following effect ;

[a] In region 1. (Symmetric disturbances predominated)

[b] In region 2. (Nonsymmetric disturbances predominated)

[c] In region 3. (Destructive jetting resulted from predomination of Shear forces.)

He further found that the jet length was maximum at the boundary between the region 1 and 2 (critical velocity), and derived an

equation similar to Smith and Moss which related the parameters as;

$$U_n \sqrt{\left[\frac{\rho_d D_n}{\sigma}\right]} = 14.2 \left[\frac{\mu_d}{D_n U_n \rho_d}\right]^{1/4} \qquad [37]$$

Where ρ_d and ρ_c are the density and the viscosity of the dispersed phase and U_n - is the nozzle velocity.

Merrington and Richardson (23) studied the jet break-up process in both liquid and air. They noted two types of disturbances :

[1] Varicose disturbances

[2] Sinuous disturbances

They considered that the varicose disturbance was caused by the effect of surface tension and sinuous disturbances could be attributed to shear. These corresponded to the symmetric and non symmetric disturbances reported by Ohnesorge (22). The growth rate of the varicose disturbance was considered to be independent of the velocity , whilst the growth of the sinuous disturbance increased rapidly with velocity and acts as a controlling mechanism for break-up. They corelated their data for liquid jet in air using equation 33 of Smith and Moss.They found that the value for the constant is 11 for water which is in line with the results of the other workers , but for the liquid with 50 cp viscosity the value of the constant was found to be 21 and for a glycerine

solution with a viscosity of 1000 cp , the value was 84. These two results contradict the finding of Tyler and Watkin(21) which indicated that the value of the constant should decrease with increasing viscosity.

Fujinawa et al (24) empirically correlated the velocity at maximum jet length for the liquid-liquid system and concluded the effect of viscosity of both the phases and obtained the following equation ;

$$U_m \sqrt{\left[\frac{\rho_d D_n}{\sigma}\right]} \quad N_{Re} = \left[\frac{19000}{N_{Re}}\right]^3 \left[\frac{\mu_d}{\mu_c}\right]^{0.42} \qquad [38]$$

Where N_{Re} - Nozzle Reynold number.

Meister and Scheele (16) studied the disintegration of a laminar liquid jet injected into another liquid. They found that the jet contracts depending on the viscosity and density of the continuous phase. They attempted to ascertain the effect of contraction on the jet break-up length and reported that the jet length was independent of the jet contraction. In their theoretical treatment they considered the case where the jet contracts to one half of its nozzle diameter(maximum possible contraction)and showed that ;

$$\frac{L = D_n/2}{L = D_n} = \frac{[2]^2}{[2]^{3/2}} \quad \frac{\ln(D_n/4\delta_o)}{\ln(D_n/2\delta_o)} \qquad [39]$$

Where :

D_n - Nozzle diameter , ∂_o - Initial amplitude of the disturbance

In their calculation they used $\ln(D_n/\partial_o) = 6.$ as suggested by most of the previous workers (18,19). Experimental values of L/D_n against Reynold number (Re) were plotted as in Figure (4).

They compared their plotted results with those of Smith and Moss (Figure 3). It can be seen that in Figure 4 (Meister and Scheele), there is a sharp increase from B-C . They suggested that the assumption of a flat velocity profile in the jet is only valid for a liquid jet injected into air , as the viscosity of the air is negligible compared with the liquid phase. In their calculation they assumed a radial velocity gradient in the jet which gives the different values of the interfacial velocities as compared to a jet in air . The disturbance waves which break-up the jet grow at the interface and are affected by the interfacial velocity. These waves determine the jet length.

The equation for the jet length , neglecting the jet contraction was given as ;

$$\ln\left[\frac{a_n}{\partial_o}\right] = \frac{1}{U_n}\int_o^L \frac{B\,U_A}{U_I}\,\partial z \qquad [40]$$

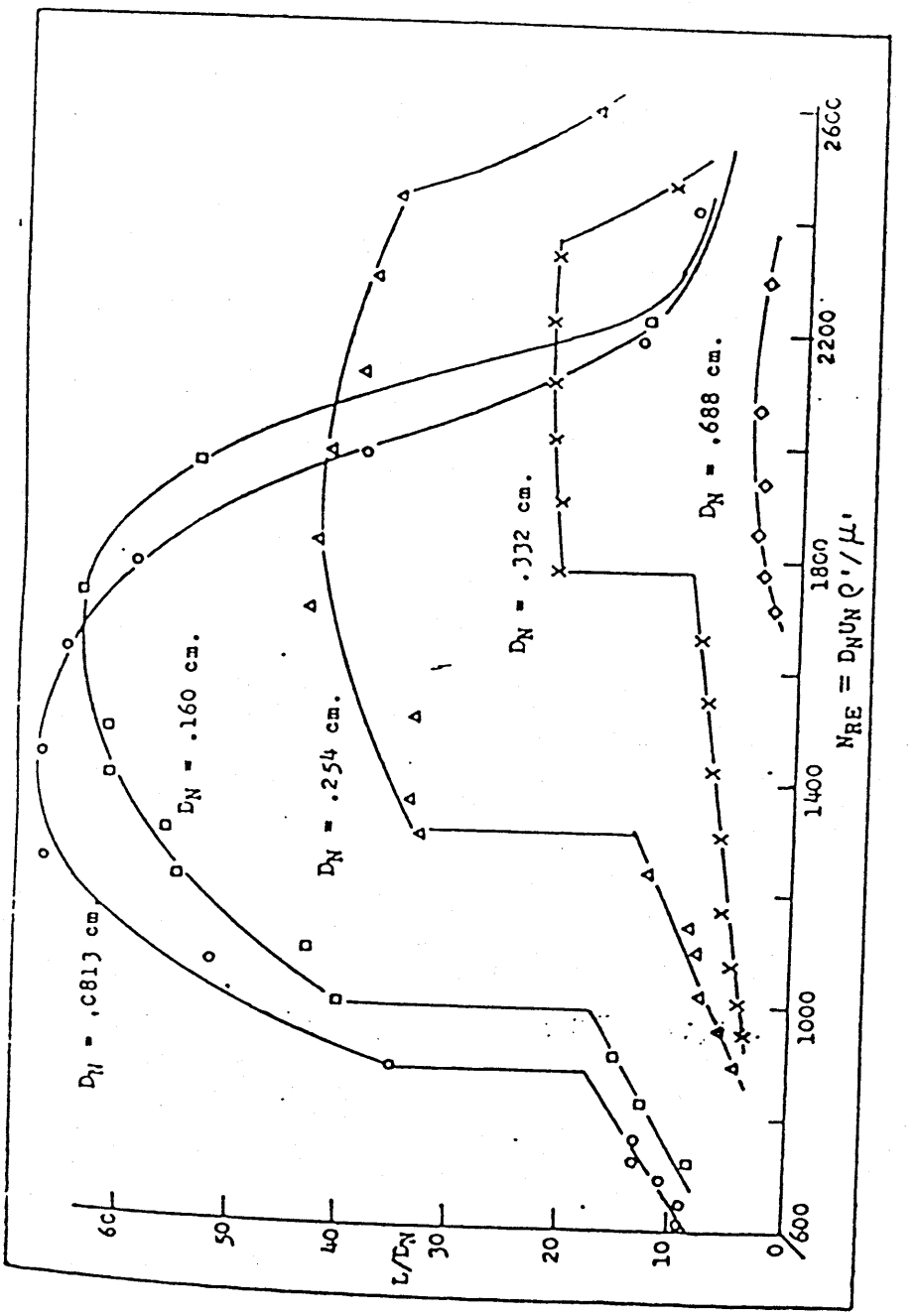

Figure 4 : Effect of nozzle diameter on jet breakup length (ref 16)

where U_A - is the average velocity of the jet and U_I - is the interfacial velocity and the ratio of the two is given by ;

$$\frac{U_I}{U_A} = [1 + e^{-A\frac{\mu_d}{\mu_c}Z^n}] \; [1 - e^{-B\frac{\mu_d}{\mu_c}Z^n}] \qquad [41]$$

Where A and B are the constants ,Z^n - is the distance between the two adjacent nodes.

They also suggested that the value of the interfacial velocity is zero at the nozzle exit and increases rapidly over a short distance. They solved the integral in equation 40 graphically and calculated the average value for $(U_I/U_A)_{ave}$ as shown in Figure (5)

Using this average value of the ratio (U_I/U_A) equation 40 can be written as ;

$$L = \frac{U_n(U_I/U_A)ave}{B} \cdot \ln\frac{a_n}{\delta_o} \qquad [42]$$

Anwar et al (25) studied the variation of the jet diameter and velocity in the axial direction of the laminar liquid jet injected into another liquid. They used the continuous phase of viscosity varying from 1.5 to 28 cp. A simple solution to the simultaneous equation of motion for dispersed and continuous phases was employed to predict the jet diameter, as ;

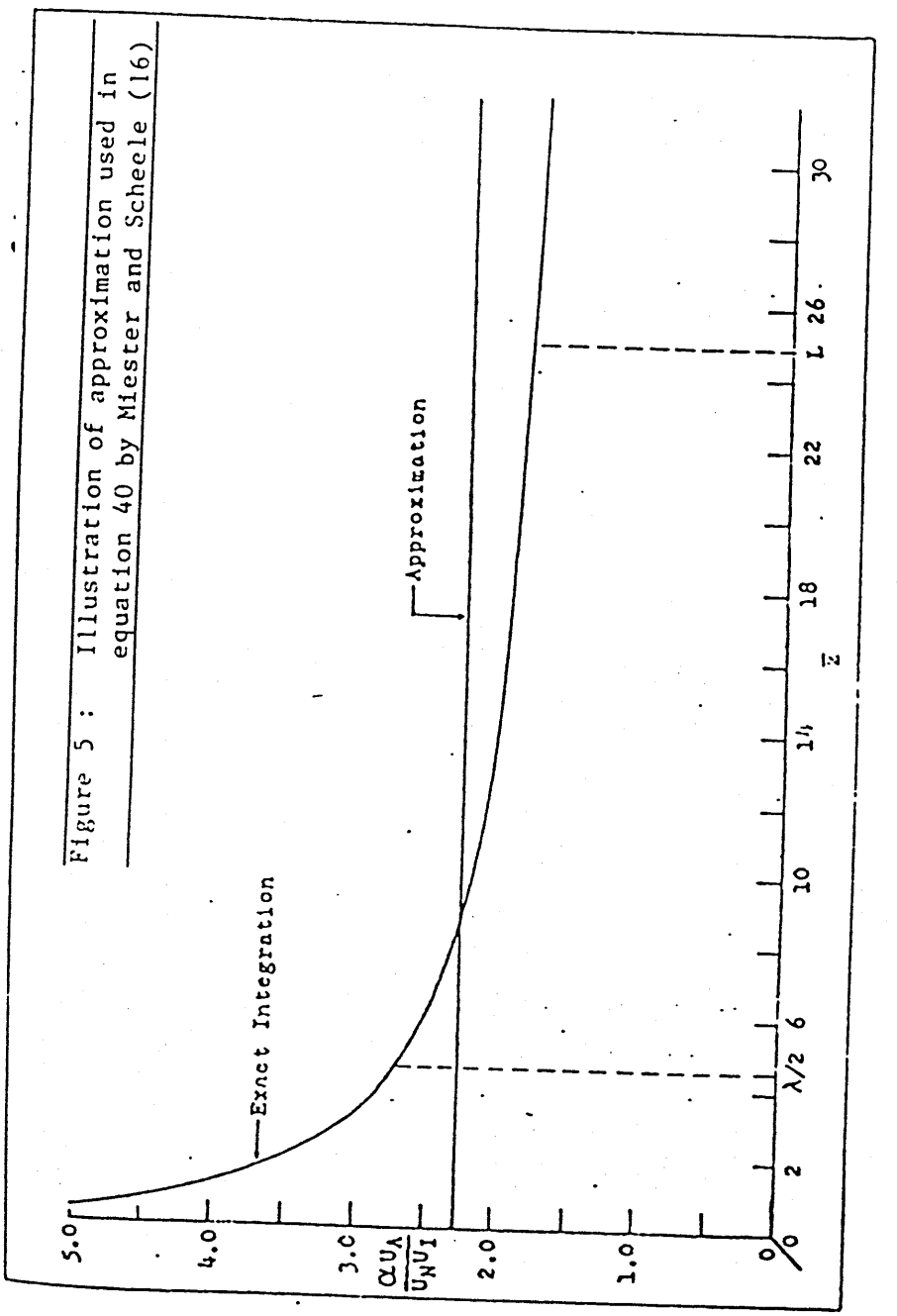

Figure 5 : Illustration of approximation used in equation 40 by Miester and Scheele (16)

$$(DP)\quad \frac{\partial}{\partial x}\left[\frac{4-2\phi+\phi^2}{6a^2} - \frac{a}{We}\right] = \pm \frac{N_j a^2}{4} - \frac{8}{a^2}\,[1-\phi] \qquad [43]$$

$$(CP)\quad \frac{\partial}{\partial x}\left[\frac{\phi^2(\Psi-1)(\Psi+5)}{30a^2}\right] = \pm \frac{8}{a^2}\left[\frac{\rho_c}{\rho_d}\right]\,[1-\phi] \qquad [44]$$

Where (+) and (-) signs correspond to a jet injected downward or upward DP and CP indicates the dispersed and continuous phase respectively.

N_j. -Buoyancy parameter $= \frac{Re}{Fr}\left(1-\frac{\rho_d}{\rho_c}\right)$

Fr. - Froude Number $= U_n^2/2a_n g$

ϕ - Variable defined by $U_I a^2$

Ψ - Variable defined by δ/a

A solution for ϕ , Ψ and a as a function of dimensionless distance z from the nozzle exit was presented. They took into account gravity , interfacial tension , and viscous shear forces on the surface of the jet . The buoyancy parameter (Nj) can be used as a rough guide to determine whether the jet will contract or expand (if Nj >> 1 the jet contracts and if Nj << 1 the jet will expand) .With the decreasing values of (Nj) from 200 to 0.1 the jet contraction effect is replaced by the jet expansion effect.

2.3 Effect of forced vibration on the instability and break-up :

Rayleigh (3) introduced the idea of imposed disturbance to induce jet instability. However this idea has not been exploited until recently. Crane et al (26,27) studied the jet instability using a flexible electronically driven vibrator to induce disturbances of different wavelengths. The growth rates of these disturbances were calculated from the break-up time . The result agreed only qualitatively with Rayleigh's (1) theory. They concluded that rotationally symmetric disturbances are required to trigger instability on the liquid jet . This could be induced by small pressure variation at the nozzle . They suggested that the external mechanical vibrations in the appropriate range of frequency and amplitude could induce such small pressure fluctuations and trigger the instability .

Donnelly and Glaberson (28) made a study of the growth rate of a liquid jet by introducing sinusoidal disturbances of different wavelengths, using a loudspeaker , driven by an audio oscillator . They investigated the growth rate of the surface wave as a function of time . Their results showed that surface waves grow exponentially , and the measured growth rates agreed well with Rayleigh's theory . They concluded that the break-up of the liquid jet was induced by the non-linear effects and non-sinusoidal surface deformation due to the presence of higher harmonics in the system ,as first suggested by Rayleigh .

Haelein (29) investigated the disintegration of cylindrical jets of liquid of different physical properties . At low velocities he related the wave length of the forced disturbance to the circumference of the liquid jet and reported that a water jet disintegrated at wave lengths varying from 1.4 - 2.2 times the circumference of the jet . At higher velocities he reported that the effect of the surrounding air gradually becomes dominant and this relationship is no longer valid .

The instability of a liquid jet of cylindrical geometry under the influence of the external vibration was studied by Yuen (30,31).He suggested that the non-sinusoidal surface deformation of the jet was induced by the non-linear effect and the agreement between Donnelly and Glaberson's experiments and Rayleigh's linearised theory was only due to their method of measurements .

Considering the effect of the finite amplitude on the instability of a liquid jet, he developed a third order theory and suggested that in Rayleigh's analysis the volume of the jet is conserved only to the first order of the wave amplitude which causes break-up. By conserving the mass to the higher order , he showed that interaction occurred between the higher harmonics of the disturbances , which extracts the energy from the Fundamental , and found that the growth of the surface disturbing wave was only dependent on the amplitude of disturbance and the dimensionless wave number (k) of the wave .

Wissema and Davies (33) studied the effect of external mechanical vibrations , in the direction normal to the liquid jet , on the disintegration of liquid jet . They used an electromagnetically driven vibrator and kept the flow rate constant , by using a metering pump. A wide range of amplitudes and frequencies , over a range of flow rates was studied. It was found that at relatively low vibrational frequencies , the disintegration pattern of the liquid jet and dropsize distributions changed very little from those observed under natural conditions.

In most of the cases they found that the maximum frequency , at which monosize drops appeared , was one half of the frequency of the maximum instability of the jet predicted from the the extension of Rayleigh's original analysis . It was also reported that uniform sized drops were formed at a rate equal to the frequency of vibration of the nozzle . They proposed an equation based on the material balance to correlate dropsizes. The equation is ;

$$D \simeq 0.98 d^{2/3} (U/f) \qquad [45]$$

Where f is the applied frequency and U is the velocity of the jet . It is also reported that under these conditions for uniform droplet formation , the break-up length of the jet decreases with both increasing frequency and amplitude of vibration .

Rutland and Jameson (34) used an experimental method similar to Donnelly and Glaberson (28) and extended Yuen's (30) idea of the

presence of higher harmonics in the system , which he called a wave undulation (i.e the presence of more than one crest per wavelength , on the surface of the jet.)

They reported that the primary wave grows exponentially as reported previously by other investigators (8,9,30,31) and the growth rate of the secondary wave is always slower , and also the amplitude of the higher harmonics depends upon the initial amplitude . They assumed the swelling between the two adjacent crests of the primary wave as the higher harmonics of the initial disturbances

Rajgopalan(35) studied the production of monosize droplets by applying an external vibration. They extended the equation of Wissema and Davies (33) for the prediction of the drop sizes , by employing the following assumptions ;

[1] The length of a cylindrical jet resulting in a drop is equal to that of one complete wave length of the disturbance applied .
[2] The wave length (λ) and the frequency (f) are related by

$$\lambda = U/f$$

A simple material balance was carried out to predict the drop diameter using the following equation ;

$$\frac{1}{6} \pi D^3 f = (\pi D^2/4) U \qquad [46]$$

They emphasised that from material balance it is impossible to obtain the equation given by Wissema and Davies .

Rajgopalan et al (36) investigated the production of monosized drops by controlled vibration of the liquid jet. The variables studied were physical properties of the liquid , capillary diameter , and the frequency and the amplitude of applied disturbance . They found that the break-up of a vibrated jet could be very effectively controlled to produce uniform size drops . They managed to produce drops at a rate equal to twice that of the imposed frequency in contrast to the finding of previous workers (33)

Schneider and Hendricks (37) studied the liquid jet under the influence of external vibration to produce monosize drops . They showed that uniform drops of low viscosity liquids could be formed by liquid jet break-up when the wave length of the external disturbance became 3.5 - 7 times the diameter of the jet . In their investigation the lower limit of the wavelength corresponds to the maximum wavelength predicted by Rayleigh's theory.

Dabora (38) applied external mechanical vibrations on a liquid jet submerged into another liquid to produce monosize drops . His theoretical treatment was based on Rayleigh's analysis of the instability of a capillary jet in air . He showed that the frequency for the maximum instability is related to the jet velocity and the jet diameter at the break-up point . He also calculated

the $\lambda_{(max)}$ at maximum instability for a given viscosity ratio (μ_d / μ_c) , applying Tomotika's theory and related the frequency of maximum instability at which monosize drops appeared as ;

$$f_{(max)} = \frac{U_z}{K\, d_j}$$

where ;

$f_{(max)}$ - Frequency of maximum instability (Hz)

K - Coefficient depend on the viscosity ratio (μ_d/μ_c)

U_z - jet velocity (cm/sec.)

d_j - jet diameter (mm)

He made simplifying assumption that the velocity and the diameter of the jet at break-up point are equal to the nozzle velocity and diameter . Experimentally he could not produce monosize drops applying this frequency . Therefore the frequency was adjusted by trial and error to achieve monosize drops.

2.4 Discussion on the literature survey :

Most previous investigators (12,13,16) used the following equation to predict the length of a liquid jet in air ;

$$\frac{L}{D_n} = K_L D_n \sqrt{\left[\frac{\rho_d D_n}{\sigma}\right]}$$

The derivation of this equation involves three simplifying assumptions ;

[1] All the disturbances are initiated at the nozzle exit.

[2] The amplitude of the disturbance grows exponentially on the surface of the jet

[3] The velocity and the diameter of the jet is the same as that of velocity and diameter at the nozzle exit.

The growth rate of the disturbance can be calculated using Rayleigh's instability theory . The value of the constant K_L in the equation above was taken by previous workers varying from 6 - 21 . A flat velocity profile was assumed and the viscosity and density of the continuous phase were neglected.

Christiansen (9) extended Tomotika's analysis for the growth rate for a liquid jet submerged into another liquid and suggested the the growth rate of the fastest growing disturbance also depended on the viscosity and density of the continuous phase.

Later it was suggested by other investigators (16,17) that for a submerged liquid jet into another liquid , the assumption of a flat velocity profile is not valid as the jet could contract or expand depending on the nozzle diameter , nozzle velocity , density and viscosity of the continuous phase . Meister and Scheele considered that the interfacial velocity plays an important role in the prediction of the jet length , and suggested in their theoretical model that the jet length is independent of the jet contraction . They ignored the viscous forces in their momentum balance equation and did not explain the process of the jet expansion observed experimentally.

A simple momentum integral approach to the simultaneous equation of motion for dispersed and continuous phases was presented by Anwar et al (25) , to predict the jet diameter at the point of break-up , considering the effect of gravity , interfacial tension and viscous forces , they suggested that the drop diameter depends on the jet diameter at the point of break-up . The jet can expand or contract depending on the physical properties of the system. This leads to a conclusion that the jet diameter is a function of the jet length ,thus to quantify drop diameter the jet length must be known.

It is obvious from the literature that there is a lack of a suitable model to predict the jet length of a liquid jet in liquid - liquid systems. In order to understand jet instability and break-up phenomena and to predict the drop diameter resulting from the disintegration of a laminar liquid jet and also to calculate

the interfacial contact area ,a suitable model is essential for the prediction of the jet length . This indicates the next step in the understanding of the phenomenon as also suggested by Das (17).

3. EXPERIMENTAL

To study the various parameters on the jet break-up length , for example , frequency and the amplitude of the forced vibrations , an experimental programme was initiated to produce data for the use in the prediction of jet break-up length .

The experimental work can be divided into the following sections :

3.1 Apparatus and procedure

3.2 Measurment of the physical properties

3.1 Apparatus and procedure :

3.1.1 Vibrating unit :

The basic unit was a vibrator 407L made by LTV Ling Altec Ltd. This vibrator was held by speed-frame to minimise most of the external vibrations . A PO-20 Type (Ling Dynamic) frequency generator was use to activate the vibrator . The signal from the frequency generator was amplified by using an amplifier made by LTV Ling Altec Ltd. The amplitude of oscillation was controlled by the power output from the frequency generator . An accelerometer , Digital Power Module 2020 type , supplied by Environmental Equipment Ltd , and an oscilloscope supplied by Golds Advance were used to measure the amplitude of vibrations in terms of acceleration values . The calibration of acceleration at constant amplitude for different frequency is presented in Figure (6). To

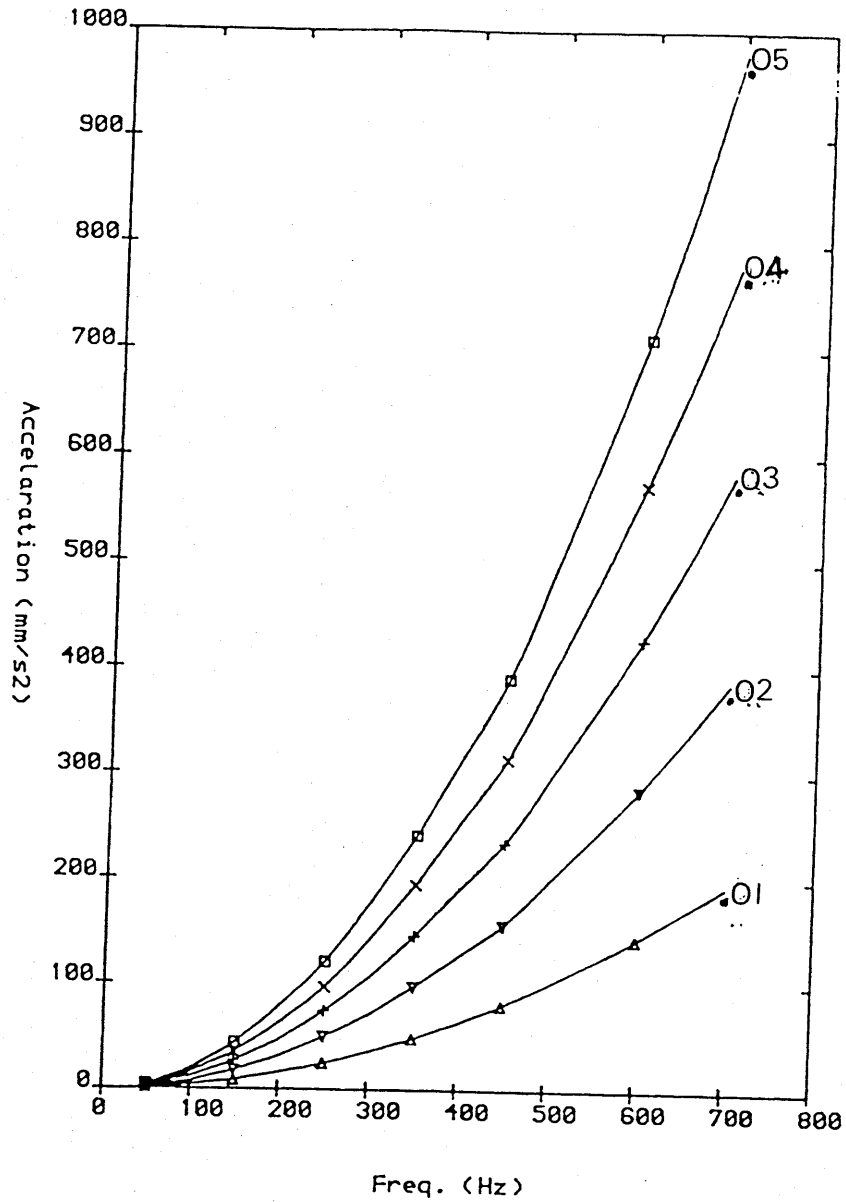

Figure 6 : Variations af acceleration values with applied frequency at constant applied amplitude

confirmd the value of frequency applied an electronic digital counter (Racals Instrument Ltd.) was employed .

3.1.2 Flow control unit :

To minimise the effect of variation of liquid flow through the nozzle and its effect on jet length , it is essential to have a steady and constant flow of liquid . Das(17) employed compressed air to obtain a constant head which gave a steady flow . For a fine control of air flow a capillary copper tube of 1 mm. inside diameter and 30 cm length was used . A mercury manometer was fitted across the capillary tube to observe the change of variation in the air flow . In the present work efforts were made to reproduce Das's results . Difficulties were experienced in the control of a very low flow rate ,because the pressure variation across the manometer was very small. The operation was laborious , took a long time to achieve a steady flow rate and stable conditions were only possible for short periods .

In gas-liquid chromatographic equipment very accurate flow rates are required . This suggests the possibility of using such system in the present work . A GLC gas flow system (Perkin Elmer) was used to test its suitability . The results were most encouraging and this system was used to produce flow rates at lower values of pressure . It was fairly good for a constant and steady flow over a long period without any variation and was unaffected by external vibrations . The set up is given in Figure (7&7a)

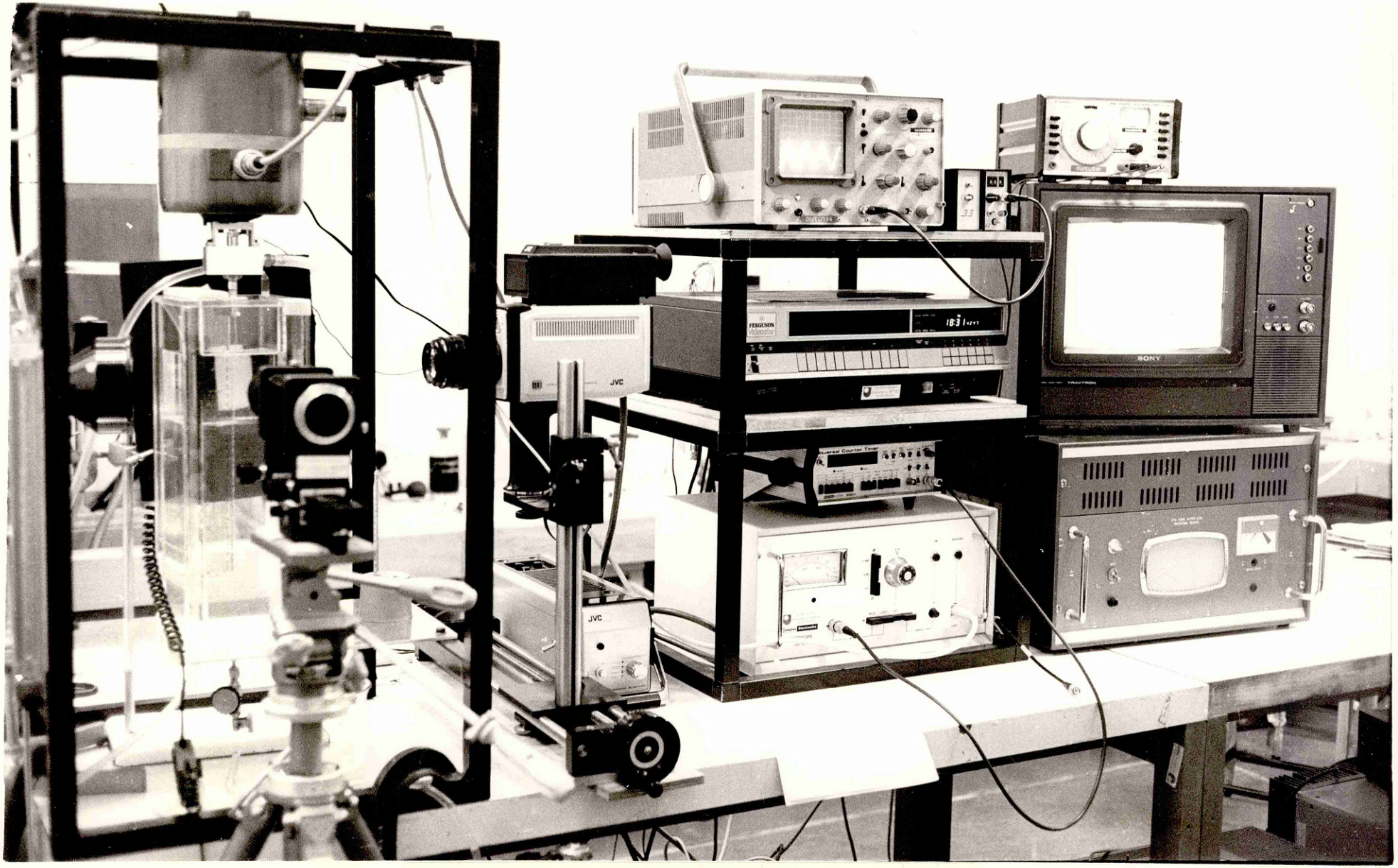

PLATE 1 : Experimental Set-up To Generate Data For The Present Work.

Figure 7 : Schematic Diagram of Flow Control Unit

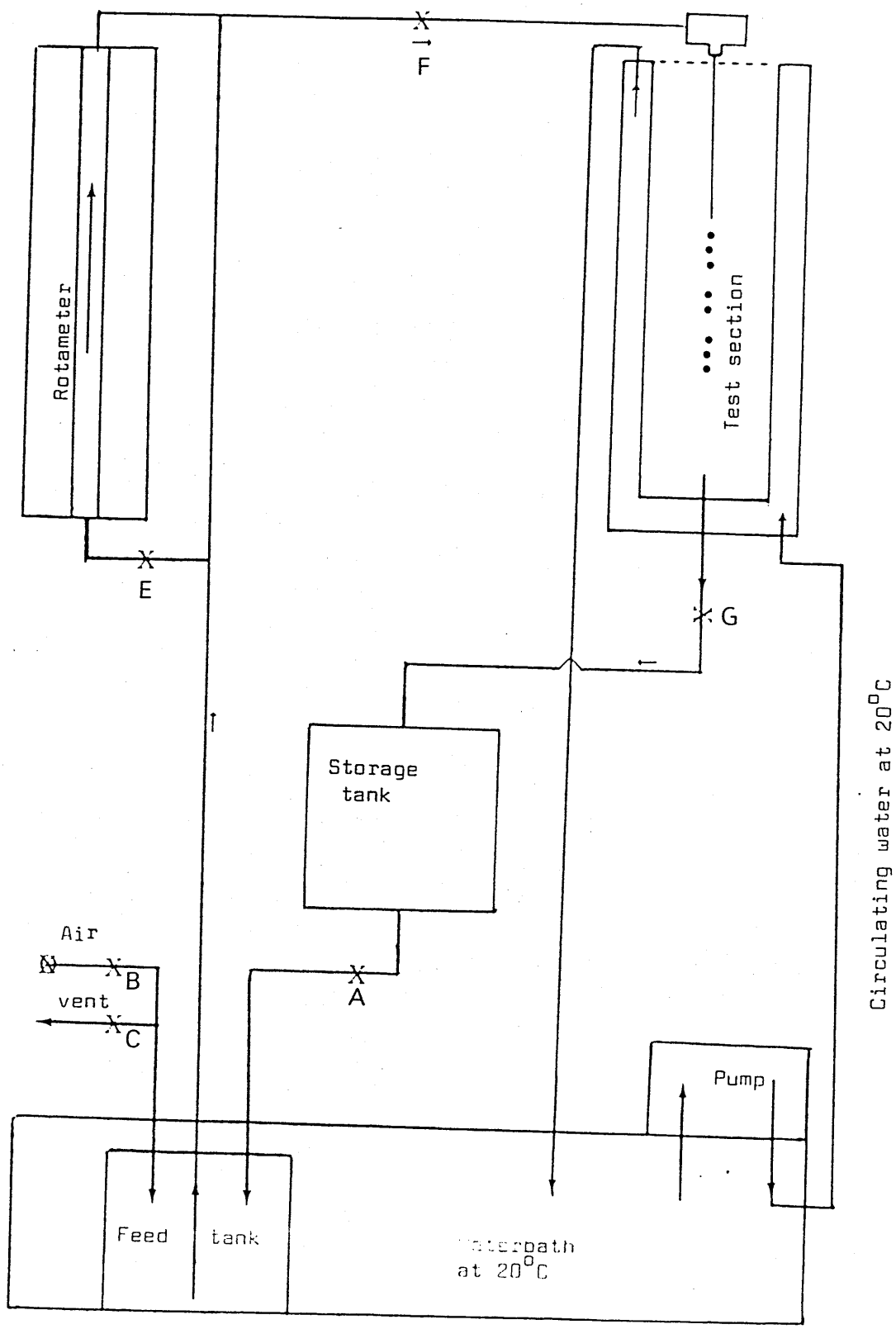

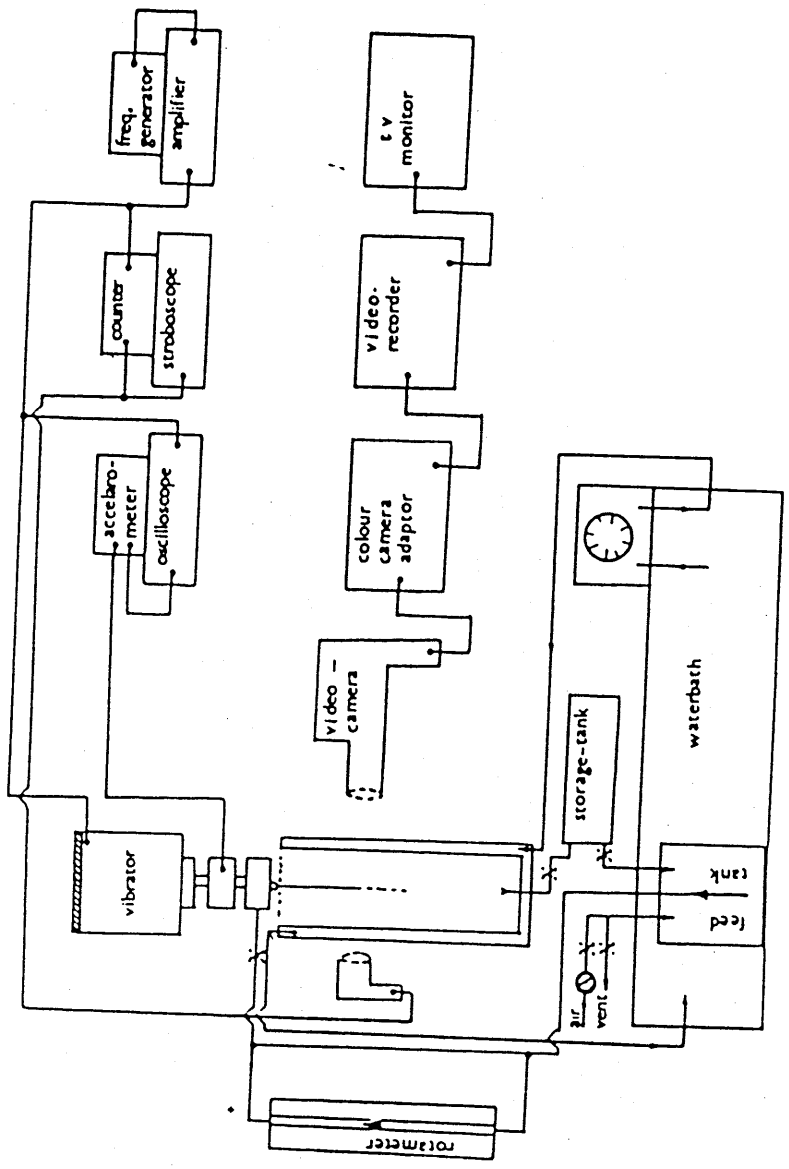

Figure 7a : Schematic diagram of the experimental apparatus.

A pressure of 30 psi was applied to the feed tank and kept constant in the present investigation. A rotameter (supplied by G A Platon Ltd.) was used to control a flow rate .The dispersed phase was kept at a constant temperature of 20°C using a Gallenkamp Thermostatic bath . A storage tank of capacity one litre was used for the dipersed phase from the contact cell . To maintain the level of the continuous phase in the contact cell, a needle valve (G) was used . The contact cell was made from a double walled perspex sheet of 0.5 cm thickness with the following dimensions :

Inside -	Length	12 cm	Breadth	12 cm	Height	37 cm
Outside-	Length	14 cm	Breadth	14 cm	Height	38 cm

The continuous phase was also maintained at 20°C by circulating water from the thermostatic bath .

OPERATING PROCEDURE

Dispersed phase (water) saturated with continuous phase was vented by valve C in the feed tank, temperature was maintained at 20°C. A pressure of 30 psi was applied to the feed tank via valve B. The required flow rate was achieved by the adjustment of valves E and F. An approximate value of volumetric flow rate of the dispersed phase was indicated by a rotameter. A calibration of the rotameter at 20°C is given in Figure 8. The indicated flow rate was confirmed by weighing the collected sample of the dispersed phase from a known time and a volumetric flow rate could then be calculated.

After having a constant flow rate through nozzle, a choosen frequency and amplitude of external vibration were applied and the variations in the jet length were recorded simulteneously by a video camera and a 35 mm still camera ,focussed on the suface of the jet. Measurements of jet length and drop diameter were taken from still photographs and the process of disintegration was studied by replaying the video recorded film in slow motion.

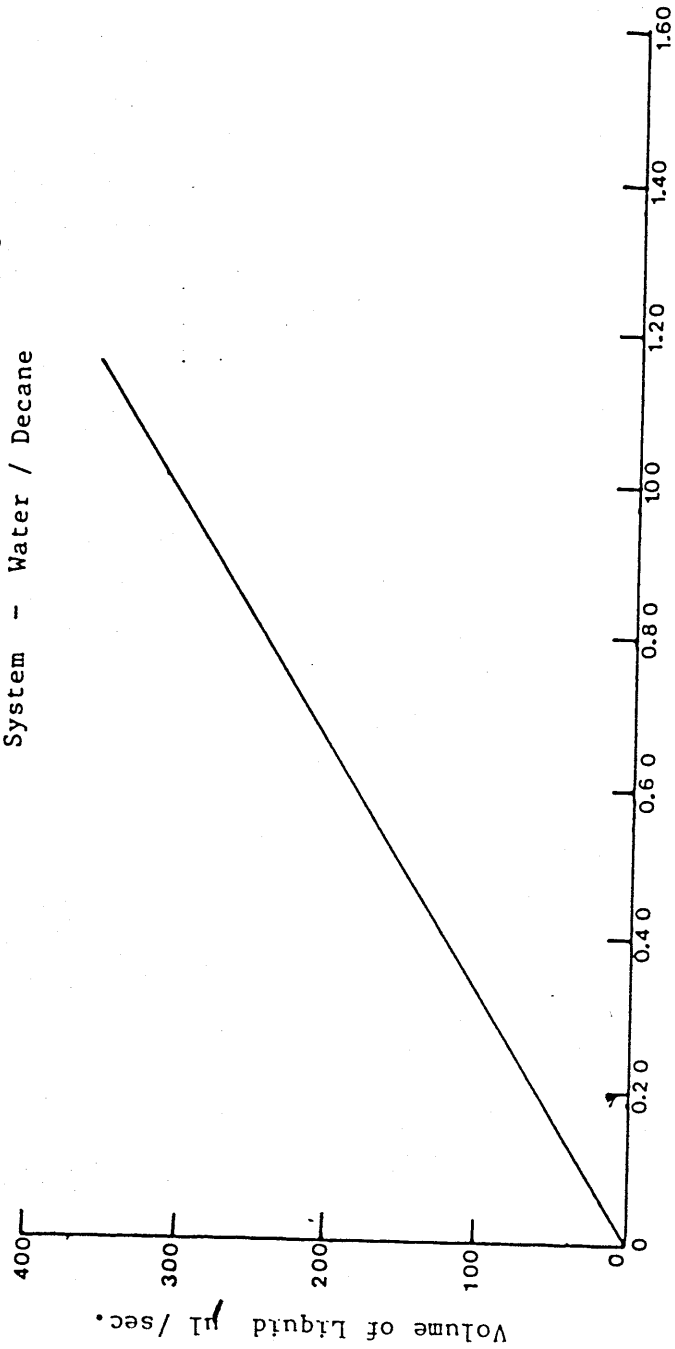

Figure 8 : Calibration of rotameter at 20°C
System - Water / Decane

3.1.3 Nozzles :

Two types of nozzle were used in the present investigation ;

3.1.3.1 - Hypodermic Needles

3.1.3.2 - Spinnerettes

3.1.3.1 Hypodermic Needles :

Stainless steel hypodermic needles were provided by Cooper's Needles Works Ltd. , Birmingham , England. Needles were 6.5 cm long and the ratio of length to the inside diameter was kept higher than required to obtain a fully developed velocity profile at the outlet. Needle tips were machined flat and smooth to reduce the rough surface effect of the nozzle on the liquid jet.A summary of the needle sizes is given in the table below :

S.No.	Nozzle No.	Inside Dia	Outside Dia
1.	5	0.61 mm	1.05 mm
2.	6	0.68 mm	1.10 mm
3.	7	0.85 mm	1.24 mm

3.1.3.2 Spinnerettes :

Spinnerettes used in the investigation were made of stainless steel plate of thicness 1 mm . Spinnerettes with four different hole sizes (250 , 200 , 150 and 100 μm diameter) were employed . These were supplied by Courtaulds Engineering Ltd , Coventry , England . An aluminium chamber was designed and constructed to hold these spinnerettes , to provide a smooth and uniform flow through the holes . A schematic plan of chamber and spinnerette is given in figure (9) and a photograph of of the two is given in plate 2 and 3 .

The needle assembly or aluminium chamber fitted with the spinnerette was mounted vertically on the extension bar of the vibrator to induce transverse vibrations .

PLATE 2 : Spinnerette Assembly.

PLATE 3 : Anatomy of Spinnerette Assembly.

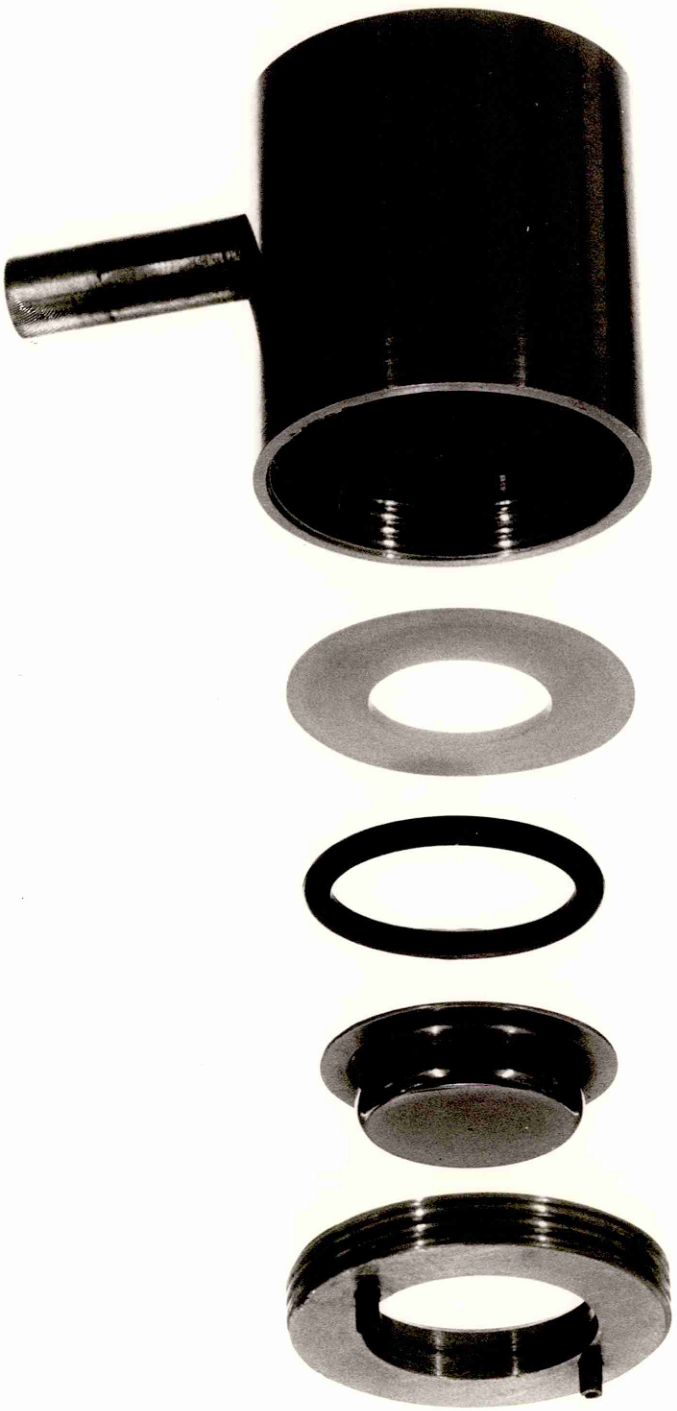

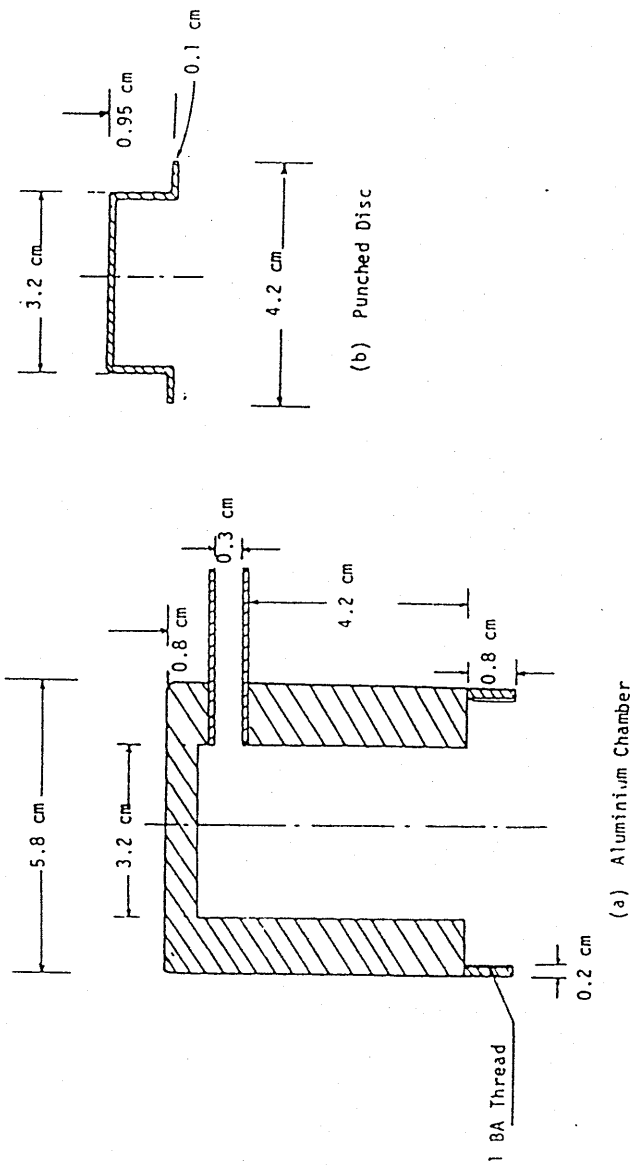

Figure 9 : Plan View of Aluminium Chamber and Punched Disc

3.1.4 Photographic Unit

3.1.4.1 - Still Photography :

A fixed rigid base stand mounted with Nikon - f2, camera with 55 mm f 3.5 lens was used for still photography . A cable release mechnism was used to prevent unnecessary movement during the photography A high speed flash (Sunpark Zoom A24000) was used to illuminate the jet and the droplets . The flash duration time was 30 μsec synchronized with the camera at a shutter speed of 1/30 of a second . The early test indicated that it was necessary to reduce the light intensity to produce a clear distinction of the objects being photographed . The reduction was achieved by inserting two sheets of typing paper in front of the flash . These acted as light diffusers and provided a uniform illumination , which produced distinct , measurable boundaries around the jet surface . A scale was fixed in the same plane as the liquid jet and within the camera field . Ilford F-P4 films were used and the exposed films were developed in Ilford Microphen developer .

3.1.4.2 Video Recording :

A video recorder (Model Video Star supplied by Ferguson Electronic Ltd.)was used , to record the pictures from a video camera (supplied by JVC). To illuminate the jet, a strobe light (supplied by Cromston Electronics Ltd) was used . The frequency of the strobe light was set manually , equal to the drop frequency . This

gave a frozen picture of the liquid jet on the TV monitor (supplied by Sony Electronics Ltd. Japan.) Films were made at every setting of frequency and amplitude using E-180 VHS video cassettes ,supplied by Victor Company Ltd , Japan.

The disintegration process of the liquid jets and drop formation could be studied in detail by replaying the recorded films in slow motion on the TV monitor . Jet lengths and sizes and inter-drop distances could be measured directly from the TV monitor by freezing the frames of the films . These results could be checked against the measurements taken from the still photographs obtained at the same time .

3.1.4.3 High Speed Photography :

The camera used was a 16 mm Wollensak Fastex WF 17T , rotating prism model of 30 m film capacity . It employed two lenses (oriented at right angles) simultaneously . The images are superimposed on the same film. Photographs can be taken at a speed between 150 - 18000 frames per second . The framed image is established on the continuously moving film by a prism . The rotation of the prism is synchronised with the movement of the film . Different film speeds are obtained by adjusting the voltage supplied to the two motors of the camera and a speed at any point is indicated by the limiting pulses registered on the films during the operation . The exposure time cannot be adjusted independently

of the picture frequency . The effective exposure time is approximately the reciprocal of five times the setting frequency . This camera was mounted on a stand which gives flexibility of adjustment with adequate stability .

A special control unit (Goose) permits the synchronisation of the camera with the events to be photographed . Regulation of the camera speed and remote control of the camera is controlled by the current supplied with an AC variable auto transformer with a maximum output of 280 volts . The camera control circuit also incorporates a 70ms delay time when operating above 130 volts . This delay brings the camera up to speed in two steps to prevent stripping of the film sprocket holes .

A model HSS/4/K-3 high power , high speed and short duration stroboscope was used to illuminate the jet and droplets for high speed photography .

Film requirement for the jet and the droplets photography are much the same as for other high speed cameras except good contrast and high resolution are required . To compensate to a certain extent for under-exposure, a controlling vigorous developer is needed . A Kodak Tri - X reversal movie film was used for the study .

The film was analysed by projecting on a large screen , the projector used gives bright , flickerless pictures at four different speeds 2 , 4 , 8 , 16 frame per second with forward and reversed running and remote control facilities . Individual frames

can be examined for any length of time and film can be studied frame by frame , forward or backward by operating a push button switch . An accurate frame counter which operates in both the directions provides a ready means of frame identification . The magnification of the jet was determined from a reference capillary tube and the diameter of the drop produced was calculated from the reference .

3.2 Measurement of Physical Properties :

Viscosities of liquids were measured by using a Syncro Lectric Viscometer supplied by Brookfield . This viscometer measures the viscosity by measuring the force required to rotate a spindle in a fluid (It measures the torque necessary to overcome the viscous resistance to the induced movement). This is accomplished by driving the immersed element , which is called a Spindle , through a baryllium copper spring , the degree to which the spindle is wound , indicated by the position of the red pointer on the viscometer's dial , is proportional to the viscosity of the fluid for any given rotational speed and spindle. The accuracy of the viscometer is very high , the instrument was found to be accurate within 1% and to reproduce within 0.2% of its full scale range .

Measurements were made by using the same spindle at different speeds to detect and evaluate the rheological properties of the test solution .

This measured value of viscosity was then checked by using an Ostwald Viscometer calibrated with water with in a temperature range of 24 -25^{o}C and the average values of these two readings were taken and used in calculation.

Density measurement of liquids were made by specific gravity bottle also calibrated with distilled water within the temperature range of 24 -25^{o}C

Interfacial tension was determined by using the Herkin Brown drop volume technique . A 3 ml microburette , fitted with a glass dropping tip having an inside diameter 0.52 mm and outside diameter 1.5 mm respectively , was used for the measurements. The microburette was cleaned with chromic acid solution and then thoroughly washed with distilled water . Unless the glass dropping tip is exceptionally clean, difficulties can be experienced in forming the drops so that it completely cover the tip .The burette was filled with the denser liquid and the tip was just submerged into the other liquid . Each drop was then formed very slowly so that all the kinetic effects were eliminated . By taking extreme care in the manipulation of the opening valve ,the correct drop volume was obtained. 15 drops were formed and average volume was used in the calculation of the interfacial tension from the equation ;

$$\sigma = \frac{Vf\,(\rho_d - \rho_c).g}{\pi\, D_n F}$$

Where F is the Herkin Brown correction factor depending on $Dn/Vf^{1/3}$ and plotted in Figure (10)

To check the reading of the interfacial tension , obtained by the above described technique , a Torsion Balance (Type O.S) was used and measured the interfacial tension -

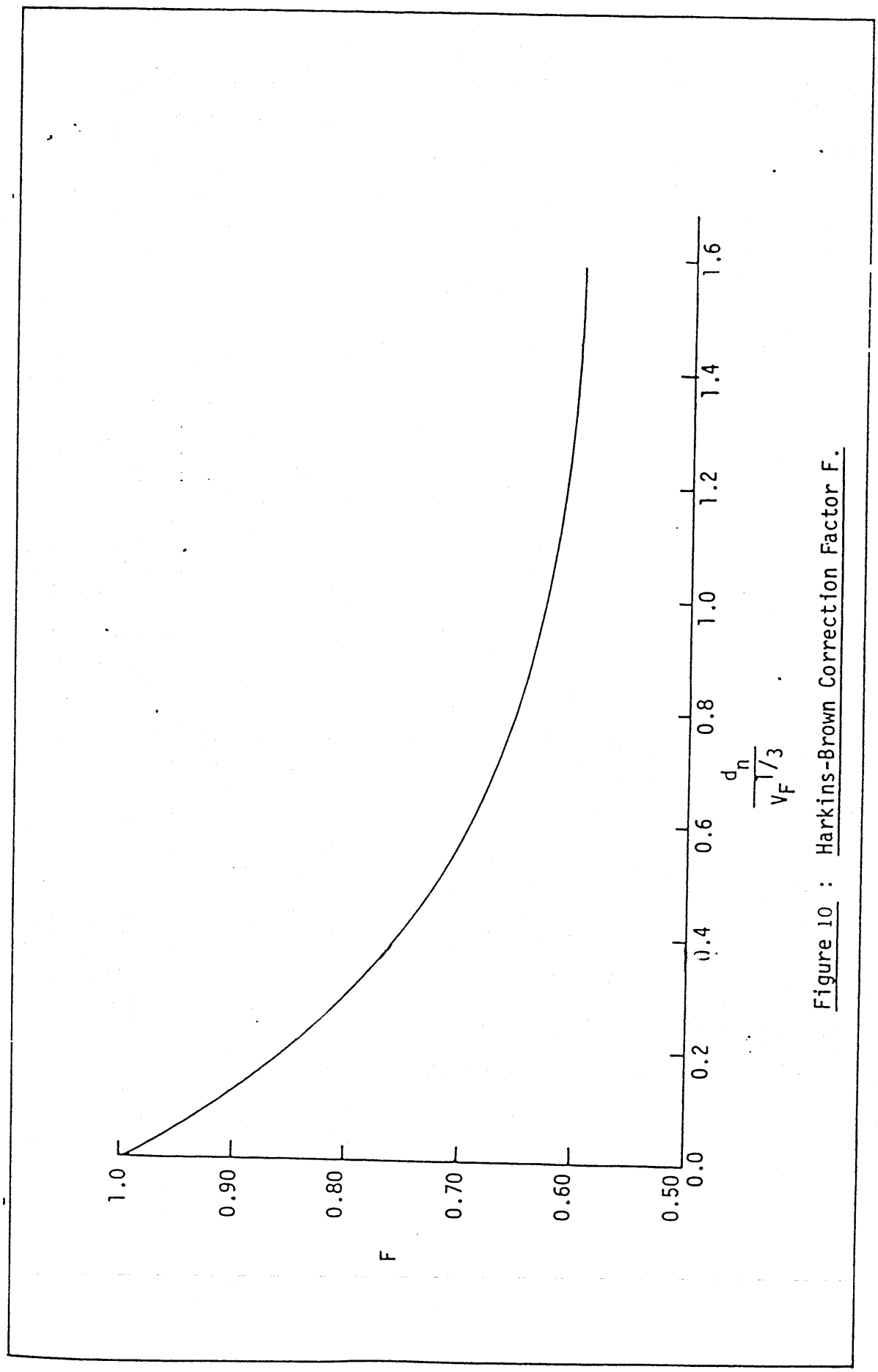

Figure 10 : Harkins-Brown Correction Factor F.

[a] By using platinum ring

[b] By using glass test plate

The torsion balance is designed for the measurement of surface tension and the interfacial tension of liquids by using a platinum ring or a glass plate . It was calibrated 0 - 0.12 Newton per meter with 240 equal divisions (1 newton per meter is equal to 1000 dynes per cm)

3.4.1 Measurement by using platinum ring :

The procedure adopted was as follows :

Set up the balance , using thinner extension hook from which the platinum ring was suspended. Check the balance for zero setting , with the platinum ring completely immersed in the upper of the two liquids . Care should be taken to ensure that the contact has not been made with the interface before the balance is checked for zero . The platinum ring was then immersed completely in the lower liquid and drawn out from interface by means of adjusting screws , the required force for this operation was read by means of a pointer on the circular dial of the torsion balance .

3.4.2 Measurement by using glass plate :

In the same manner as described in the previous section interfacial tension was also measured using a glass plate .

Thus in practice , average values of the three above described techniques of measuring interfacial tension for each system were taken

A list of these physical properties of the liquid pair studied in this investigation is given in the Table 2

TABLE 2

AVERAGE PHYSICAL PROPERTIES OF MUTUALLY SATURATED LIQUIDS USED IN THE PRESENT INVESTIGATION

S. No	SYSTEMS	DISPERSED PHASE DENSITY	CONTINUOUS PHASE DENSITY	DISPERSED PHASE VISCOSITY	CONTINUOUS PHASE VISCOSITY	INTER FACIAL TENSION
1.	Water-Kerosene	1.0	0.78	1.0	1.6	44.20
2.	Water-Kerosene (75%) + Paraffin (25%)	1.0	0.82	1.0	2.27	42.48
3.	Water-Kerosene (50%) + Paraffin (50%)	1.0	0.83	1.0	8.04	41.50
4.	Water-Kerosene (25%) + Paraffin (75%)	1.0	0.84	1.0	15.2	40.10
5.	Water-Paraffin	1.0	0.86	1.0	28.0	39.11
6.	Water-Decane	1.0	0.73	1.0	1.25	25.00

Note : Above mentioned mixing percentages by volume are approximated.

25. Anwar,M M. Bright, A. Das, T K. and Wilkinson, W L. Trans I ChemE 60 , 306 , 1982.

26. Craine,L E. Birch,S. and Mc Cormack Brit.J. Appl.Phys. 15,743,1964.

27. ibid ibid 16,395,1965.

28. Donnelly,R J and Glaberson,W. Proc.Roy.Soc. A290 , 547 , 1966.

29. Haelein, A. N A C A Tech.Memo No.659 , 1932.

30. Yuen,M C. J Fluid.Mech. 33 , 151 , 1968.

31. Goedde,E F. and Yuen,M C. J Fluid Mech 40 , 4945 , 1970.

32. Wang,D P. J. Fluid Mech. 34 , 299 , 1968.

33. Wissema,J G. and Davies,G.A. Can. J Chem.Eng. 47 , 530 , 1969.

34. Rutland,D F. and Jameson,G J. J.Fluid Mech. 46 , 267 , 1971.

35. Rajgopalan,R.,Tien,C. and Suramanyam Can. J. Chem. Eng. 50,410,1972.

36. Rajgopalan,R. and Tien,C Can. J. Chem. Eng. 51 , 272 , 1973.

37. Schneider,J M. and Hendricks C D. Rev. Sci. Inst 35 , 1349 , 1964.

38. Dabora E K. Rev. Sci. Inst. 38 , 502 , 1967.

39. Nelder, J A and Mead, R. Computer Journal 7 , 308 , 1664

40. Spendley, W. Hexr ,G R and Hinsworth, F R. Journal of Math 4 , 441 , 1962.

4.0 RESULTS AND DISCUSSION

An understanding of the disintegration process of a liquid jet into an immiscible phase is essential for determination of drop size and for the calculation of interfacial area produced under the jetting conditions. Das(17) reported that the size of droplets depends on the jet diameter at the point of break-up. Anwar et al(25) demonstrated that the diameter of the jet varies with jet length (i.e distance from orifice) and they developed a model for the calculation of the diameter at various known distances from an orifice but their model can not be applied to determine jet break-up length.In the present work knowledge of the variation of the jet diameter coupled with jet instability analysis is used as a theoretical basis for the prediction of the jet length and the drop diameter.

4.1 JET INSTABILITY CURVE

Experimental values of the jet break-up lengths against nozzle velocities (as shown in Figure 11,Table 3) for an orifice of 0.25 mm diameter were obtained. From these figures various well defined regions can be identified.

In the initial region (A-B) the jet length increases linearly with nozzle velocity (Fig 11). Subsequently there is an abrupt lengthening of the jet from B to C without any noticeable change in velocity. With further increase in the velocity , the jet

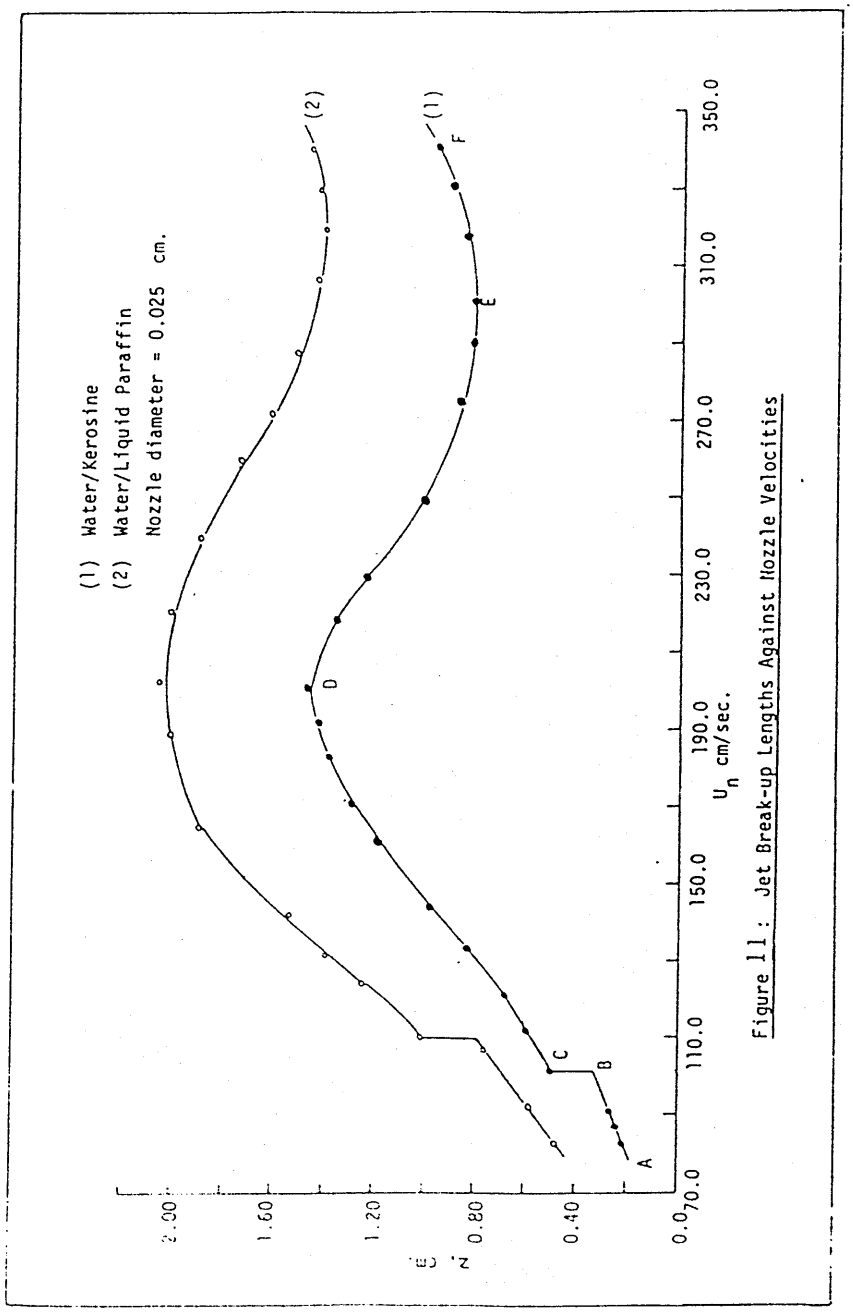

Figure 11 : Jet Break-up Lengths Against Nozzle Velocities

TABLE 3

Experimental Data on Jet Break-up Length Against Nozzle Velocity.

Nozzle Diameter - 0.025 cm

Serial No.	System - Water/Kerosene		System - Water/Paraffin	
	Nozzle Velocity cm / sec.	Jet Length cm.	Nozzle Velocity cm /sec	Jet Length cm.
1.	83.2	0.22	86.6	0.46
2.	87.0	0.29	92.9	0.57
3.	95.1	0.45	105.8	0.75
4.	102.0	0.54	107.8	1.09
5.	114.0	0.66	124.3	1.24
6.	121.3	0.75	135.3	1.38
7.	133.0	0.86	143.5	1.53
8.	146.1	0.96	166.6	1.92
9.	156.0	1.10	186.3	2.04
10.	160.0	1.18	198.0	2.15
11.	161.3	1.21	216.2	2.05
12.	168.0	1.31	237.3	1.90
13.	180.0	1.38	256.9	1.75
14.	191.2	1.41	268.9	1.59
15.	199.2	1.47	284.3	1.52
16.	216.0	1.35	303.9	1.42
17.	230.0	1.27	318.4	1.41
18.	235.2	1.22	330.2	1.44
19.	248.5	1.08	337.6	1.47
20.	260.0	1.00		
21.	274.0	0.88		
22.	289.1	0.80		
23.	302.3	0.80		
24.	318.1	0.84		
25.	329.0	0.88		
26.	338.2	0.92		

length reaches a maximum along C - D, after a critical velocity at which maximum jet length occurs, the jet length starts decreasing with increase in the jet velocity along D - E. Finally a further increase in the jet velocity causes a small increase in the jet length along E - F.

Fig 11 also shows the effect of viscosity on the jet break-up length. The results confirmed previous worker's (16,17,25) conclusions that the jet break-up length increases with the increase in the viscosity of the continuous phase.

Attempts by previous workers(18,19,23) to model the effect of various parameters e.g. viscosity, nozzle diameter, nozzle velocity, etc. on jet break-up length were restricted to the region A - D, where the dispersed phase flow rate is low. However interfacial area created is directly proportional to the flow rate of the dispersed phase. Therefore in any contacting equipment high flow rates of dispersed phase are desirable to achieve high interfacial area. Hence the first part of the present work was mainly concentrated in the region D - E.

4.2 JET BREAK-UP LENGTH AT HIGH FLOW RATES

A nozzle of 0.20 mm diameter was used and a nozzle velocity was fixed at 261 cm/sec. The viscosity of the continuous phase was varied from 1.5 - 28.0 c.p using Kerosene and Liquid paraffin in different proportions. The data obtained under the influence of

externally applied vibrations , are given in Tables (4,5,6,7) and plots of the jet lengths against applied amplitude are given in figures (12,13,14,15).

4.2.1 EFFECT OF EXTERNAL VIBRATION ON JET LENGTH

It is apparent from the figures (12,13,14,15) that both amplitude and frequency of applied vibrations play an important role in determining the jet break-up length , e.g with the increase of applied amplitude (Table 6) from 0.00183 mm to 0.0433 mm , the jet length decreases from 7.0 to 4.0 mm. Similarly with the variation of the frequency from 200 Hz to 400 Hz at known applied amplitude (Table 6) , the jet length decreases from 7.0 to 4.7 mm.

Rayleigh's theory of instability relates the jet length with the nozzle diameter and velocity as follows ;

$$L = \frac{U_n}{B} \ln \frac{a_n}{\partial_o} \qquad [R1]$$

Where ; U_n - Nozzle velocity, B - Growth rate of maximum growing disturbance, a_n - Nozzle radius, and ∂_o - Initial amplitude of maximum growing disturbance at the nozzle exit.

Figure 12 : Plot of Experimental Jet Length and Applied Amplitude

System - Water / Kerosene
× - 200 Hz
▽ - 250 Hz
+ - 300 Hz
○ - 350 Hz
◇ - 400 Hz
✳ - 450 Hz

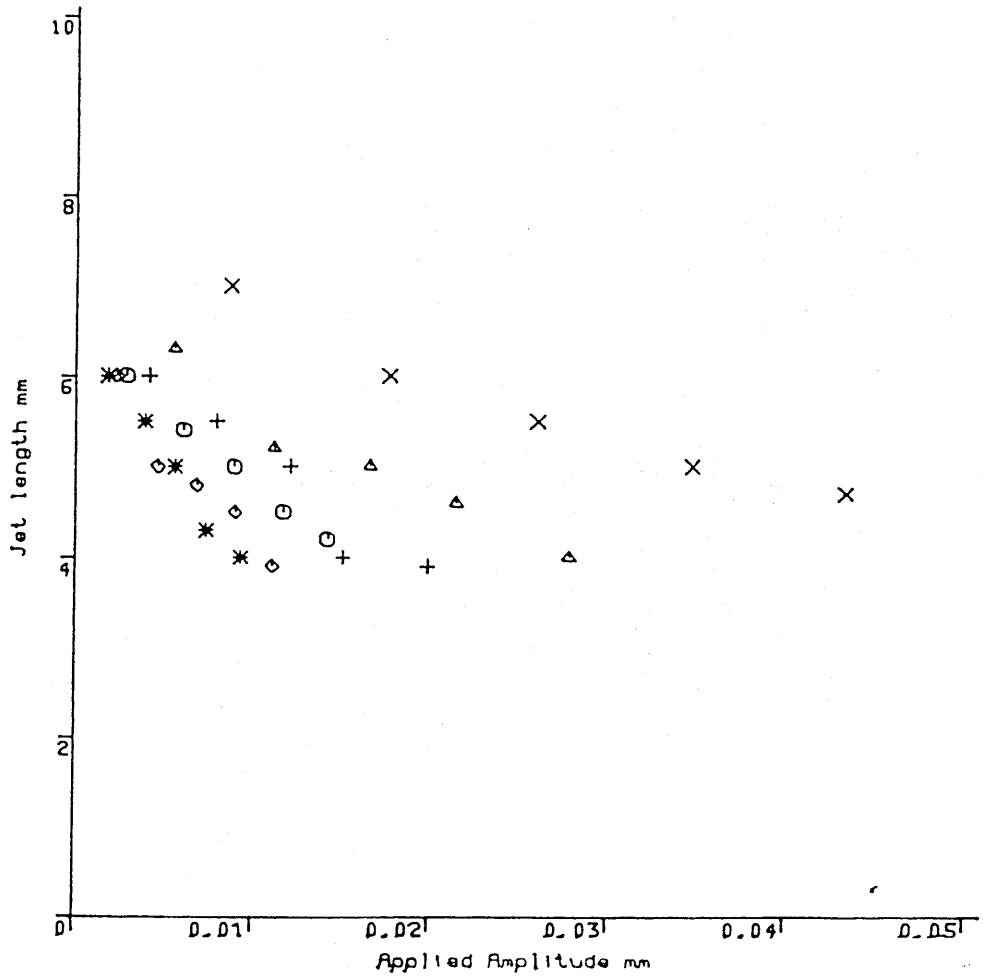

Figure 13 : Plot of Experimental Jet Length and Applied Amplitude

System - Water / 25P + 75K
× - 200 Hz
▽ - 250 Hz
+ - 300 Hz
○ - 350 Hz
◇ - 400 Hz
✱ - 450 Hz

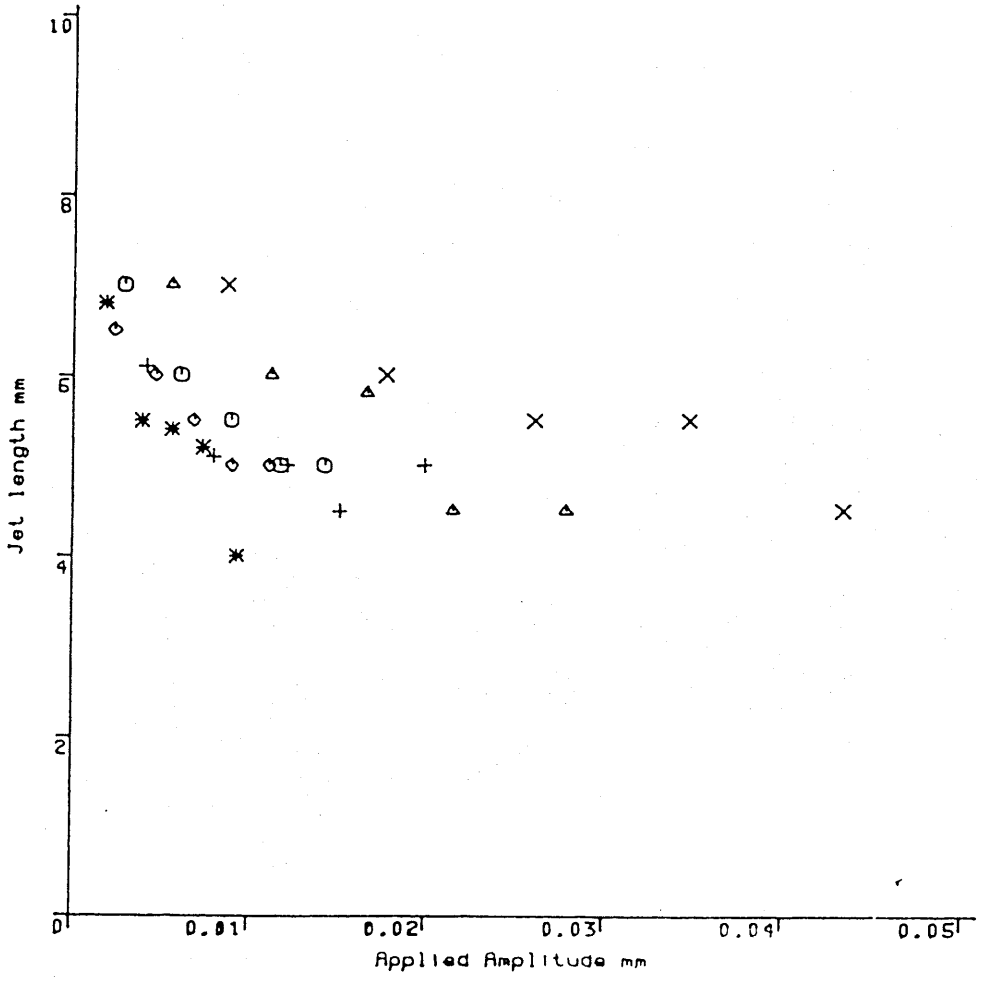

Figure 14 : Plot of Experimental Jet Length and Applied Amplitude

System - Water / 50P + 50K
× - 200 Hz
▼ - 250 Hz
\+ - 300 Hz
⊙ - 350 Hz
◇ - 400 Hz
✱ - 450 Hz

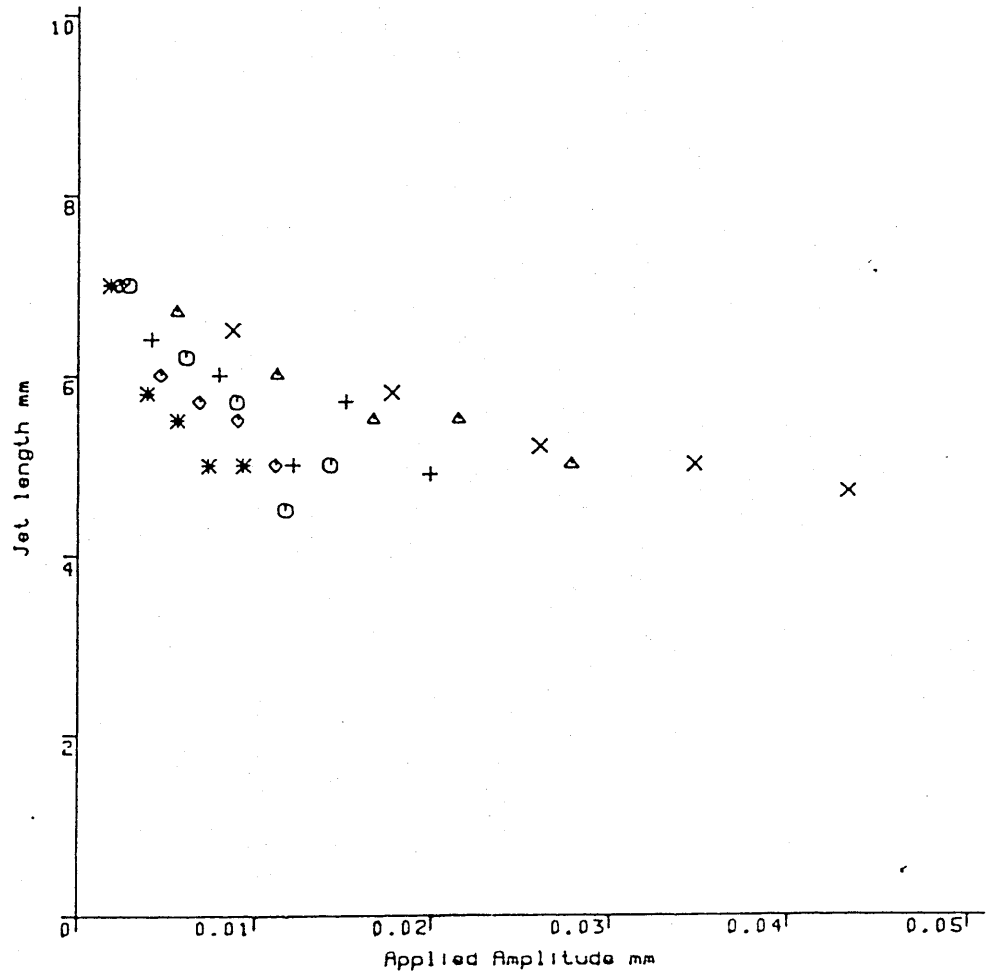

Figure 15 : Plot of Experimental Jet Length and Applied Amplitude

System - Water / 75P + 25K
× - 200 Hz
▽ - 250 Hz
+ - 300 Hz
○ - 350 Hz
◇ - 400 Hz
✱ - 450 Hz

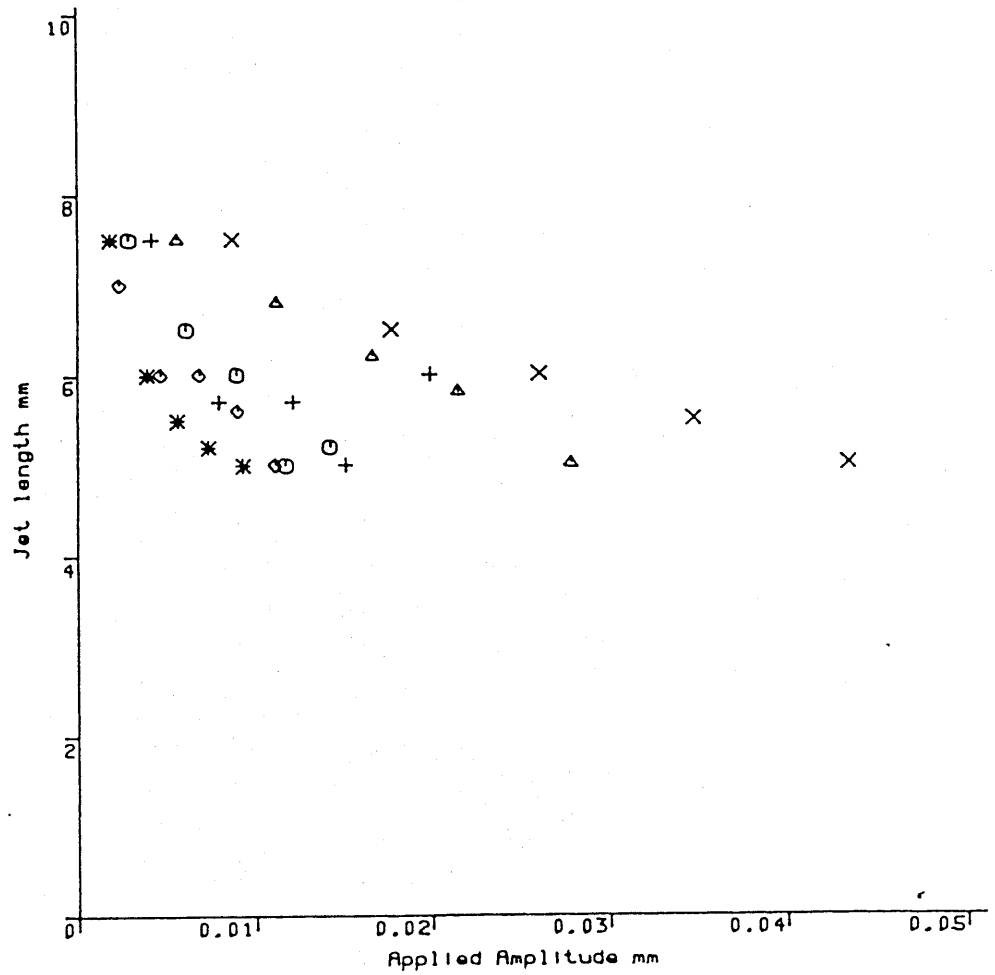

TABLE 4

ORIFICE DIAMETER : 0.020 Cm

SYSTEM : WATER / Kerosene

JET VELOCITY : 2610 mm/Sec

SEQUENCE NUMBER	EXPERIMENTAL JET LENGTH mm	AMPLITUDE mm	FREQUENCY H_Z
1	7.0	.00868	200
2	6.0	.01768	200
3	5.5	.02600	200
4	5.0	.03475	200
5	4.7	.04344	200
6	6.3	.00556	250
7	5.2	.01120	250
8	5.0	.01660	250
9	4.6	.02144	250
10	4.0	.02780	250
11	6.0	.00413	300
12	5.5	.00794	300
13	5.0	.01210	300
14	4.0	.01509	300
15	3.9	.01985	300
16	6.0	.00283	350
17	5.4	.00608	350
18	5.0	.00892	350
19	4.5	.01170	350
20	4.2	.01418	350
21	6.0	.00232	400
22	5.0	.00465	400
23	4.8	.00682	400
24	4.5	.00899	400
25	3.9	.01110	400
26	6.0	.00183	450
27	5.5	.00392	450
28	5.0	.00563	450
29	4.3	.00735	450
30	4.0	.00931	450

TABLE 5

ORIFICE DIAMETER : 0.020 Cm

SYSTEM : WATER / 25P+75K

JET VELOCITY : 2610 mm/Sec

SEQUENCE NUMBER	EXPERIMENTAL JET LENGTH mm	AMPLITUDE mm	FREQUENCY Hz
1	7.0	.00868	200
2	6.0	.01768	200
3	55.0	.02600	200
4	5.5	.03475	200
5	4.5	.04344	200
6	7.0	.00556	250
7	6.0	.01120	250
8	5.8	.01660	250
9	4.5	.02144	250
10	4.5	.02780	250
11	6.1	.00413	300
12	5.1	.00794	300
13	5.0	.01210	300
14	4.5	.01509	300
15	5.0	.01985	300
16	7.0	.00283	350
17	6.0	.00608	350
18	5.5	.00892	350
19	5.0	.01170	350
20	5.0	.01418	350
21	6.5	.00232	400
22	6.0	.00465	400
23	5.5	.00682	400
24	5.0	.00899	400
25	5.0	.01110	400
26	6.8	.00183	450
27	5.5	.00392	450
28	5.4	.00563	450
29	5.2	.00735	450
30	4.0	.00931	450

TABLE 6

ORIFICE DIAMETER : 0.020 Cm

SYSTEM : WATER / 50P+50K

JET VELOCITY : 2610 mm/Sec

SEQUENCE NUMBER	EXPERIMENTAL JET LENGTH mm	AMPLITUDE mm	FREQUENCY Hz
1	6.5	.00868	200
2	5.8	.01768	200
3	5.2	.02600	200
4	5.0	.03475	200
5	4.7	.04344	200
6	6.7	.00556	250
7	6.0	.01120	250
8	5.5	.01666	250
9	5.5	.02144	250
10	5.0	.02780	250
11	6.4	.00413	300
12	6.0	.00794	300
13	5.0	.01210	300
14	5.7	.01509	300
15	4.9	.01985	300
16	7.0	.00283	350
17	6.2	.00607	350
18	5.7	.00892	350
19	4.5	.01170	350
20	5.0	.01418	350
21	7.0	.00232	400
22	6.0	.00465	400
23	5.7	.00682	400
24	5.5	.00899	400
25	5.0	.01111	400
26	7.0	.00183	450
27	5.8	.00382	450
28	5.5	.00563	450
29	5.0	.00735	450
30	5.0	.00931	450

TABLE 7

ORIFICE DIAMETER : 0.020 Cm

SYSTEM : WATER / 75P+25K

JET VELOCITY : 2610 mm/Sec

SEQUENCE NUMBER	EXPERIMENTAL JET LENGTH mm	AMPLITUDE mm	FREQUENCY Hz
1	7.5	.00868	200
2	6.5	.01768	200
3	6.0	.02600	200
4	5.5	.03475	200
5	5.0	.04344	200
6	7.5	.00556	250
7	6.8	.01120	250
8	6.2	.01660	250
9	5.8	.02144	250
10	5.0	.02780	250
11	7.5	.00413	300
12	5.7	.00794	300
13	5.7	.01210	300
14	5.0	.01509	300
15	6.0	.01985	300
16	7.5	.00283	350
17	6.5	.00607	350
18	6.0	.00892	350
19	5.0	.01170	350
20	5.2	.01418	350
21	7.0	.00232	400
22	6.0	.00465	400
23	6.0	.00682	400
24	5.6	.00899	400
25	5.0	.01111	400
26	7.5	.00183	450
27	6.0	.00392	450
28	5.5	.00563	450
29	5.2	.00735	450
30	5.0	.00931	450

Previous workers (18,19) who have used this equation in attempting to correlate their results in the region A-D (Fig 11) have taken the initial amplitude of maximum growing natural disturbance (∂_o) as a function of the individual nozzle (depending on the type and on the roughness at the surface of the nozzle). A number of investigators (16,17,18,19) have reported the value of $\ln\frac{a}{\partial_o}$ as a constant for an individual nozzle and taken the value as 6.

From figures (12,13,14,15) it can be seen that when an external forced vibration is applied , the experimental jet length shows a clear effect of the applied vibration, which lead to the conclusion that $\ln\frac{a}{\partial_o}$ cannot be a constant value. In the present investigation attempts have been made to modify Rayleigh's equation to take into account this effect. Initially it is assumed that the applied vibrations is the over-riding factor in the disintegration of the jet, and the amplitude of maximum growing disturbance (∂_o) can be replaced by the value of applied amplitude (∂). Thus equation 1 can be written as ;

$$L = \frac{U_n}{B} \ln\frac{a_n}{\partial} \qquad [R2]$$

Where ; ∂ - is the applied amplitude

Plots of experimental jet length vs $\ln \frac{a_n}{\delta}$ are given in figures 16,17,18,19 .

Figure 16

SYSTEM - WATER / KEROSENE

Nozzle diameter - 0.020Cm

* - 200 Hz
▽ - 250 Hz
◇ - 300 Hz
□ - 350 Hz
△ - 400 Hz
○ - 450 Hz

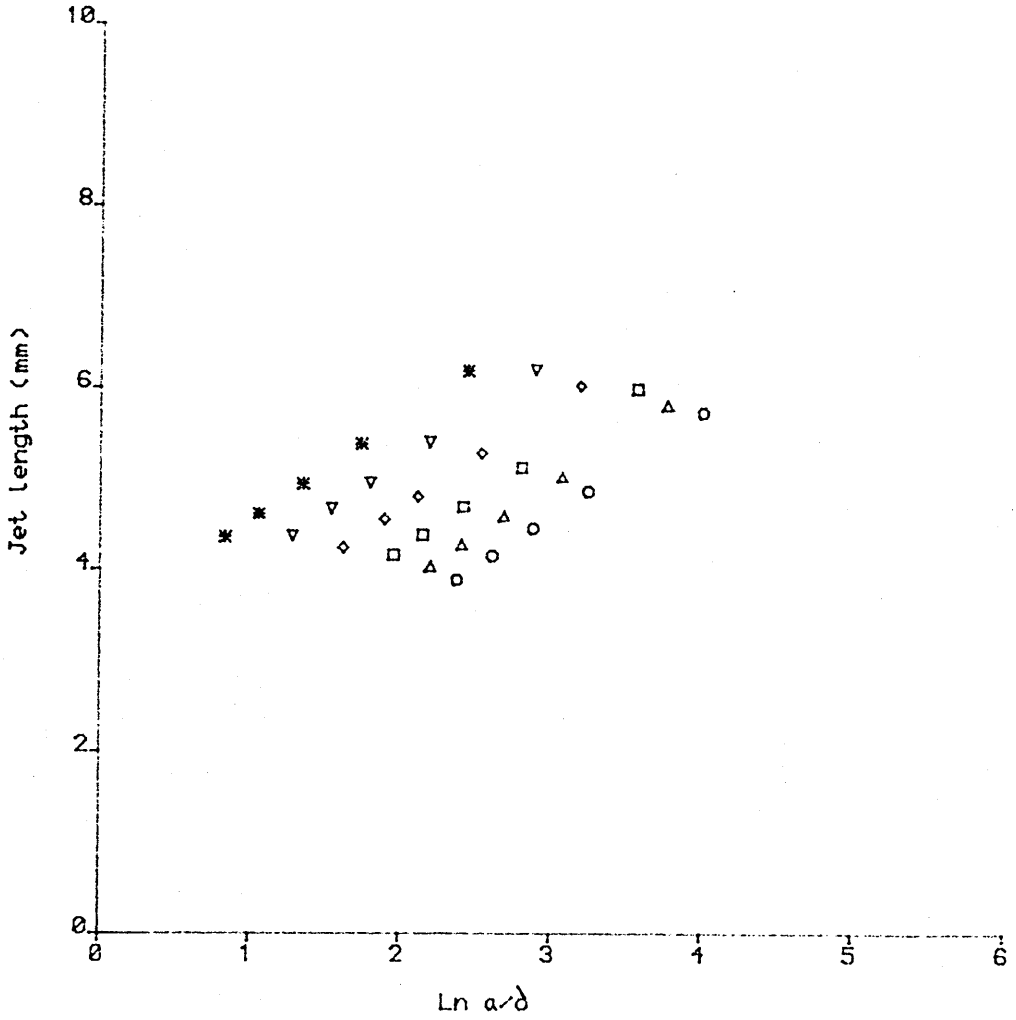

Figure 17

SYSTEM - WATER / 25P+75K

Nozzle diameter - 0.020 Cm

* - 200 Hz
▽ - 250 Hz
◇ - 300 Hz
□ - 350 Hz
△ - 400 Hz
○ - 450 Hz

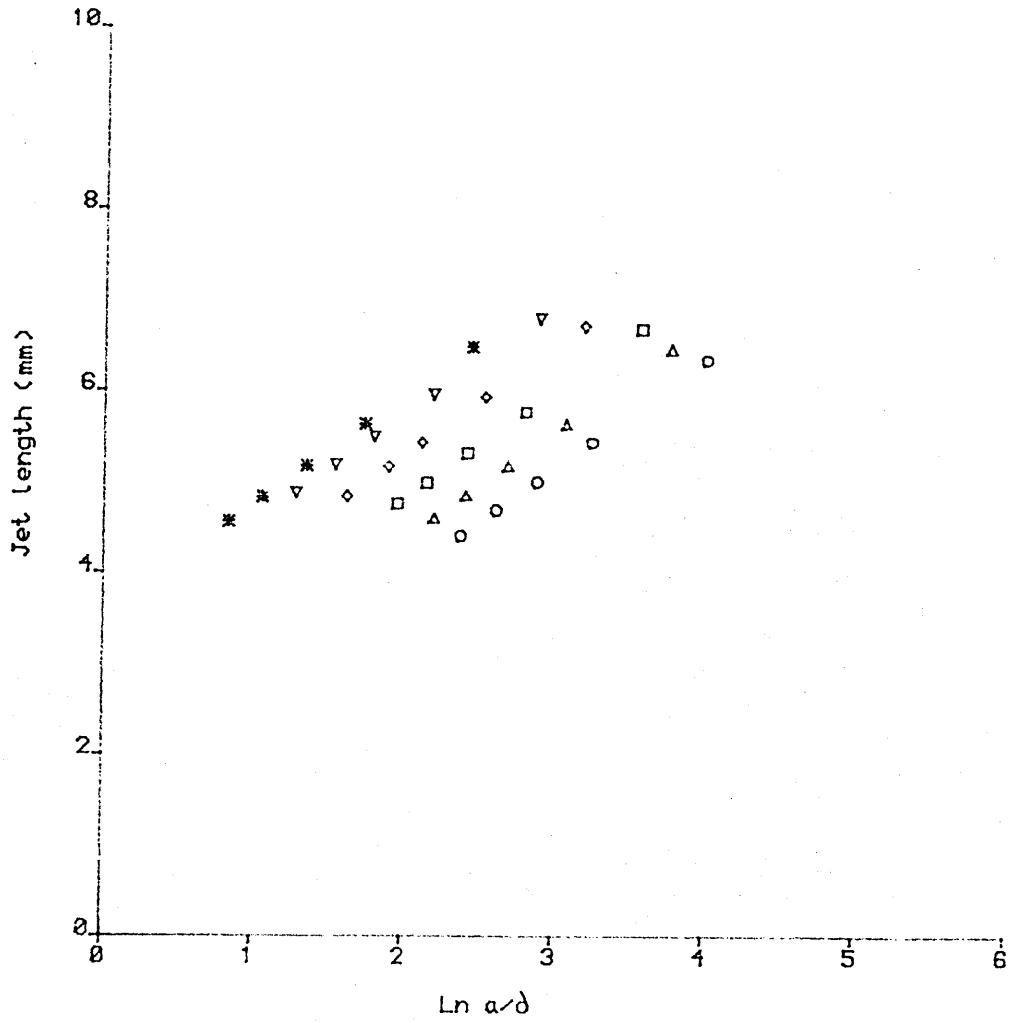

Figure 18

SYSTEM - WATER / 50P+50K

Nozzle diameter - 0.020 Cm

* - 200 Hz
▽ - 250 Hz
◇ - 300 Hz
□ - 350 Hz
△ - 400 Hz
○ - 450 Hz

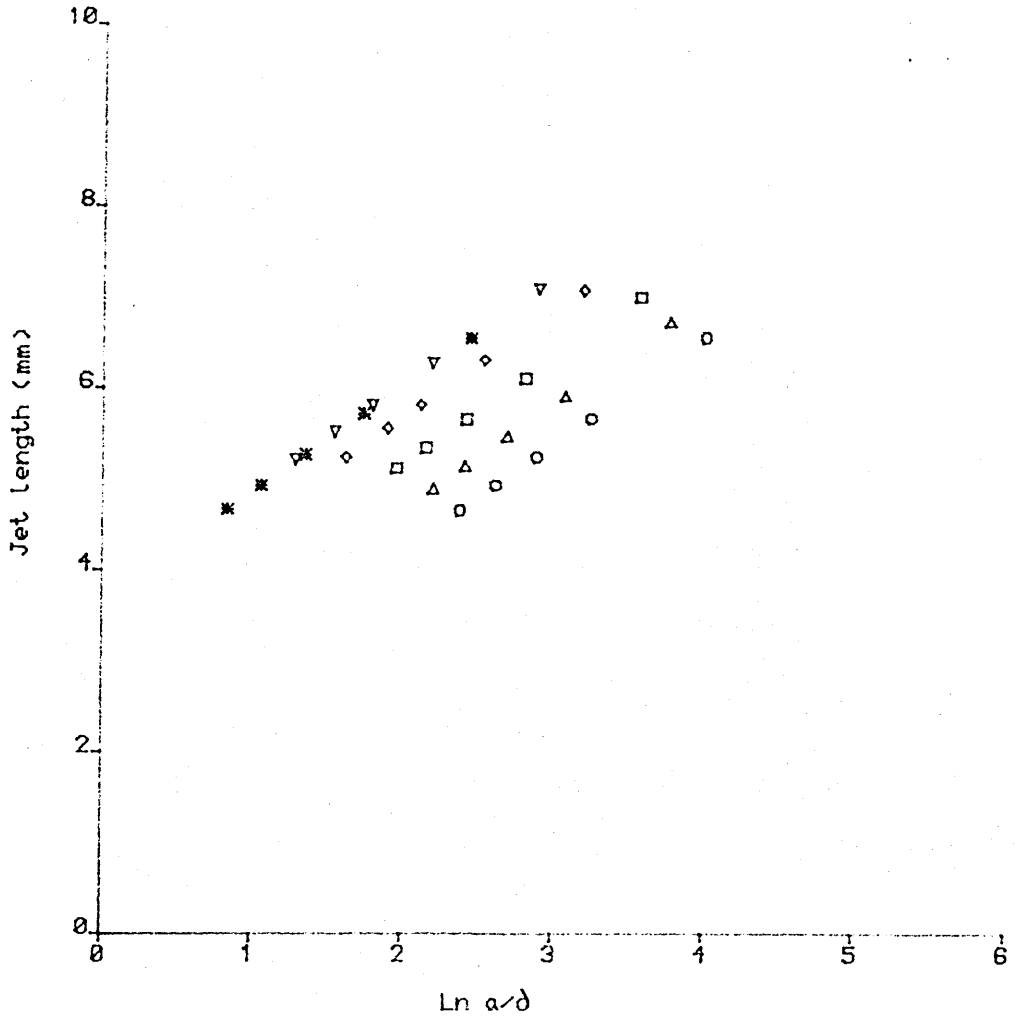

Figure 19

SYSTEM - WATER / 75P+25K

Nozzle diameter - 0.020 Cm

* - 200 Hz
▽ - 250 Hz
◇ - 300 Hz
□ - 350 Hz
△ - 400 Hz
○ - 450 Hz

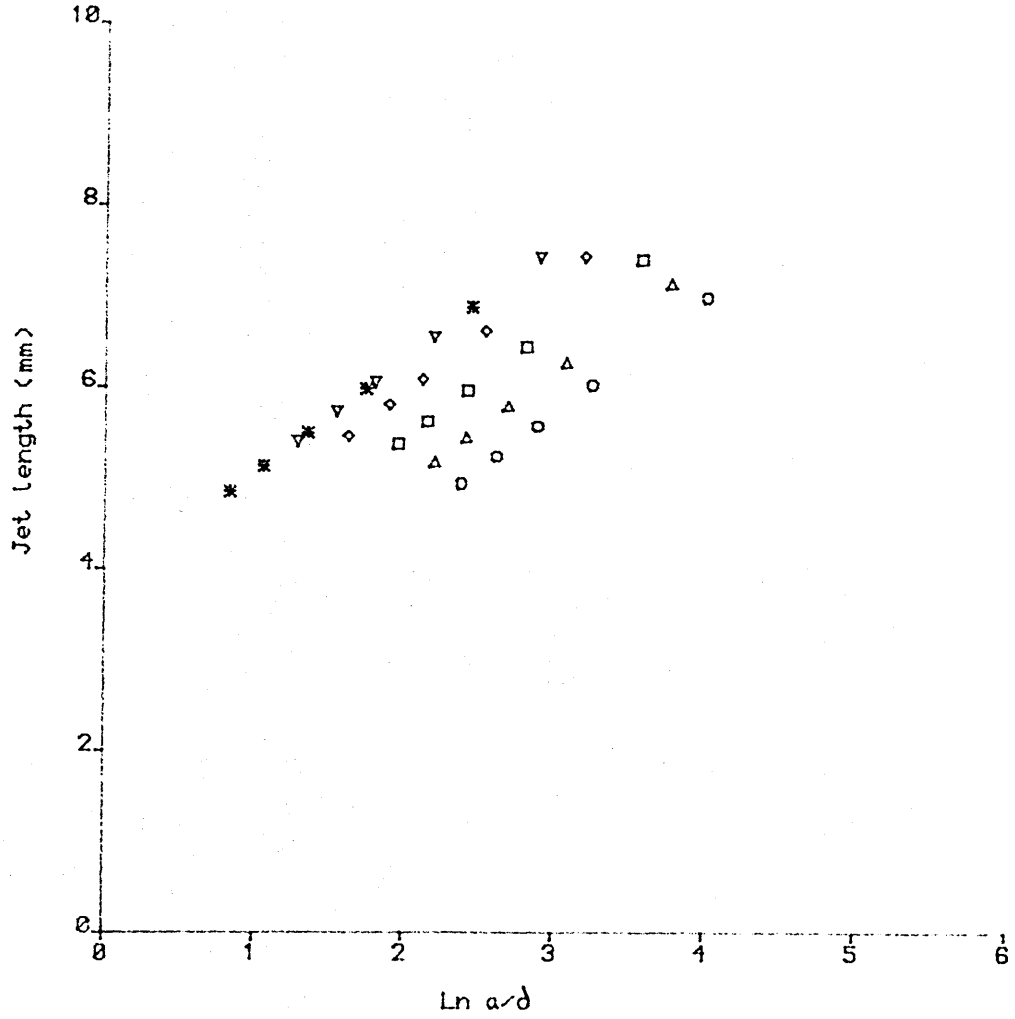

4.2.2 GROWTH RATE OF DISTURBANCE

It can be seen from the Figures (16,17,18,19) that at a fixed frequency a linear relationship does exist between jet length and $\ln\frac{a_n}{\delta}$, but for the range of frequency investigated , the plots shows a constant slope (Fig 16,17,18,19) indicating U_n/B is constant (equation R2). As the value of U_n is fixed it follows that B must also take a constant value , which lead to the conclusion that B is independent of the applied frequency.

Tomotika (8) developed a relationship for the growth rate(B) of the disturbance on the surface of the jet as ;

$$B = \frac{8\sigma}{D_j^3 \rho_d}\left[\frac{(1-k^2a^2)ka}{\frac{I_0(ka)}{I_1(ka)} + \frac{\rho_c}{\rho_d}\frac{K_0(ka)}{K_1(ka)}}\right] \qquad [R3]$$

Where ka is the wave number and can be related to the frequency as

$$ka = \frac{2\pi a}{\lambda} = \frac{2\pi f a}{U_n} \qquad [R4]$$

Where f is the frequency of the disturbance on the surface of the jet and U_n is the nozzle velocity. A number of workers (17,25) have used this equation to determine the value of growth rate(B) of the applied disturbance. Theoretically calculated B values

(using equation R3) for the condition employed in the present work are plotted against wave number , ka , in Figure 20,21 and for the range of experimental frequencies (200 Hz to 400 Hz) values are given in Table (8)

The plots in Figures (16,17,18,19) have already demonstrated that the growth rate (B) is constant (constant slope U_n/B), i.e applied vibration has no effect on the growth rate. In the light of this fact , Tomotika's equation can not be applied to generate 'B' values to be used in the prediction of the jet length.

4.2.3 PREDICTION OF THE JET LENGTH

The plots in figures (16,17,18,19) also show that the jet length is a function of the applied frequency , But Rayleigh's equation does not allow for this interaction. The growth rate (B) is constant and independent of the applied frequency , hence the effect of the interaction can only be contained in the value of ∂ .

It is clear from these plots (Figures 16,17,18,19) that the slope U_n/B is constant for a fixed frequency and the value of intercept varies with frequency. Thus equation R2 should be modified to allow for this behaviour. We can write equation R2 as ;

Figure 20

SYSTEM : WATER / KEROSENE
ORIFICE DIAMETER : 0.015 cm △
: 0.020 cm ✱
: 0.025 cm ▽

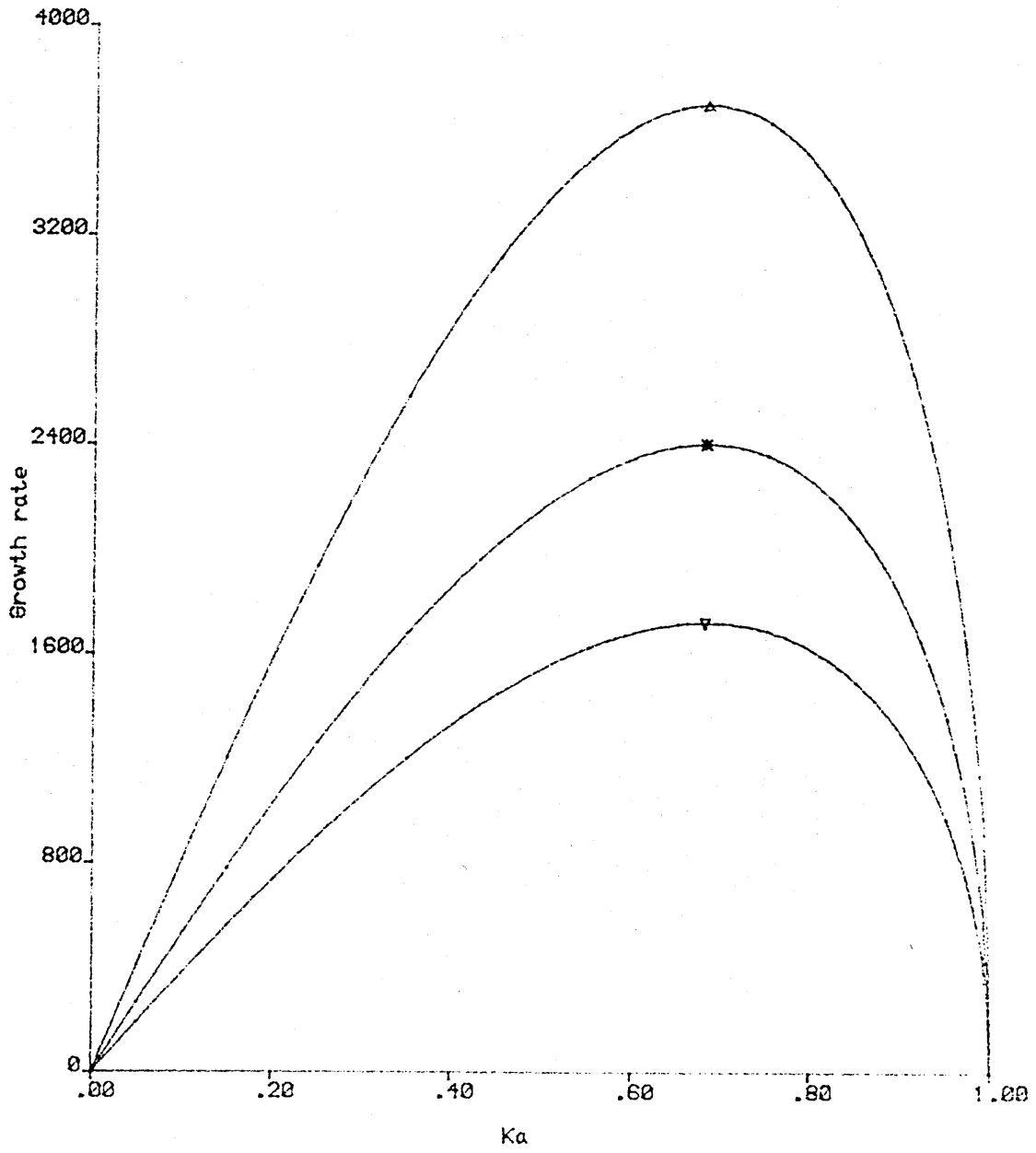

Figure 21

ORIFICE DIAMETER : 0.020 cm
SYSTEM : WATER / KEROSENE △
: WATER / 25P+75K ✱
: WATER / 50P+50K ▽
: WATER / 25P+75K □

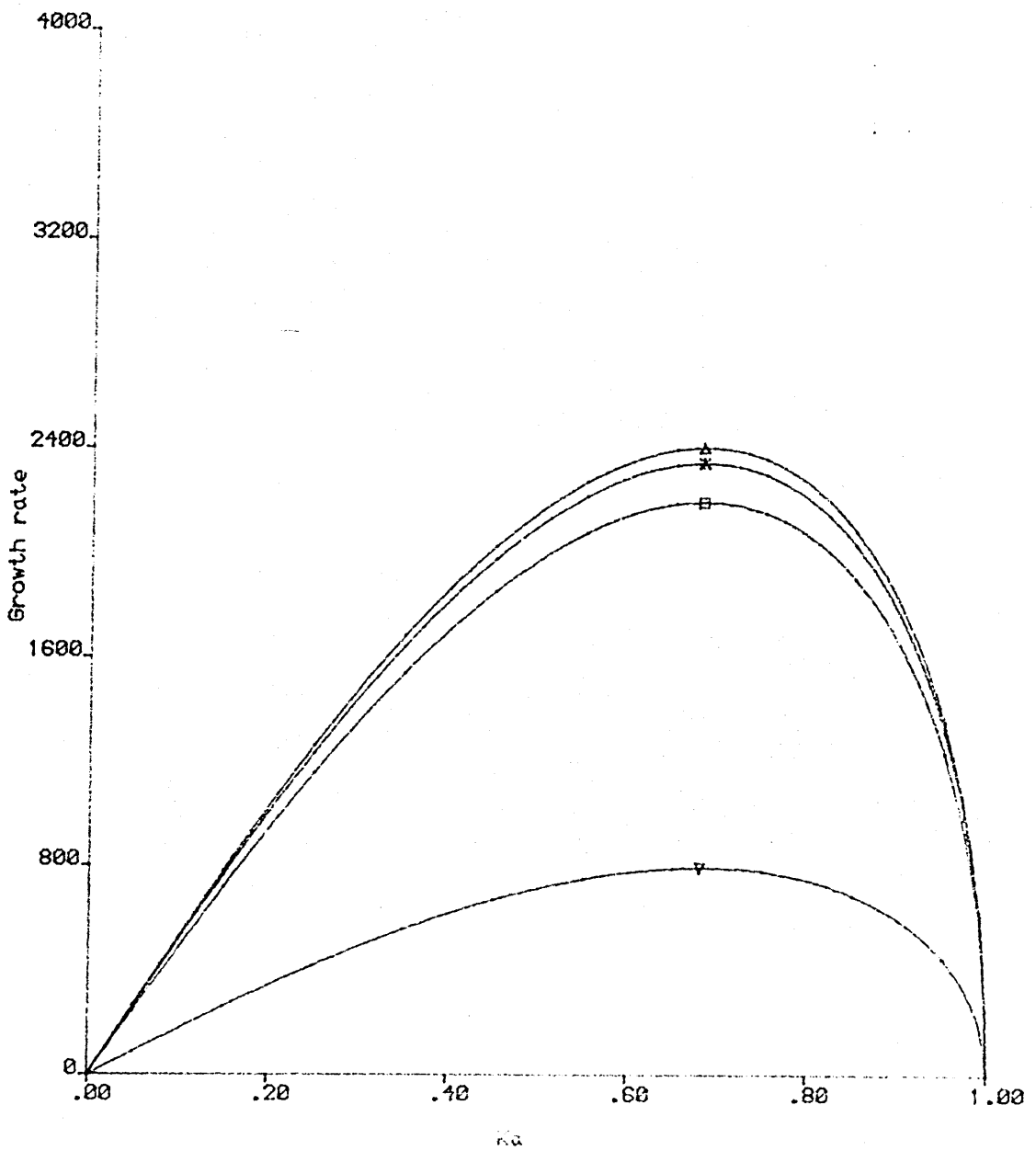

TABLE - 8

Variation of the growth rate with applied frequency.

Serial No.	Applied Frequency (Hz)	Wave Number (ka)	Growth rate (sec^{-1})
1.	200	0.048	265
2.	250	0.050	318
3.	300	0.072	370
4.	350	0.082	450
5.	400	0.096	500
6.	450	0.108	526

$$L = \frac{U_n}{B} \ln\frac{a_n}{\partial} + C \qquad [R5]$$

Where intercept ,C, is a function of applied frequency.

To take into account the effect of frequency on ∂ and develop a relationship to correlate the experimental data without generating a series of intercept values , for different frequencies , we can write ;

$$C = \frac{U_n}{B} \ln K \qquad [R6]$$

Therefore

$$L = \frac{U_n}{B} \ln\frac{a_n}{\partial} \pm \frac{U_n}{B} \ln K \qquad [R7]$$

or

$$L = \frac{U_n}{B}\left[\ln\frac{a_n K}{\partial}\right] \quad \text{or} \quad L = \frac{U_n}{B}\left[\ln\frac{a_n}{\partial K}\right] \qquad [R8]$$

Where K is a function of frequency which can be related interms of a polynomial function as

$$\frac{K}{\partial} \quad \text{or} \quad \frac{1}{\partial K} = \frac{1}{\partial(Pol)} \qquad [R9]$$

Where

$$Pol = A_1 + A_2 f + A_3 f^2$$

Where f is the frequency of the applied vibration. The final equation thus can be written as ;

$$L = \frac{U_n}{B} \ln \frac{a_n}{\partial(Pol)} \qquad [R10]$$

4.2.4 CORRELATION OF DATA

The value of the constants in equation R9 were determined by using a minimisation technique proposed by Nelder and Mead (39). They have generalised the simplex method described by Spendley et al (40) for minimisation of a function of n variables. The Nelder and Mead method accelerates the simplex method and makes it more general. It adapts itself to a local landscape , using reflected , expanded and contracted point to locate the minimum.

The minimisation is accomplished in the following steps

1. Start an initial simplex ($x_1, x_2, x_3, \ldots\ldots x_{n-1}$) by selecting

$x_{i+1} = x_i + a_i$

Where x_i is chosen arbitrarily a_i can be determined from the following table

i	$a_{1,i}$	$a_{2,i}$	$\ldots\ldots\ldots a_{n-1,i}$	$a_{n,i}$
2	P	Q	Q	Q
3	Q	P	Q	Q
n	Q	Q	P	Q
n+1	Q	Q	Q	P

Where n-is total number of variable

a-is the side length of the simplex

$$P = \frac{a}{n\sqrt{2}} [n+1] + n-1$$

$$Q = \frac{a}{n\sqrt{2}} [n+1] - 1$$

2. Once the simplex is formed , the objective function is evaluated at each point. The worst point (high value of objective function in minimisation) is replaced by a new point. To do this Nelder and Mead applied three basic operations to find a minimum as follows

a. REFLECTION STEP : Where x_H is replaced by replacing x_R as

$$x_R = x_P + \alpha (x_P - x_G)$$

Where is a positive constant ($\alpha > 0$) determining the amount of reflection.

b. EXPANSION STEP : Where x_R is expanded in the direction along which a better objective function value is expected by using the relation

$$x_E = x_P + \gamma(x_P + x_R)$$

Where γ is a positive expansion factor , greater than 1 , determining the amount of expansion.

c. CONTRACTION STEP : For contracting the simplex by computing

$$x_C = x_P + \beta (x_H - x_P)$$

Where $0 < \beta < 1$ so that this vertex does not correspond to the largest function value.

If the calculation expansion point is an improvement over the reflected point , the reflected point is replaced by expansion point and we start the process , otherwise reflection point is retained and we start the process.

3. The procedure is terminated when a stated convergence criterion is satisfied or a specified number of iterations is exceeded. The convergence criterion used in this method is

$$Con = \left[\sum_{i=1}^{n}(z_i - z_C)^2 - (z_H - z_i)^2/N\right]^{1/2}$$

Where z_i objective function

z_C the function value of the centroid

z_H the highest function value in simplex

To apply this method the objective function ,F, is defined as;

$F = WILL(I) - HALA(I)$

Where

$$WILL(I) = EXP\left[-\frac{L*B}{U_n}\right]$$

$$HALA(I) = -\frac{a_n}{\partial*Pol}$$

$$Pol = A_1 + A_2 f + A_3 f^2$$

Putting the guessed values of the constants the objective function F, is calculated for every experimental point.

The flow chart for the algorithim is given in Fig.22 and a listing of the computer program is given in appendix (A1)

The values of the constants of the equation R9 obtained by this optimisation technique were substituted to predict the jet length. The experimental and predicted results are given in Tables 9,10,11,12 and plots of jet length vs $\ln \frac{a_n}{\delta_{Pol}}$ are given in Figures 23,24,25,26

These results show a reasonably good agreement between the experimental and predicted results (Table 9,10,11,12). The maximum difference between the experimental and predicted jet lengths lies within the range of 0.8 mm. (Table 9,10,11,12).

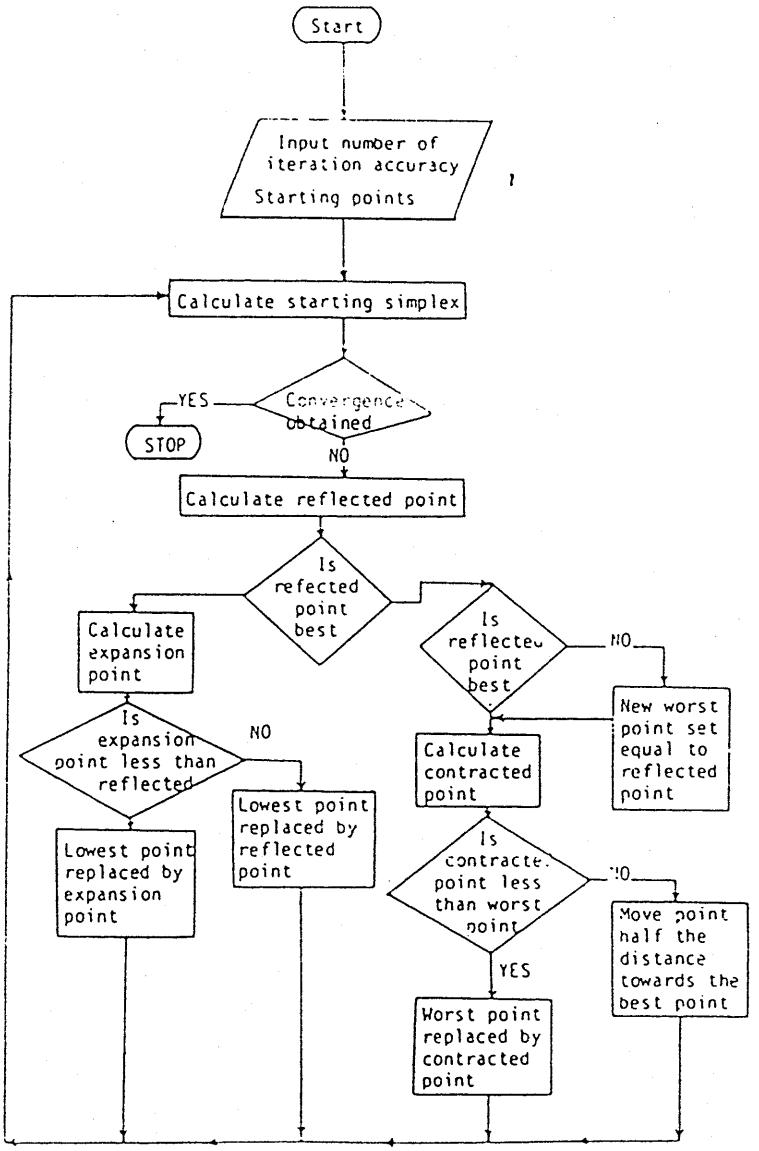

Figure 22 : Flow Sheet For Simplex Minimization.

Figure 23

SYSTEM - WATER / KEROSENE

Nozzle diameter - 0.020Cm

× EXPERIMENTAL
—— THEORETICAL

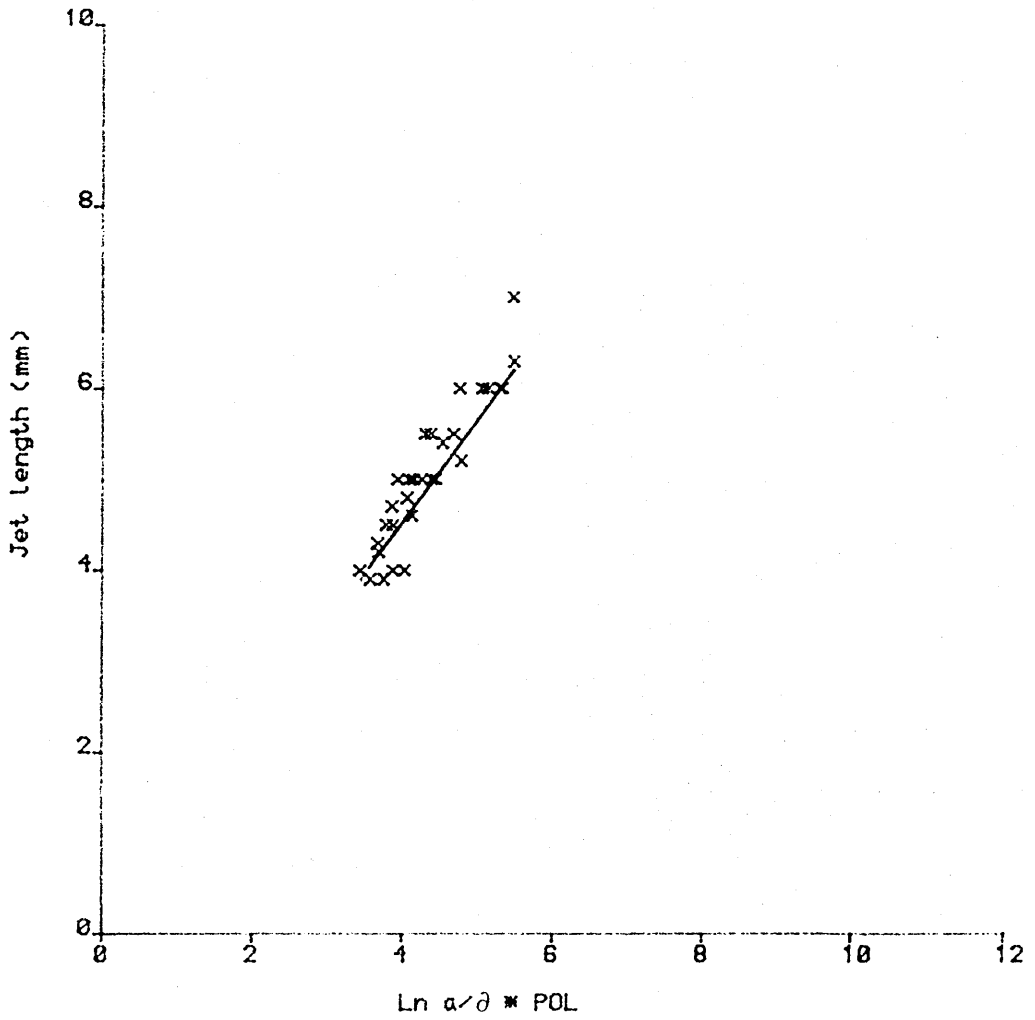

Figure 24

SYSTEM - WATER / 25P+75K

Nozzle diameter - 0.020 Cm

× EXPERIMENTAL
—— THEORETICAL

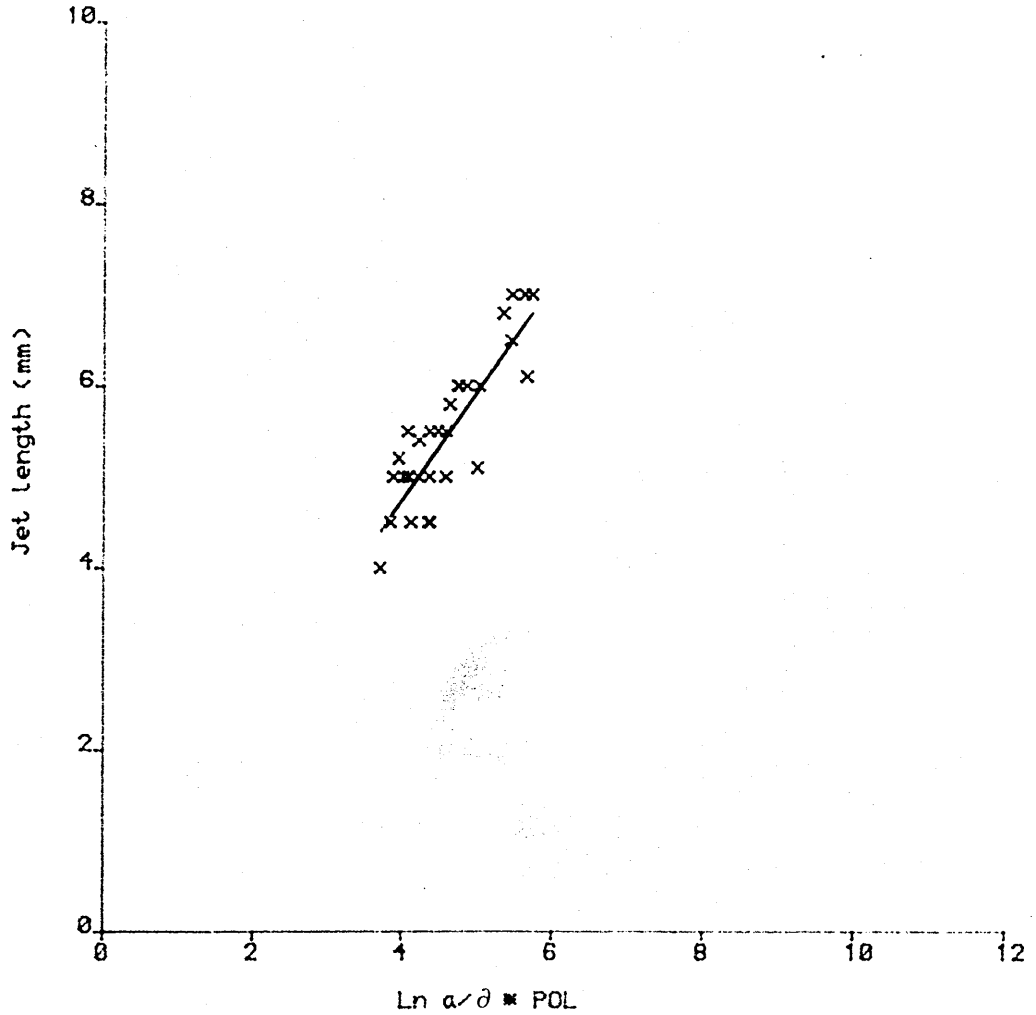

Figure 25

SYSTEM - WATER / 50P+50K

Nozzle diameter - 0.020 Cm

× EXPERIMENTAL

—— THEORETICAL

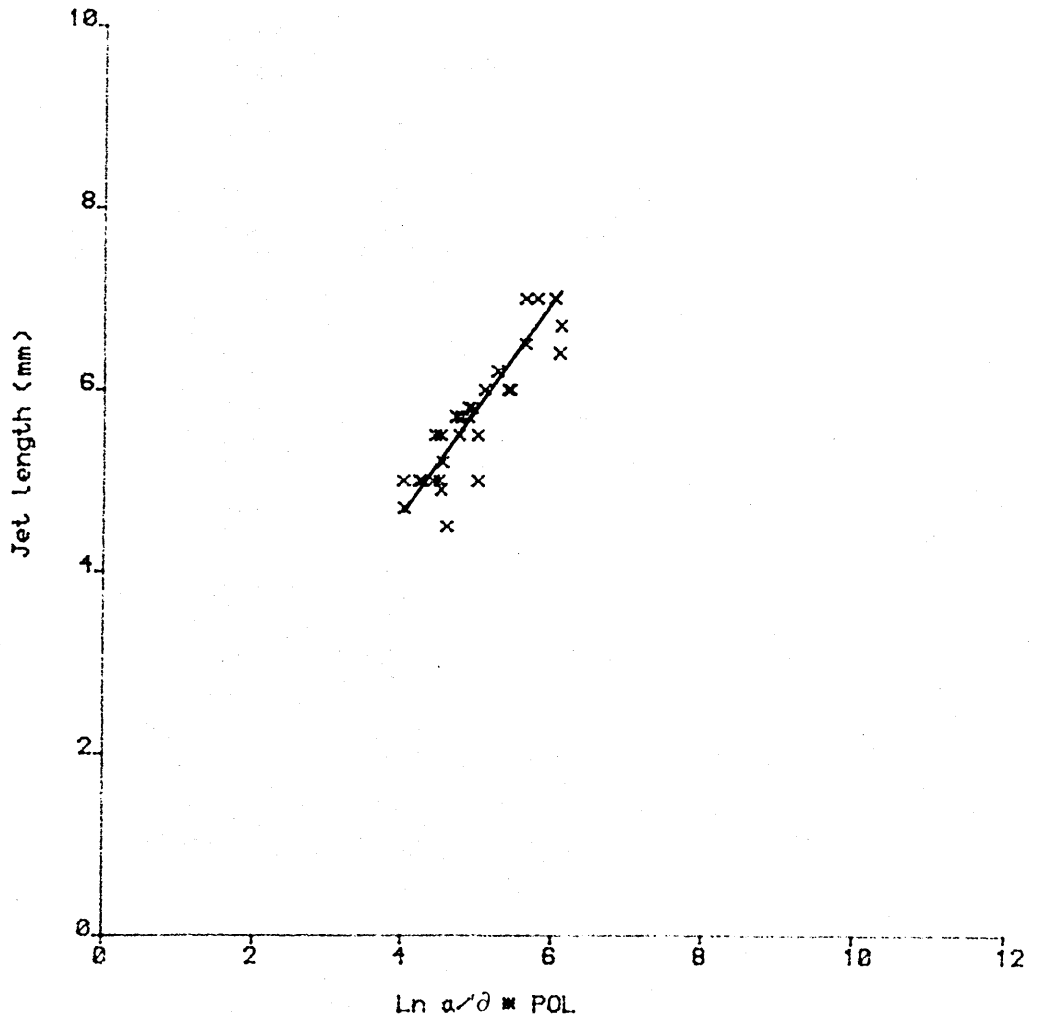

Figure 26

SYSTEM - WATER / 75P+25K

Nozzle diameter - 0.020 Cm

× EXPERIMENTAL

—— THEORETICAL

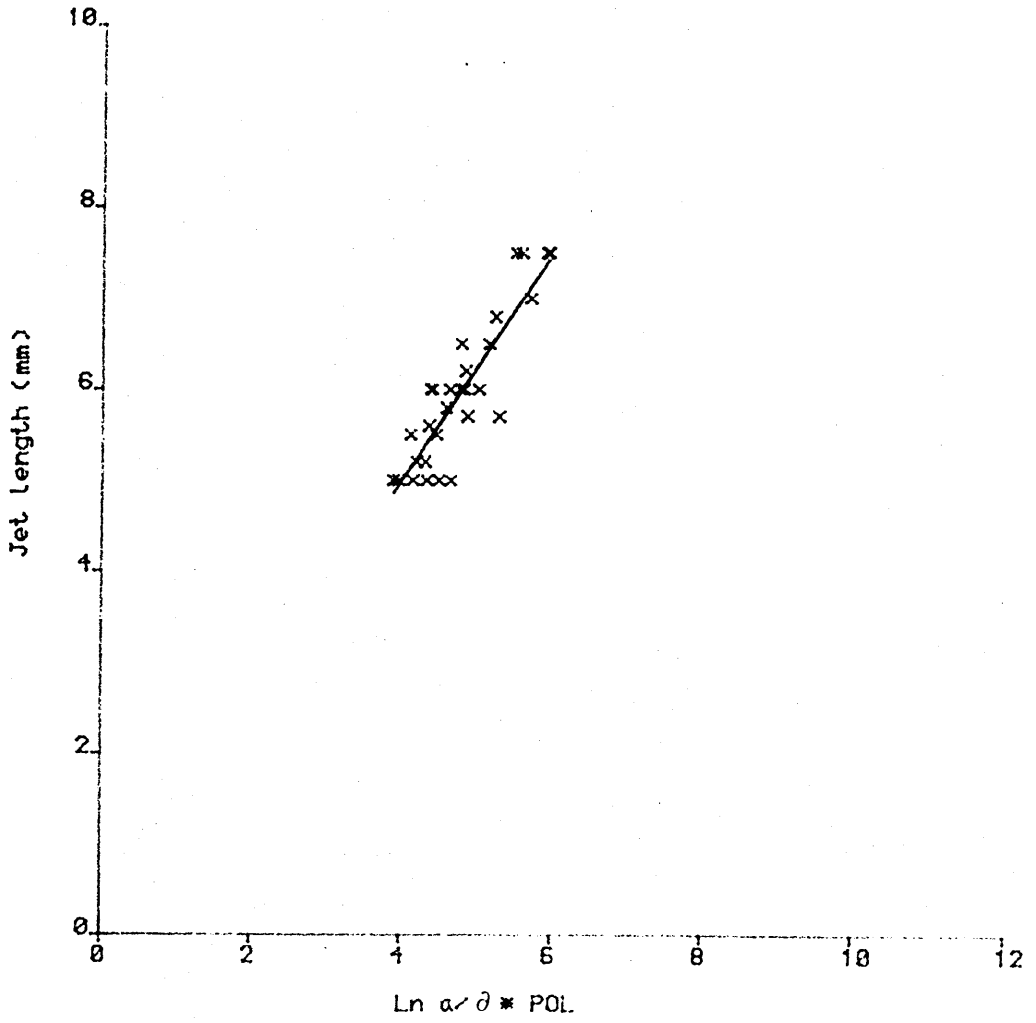

TABLE 9

ORIFICE DIAMETER : 0.020Cm

SYSTEM : WATER / KEROSENE

JET VELOCITY : 2610 mm/Sec

SEQUENCE NUMBER	EXPERIMENTAL JET LENGTH mm	THEORETICAL JET LENGTH mm
1	7.0000	6.1847
2	6.0000	5.3795
3	5.5000	4.9430
4	5.0000	4.6147
5	4.7000	4.3620
6	6.3000	6.1970
7	5.2000	5.4044
8	5.0000	4.9590
9	4.6000	4.6695
10	4.0000	4.3754
11	6.0000	6.0212
12	5.5000	5.2814
13	5.0000	4.8046
14	4.0000	4.5546
15	3.9000	4.2443
16	6.0000	5.9871
17	5.4000	5.1215
18	5.0000	4.6877
19	4.5000	4.3807
20	4.2000	4.1631
21	6.0000	5.8086
22	5.0000	5.0216
23	4.8000	4.5882
24	4.5000	4.2755
25	3.9000	4.0369
26	6.0000	5.7250
27	5.5000	4.8628
28	5.0000	4.4530
29	4.3000	4.1513
30	4.0000	3.8838

TABLE 10

ORIFICE DIAMETER : 0.020 Cm

SYSTEM : WATER / 25P+75K

JET VELOCITY : 2610 mm/Sec

SEQUENCE NUMBER	EXPERIMENTAL JET LENGTH mm	THEORETICAL JET LENGTH mm
1	7.0000	6.4740
2	6.0000	5.6285
3	5.0000	5.1701
4	5.5000	4.8253
5	4.5000	4.5600
6	7.0000	6.7886
7	6.0000	5.9562
8	5.8000	5.4885
9	4.5000	5.1844
10	4.5000	4.8757
11	6.1000	6.7044
12	5.1000	5.9275
13	5.0000	5.4268
14	4.5000	5.1643
15	5.0000	4.8385
16	7.0000	6.6705
17	6.0000	5.7616
18	5.5000	5.3060
19	5.0000	4.9836
20	5.0000	4.7551
21	6.5000	6.4545
22	6.0000	5.6281
23	5.5000	5.1729
24	5.0000	4.8446
25	5.0000	4.5940
26	6.8000	6.3327
27	5.5000	5.4273
28	5.4000	4.9970
29	5.2000	4.6802
30	4.0000	4.3992

TABLE 11

ORIFICE DIAMETER : 0.020 Cm

SYSTEM : WATER / 50P+50K

JET VELOCITY : 2610 mm/Sec

SEQUENCE NUMBER	EXPERIMENTAL JET LENGTH mm	THEORETICAL JET LENGTH mm
1	6.5000	6.5405
2	5.8000	5.7123
3	5.2000	5.2634
4	5.0000	4.9257
5	4.7000	4.6658
6	6.7000	7.0848
7	6.0000	6.2695
8	5.5000	5.8072
9	5.5000	5.5136
10	5.0000	5.2112
11	6.4000	7.0645
12	6.0000	6.3036
13	5.0000	5.8131
14	5.7000	5.5561
15	4.9000	5.2369
16	7.0000	6.9896
17	6.2000	6.1013
18	5.7000	5.6531
19	4.5000	5.3373
20	5.0000	5.1135
21	7.0000	6.7172
22	6.0000	5.9078
23	5.7000	5.4619
24	5.5000	5.1403
25	5.0000	4.8938
26	7.0000	6.5444
27	5.8000	5.6576
28	5.5000	5.2362
29	5.0000	4.9258
30	5.0000	4.6506

TABLE 12

ORIFICE DIAMETER : 0.020 Cm

SYSTEM : WATER / 75P+25K

JET VELOCITY : 2610 mm/Sec

SEQUENCE NUMBER	EXPERIMENTAL JET LENGTH mm	THEORETICAL JET LENGTH mm
1	7.5000	6.8672
2	6.5000	5.9766
3	6.0000	5.4938
4	5.5000	5.1307
5	5.0000	4.8513
6	7.5000	7.4172
7	6.8000	6.5405
8	6.2000	6.0479
9	5.8000	5.7276
10	5.0000	5.4025
11	7.5000	7.4251
12	5.7000	6.6069
13	5.7000	6.0795
14	5.0000	5.8031
15	6.0000	5.4599
16	7.5000	7.3904
17	6.5000	6.4352
18	6.0000	5.9533
19	5.0000	5.6137
20	5.2000	5.3731
21	7.0000	7.1326
22	6.0000	6.2622
23	6.0000	5.7828
24	5.6000	5.4370
25	5.0000	5.1720
26	7.5000	6.9705
27	6.0000	6.0169
28	5.5000	5.5637
29	5.2000	5.2300
30	5.0000	4.9341

4.3 JET BREAK-UP LENGTH AT LOW FLOWRATES

Most previous workers (16,17,18,23) employed relatively low velocities (Fig. 3, A - D) in their studies of disintegration of laminar liquid jets. In their analysis they assumed a fastest growing natural wave on the surface of the jet and calculated its growth rate using Tomotika's model. In practice it was found necessary to adjust the frequency by trial and error to achieve monosize droplets. This confimed the conclusion drawn in the previous section that Tomotika's analysis does not adequately cover the behaviour of the jet.

During the present investigation it was observed that by trial and error, it was easier to locate the frequency of the imposed vibration for the production of the monosize droplets in the region A - D than in the region D - F. These observations are consistent with the assumption made by previous workers(16,17) that one fastest natural disturbance is predominant in the disintegration of the jet in the region A - D. Their assumption makes the theoretical analysis easier and it should be possible to combine the effect of one natural and one imposed vibration on the jet. The resultant simplified model is expected to give a better representation of the behaviour of the jet.

The model developed previously for the region D - F employed a polynomial to take into account the effect of natural and applied disturbances on the jet. At low flowrates,this model will be

simplified to take into account this assumption that only one natural wave is predominant.

It was reported in the previous section that the jet length measurements were taken without considering the production of monosized droplets. The disintegration of the liquid jet in these experiments did not produce monosize droplets (it was producing mixed drops at 1 Node, 2 Node or 3 Node etc.) and the resultant drop diameter varied from 0.2 mm. (smallest drop) to 1.2 mm (largest drop) as shown in the plate (4). The Still photographic technique applied to determine the jet length was not sufficiently accurate to capture exact point of break-up on every occasion, and the jet length measurement varied with the resultant drop-size, as shown in plate 5. This introduced an error in the measured jet length equal to the difference in drop diameters. This agrees with the difference between the experimental and predicted values of the jet length in the previous section.

These observations lead to the conclusion that the jet length variation due to different sized resultant drops should be avoided; jet length measurement should only be taken where monosize drops are produced. At this stage of experimental work a video film technique was also available which helped to determine the exact point of break-up for the measurement of the jet length.

A nozzle of 0.61 mm diameter was used and a continuous phase (decane) of viscosity 1.25 cp was employed. Three different

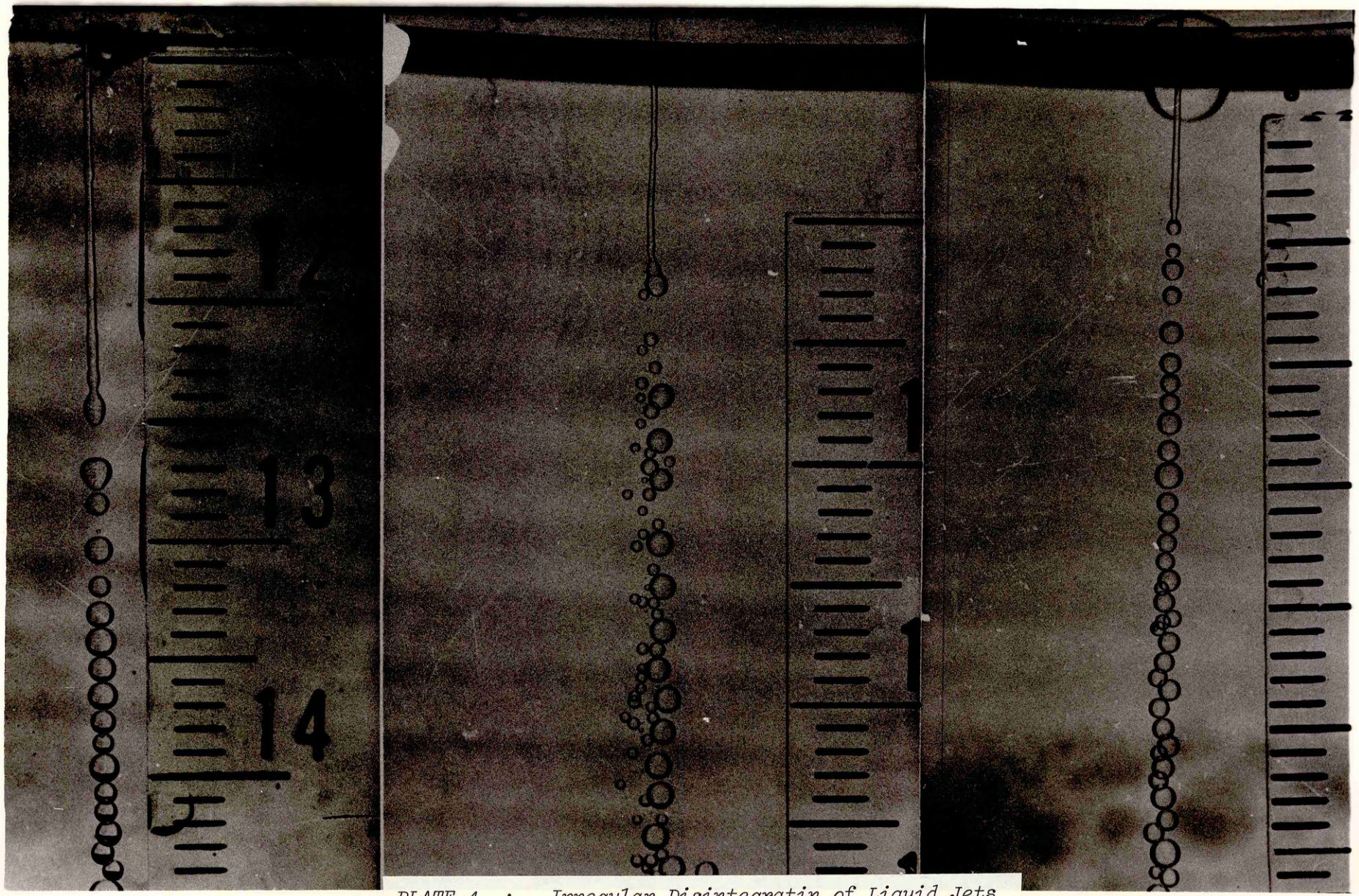

PLATE 4 : *Irregular Disintegratin of Liquid Jets In High Flow Rate Region.*
Nozzle Diameter - 0.20 mm
Nozzle Velocity - 2610 mm / sec.

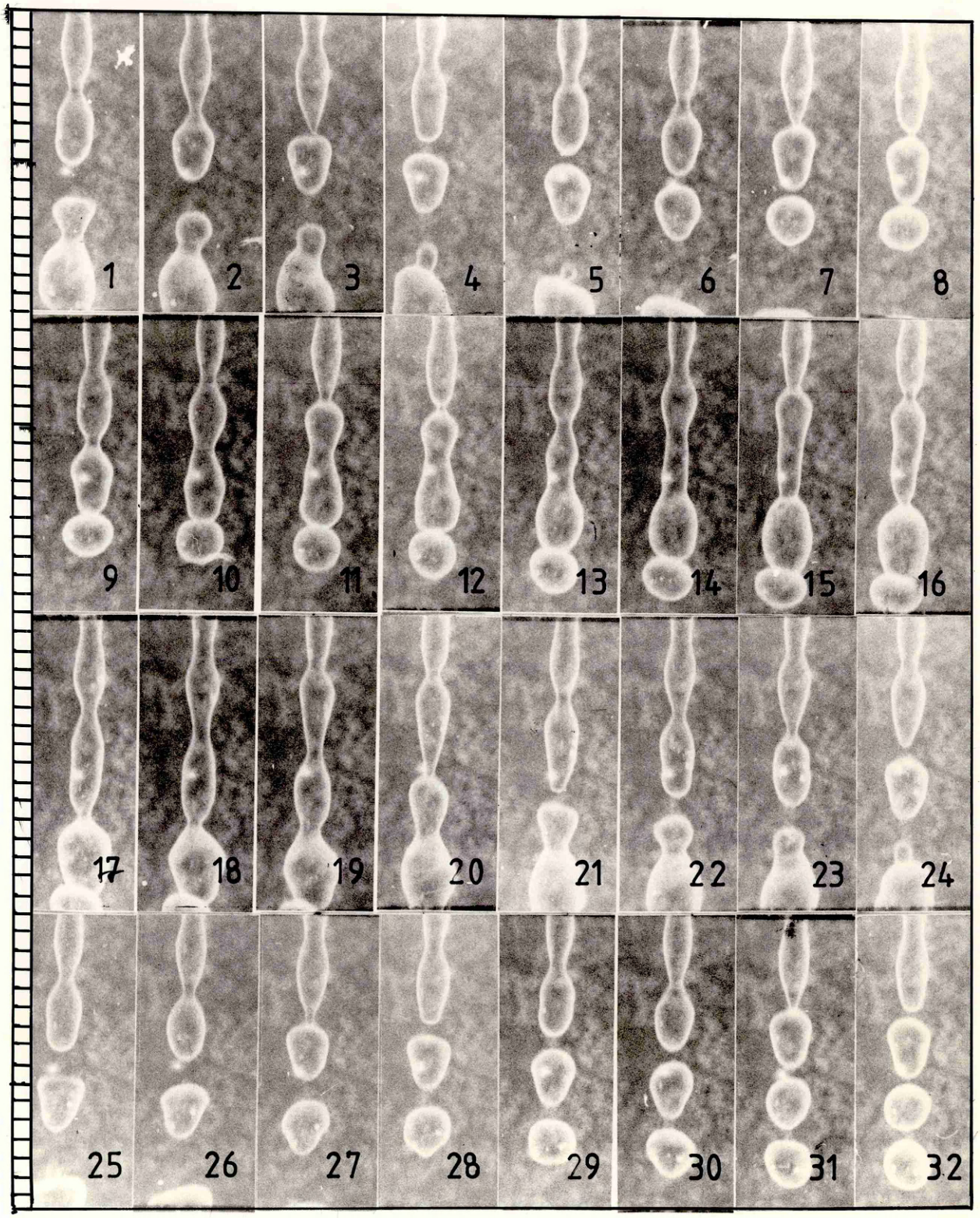

PLATE 5 : *High Speed Film Indicating Variations In The Jet Length Under Irregular Disintegration Process.*

Film Rate - *500 Frames / sec*
Nozzle Diameter - *0.61 mm*
System - *Water / Decane*

dispersed phase velocities (564,510 and 464 mm/sec) were studied. The frequency of vibration was varied between 200 to 350 Hz and the amplitude was adjusted to get monosize droplets. The experimental results are given in Tables 13,14,15 and plots of jet length vs amplitude are given in Figure 27,28,29

It can be seen from these figures that at a fixed flowrate there is a linear relationship between the jet break-up length and $\ln\frac{a_n}{\delta}$, the applied amplitude. The slope of the lines does not change with any change in the applied frequency. This confirmed the conclusion drawn in the previous section that the growth rate is independent of the frequency and amplitude of the applied vibration. The plots of data for jet break-up length in Fig.27,28,29 are parallel lines with different intercepts at different applied frequencies. This confirmed that although the jet break-up length is effected by the applied vibration, the growth rate is constant.

Rayleigh's equation relates the jet break-up length with growth rate (B) and amplitude (δ) as follows ;

$$L = \frac{U_n}{B}\ln\frac{a_n}{\delta} \qquad [R11]$$

As discussed in the previous section U_n and a_n in the above equation are constant and growth rate ,B, does not depend on the

Figure 27 : Plot of jet breakup length agaist applied amplitude.
Nozzle velocity - 562 mm /sec.
nozzle Diameter - 0.61 mm.
System - Water / Decane

o - 200 Hz.
◂ - 275 Hz.
+ - 300 Hz.
✱ - 350 Hz.

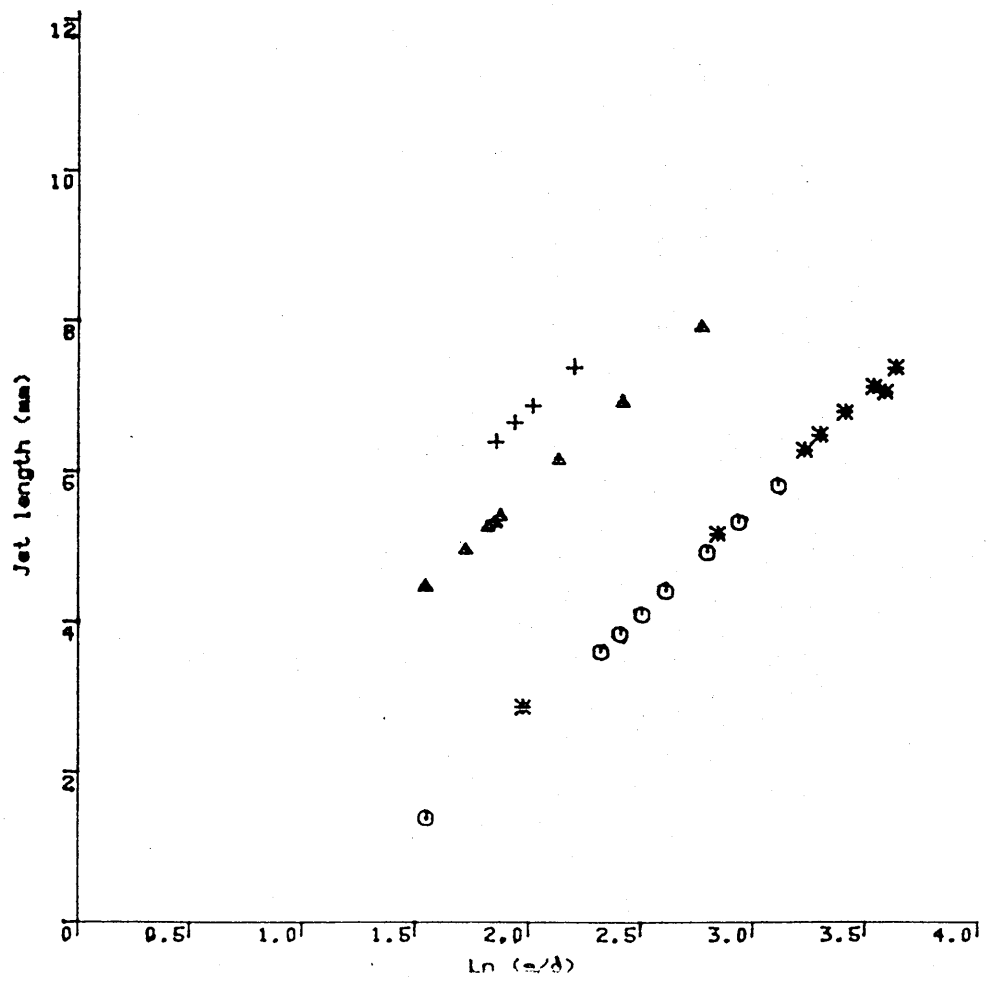

Figure 28 : Plot of jet breakup length against applied amplitude.
Nozzle velocity - 510 mm /sec.
Nozzle diameter - 0.61 mm.
System - Water /Decane

o - 200 Hz.
◂ - 275 Hz.
+ - 300 Hz.
✱ - 350 Hz.

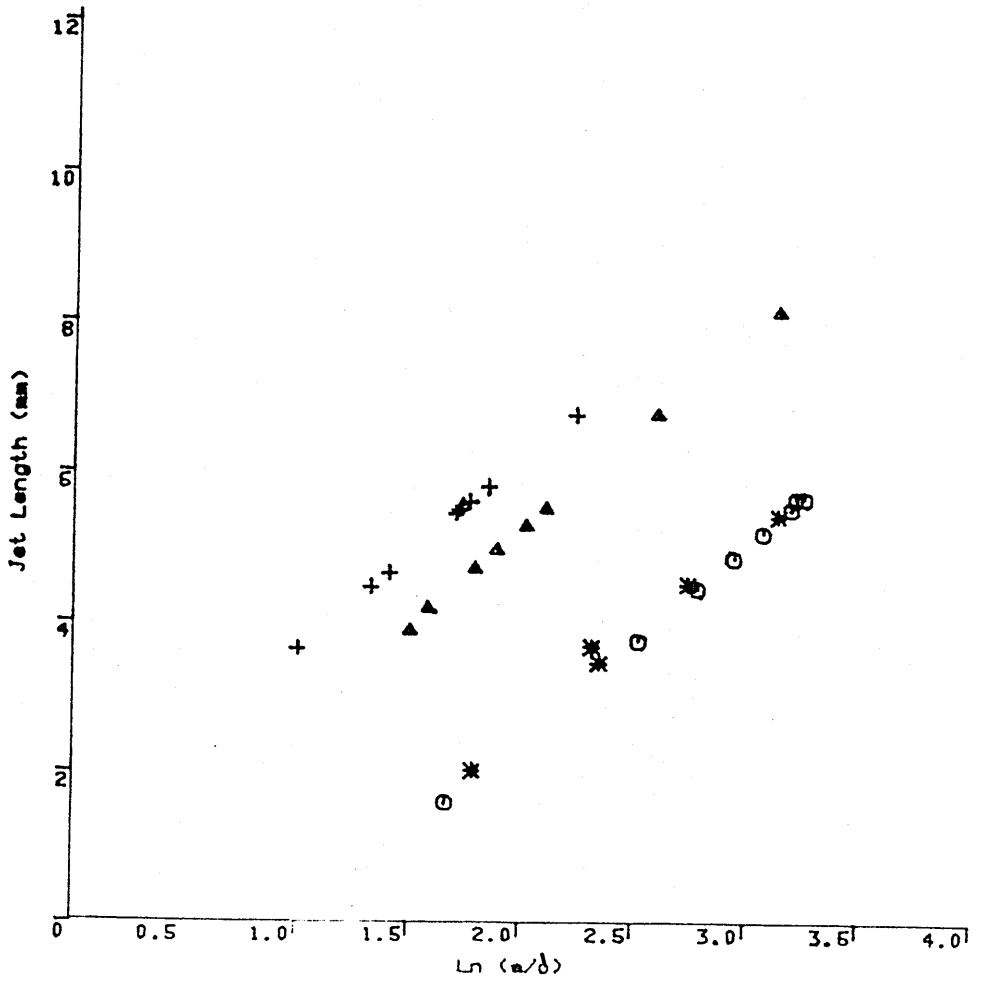

Figure 29 : Plot of jet breakup length against applied amplitude.
Nozzle velocity - 464 mm /sec.
Nozzle diameter - 0.61 mm.
System - Water /Decane

o - 200 Hz.
◂ - 275 Hz.
+ - 300 Hz.
* - 350 Hz.

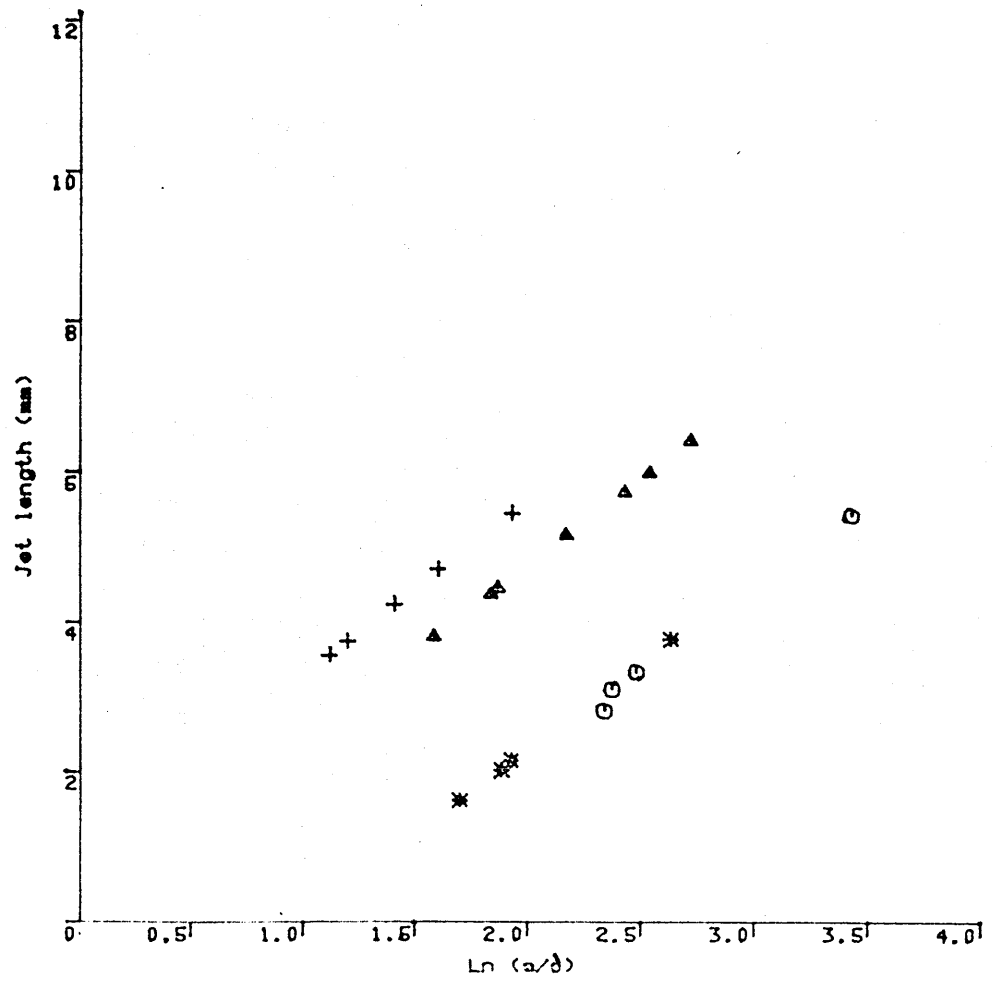

TABLE 13

Experimental Data On Jet Break-up Length Under The Influence Of Externally Applied Vibration

Jet velocity - 564 mm/sec.
Nozzle diameter - 0.61 mm.
System - Water/Decane

Serial No	Applied Frequency (Hz)	Applied Amplitude (mm)	Experimental Jetlength (mm)
1.	200	0.0137	5.80
2.	200	0.0163	5.50
3.	200	0.0188	4.70
4.	200	0.0226	4.20
5.	200	0.0251	4.00
6.	200	0.0276	3.80
7.	200	0.0301	3.50
8.	200	0.0650	1.50
9.	275	0.0194	7.90
10.	275	0.0275	7.10
11.	275	0.0364	6.50
12.	275	0.0471	5.50
13.	275	0.0484	5.10
14.	275	0.0498	5.00
15.	275	0.0549	4.50
16.	275	0.0655	4.10
17.	300	0.0340	7.50
18.	300	0.0409	7.00
19.	300	0.0443	6.50
20.	300	0.0481	6.30
21.	350	0.0082	7.20
22.	350	0.0086	7.00
23.	350	0.0090	7.40
24.	350	0.0102	6.80
25.	350	0.0114	6.50
26.	350	0.0122	6.00
27.	350	0.0179	4.80
28.	350	0.0424	2.50

TABLE 14

Experimental Data On Jet Break-up Length Under The Influence Of Externally Applied Vibration

Jet velocity - 510 mm/sec.
Nozzle diameter - 0.61 mm.
System - Water/decane

Serial No.	Applied Frequency (Hz)	Applied Amplitude (mm)	Experimental Jetlength (mm)
1.	200	0.0119	5.80
2.	200	0.0124	5.50
3.	200	0.0126	5.50
4.	200	0.0143	5.20
5.	200	0.0162	4.60
6.	200	0.0191	4.30
7.	200	0.0247	3.65
8.	200	0.0576	1.80
9.	275	0.0135	8.20
10.	275	0.0230	7.00
11.	275	0.0374	5.80
12.	275	0.0408	5.50
13.	275	0.0464	5.20
14.	275	0.0510	5.10
15.	275	0.0541	4.50
16.	275	0.0623	4.00
17.	275	0.0680	3.75
18.	300	0.0330	7.00
19.	300	0.0483	5.30
20.	300	0.0525	5.70
21.	300	0.0552	5.50
22.	300	0.0556	5.10
23.	300	0.0751	4.90
24.	300	0.0815	4.70
25.	300	0.1128	3.60
26.	350	0.0134	5.60
27.	350	0.0199	4.60
28.	350	0.0293	3.60
29.	350	0.0302	3.40
30.	350	0.0511	2.00

TABLE 15

Experimental Data On Jet Break-up Length Under The Influence Of Externally Applied Vibration

Jet velocity - 464 mm/sec.
Nozzle diameter - 0.61 mm.
System - Water/Decane

Serial No.	Applied Frequency (Hz)	Applied Amplitude (mm)	Experimental Jetlength (mm)
1.	200	0.0100	5.60
2.	200	0.0257	3.30
3.	200	0.0286	2.90
4.	200	0.0295	2.60
5.	275	0.0203	6.50
6.	275	0.0243	6.30
7.	275	0.0272	5.20
8.	275	0.0351	4.80
9.	275	0.0473	4.50
10.	275	0.0489	4.20
11.	275	0.0628	3.70
12.	300	0.0446	5.50
13.	300	0.0618	4.70
14.	300	0.0750	4.30
15.	300	0.0924	4.00
16.	300	0.1002	3.50
17.	350	0.0221	4.00
18.	350	0.0445	2.30
19.	350	0.0464	2.00
20.	350	0.0558	1.50

applied vibrations. This suggests that the amplitude ,∂, in the above equation is the only quantity which could be effected by the externally applied vibrations.

When two or more waves travel in the same direction then the combined effect of these waves results in a composite wave. Depending on the frequency of the original wave , the amplitude of the resultant wave will vary from the difference of their amplitude (interference) to the sum of their amplitude(resonance). According to Rayleigh when the amplitude of a wave on a liquid jet becomes equal to or greater than the radius of the jet, the jet breaks-up into drops. Under the influence of the applied and natural waves the value of the actual amplitude ,Ac, (amplitude of the composite wave) reaches the value of the jet radius, the jet breaks-up. Therefore it is desirable to determine the actual amplitude ,Ac, of the composite wave and to modify Rayleigh's equation to take into account the effect of wave interaction as ;

$$L = \frac{U_n}{B} - \ln \frac{a_n}{Ac} \qquad [R12]$$

Where Ac, is actual amplitude of the composite wave at the nozzle exit and is a function of the amplitude and the frequency of the applied vibration.

Experimentally actual amplitude ,Ac, is measured by a video film technique (as described in Chapter 3),for different frequencies

at constant applied amplitude. Theoretically the ratio of the measured amplitude,Am, and applied amplitude,δ, should be unity under non interacting conditions. Experimental results of measured amplitude from video film and applied amplitude for different frequencies are given in Table 16 and plot of Am/δ vs frequecy is given in Fig 30.

4.3.1 RESONANCE CORRECTION FACTOR

It is apparent from figure 20 that the ratio of measured amplitude and applied amplitude (Am/δ = Rf) is different for different frequencies. For example at 200 Hz frequency the value of Rf is 2.7 while at 300 Hz the value is only 0.66, Table.16 The value of frequency and amplitude of the natural wave are not known. The value of Rf indicates the interaction of the two waves at a particular point and shows that at 200 Hz frequency resonance is occuring and the amplitude of the composite wave is 2.7 times the applied amplitude ; at 300 Hz frequency interference is occuring and the amplitude of the composite wave is 0.66 times the applied amplitude. This is consistent with the experimental results for the jet break-up length table (13,14,15), which shows that with the applied vibration at 200 Hz frequency the jet length is shorter than at 300 Hz frequency. This is a result of the amplitude of the composite wave reaching the value equal to or greater than

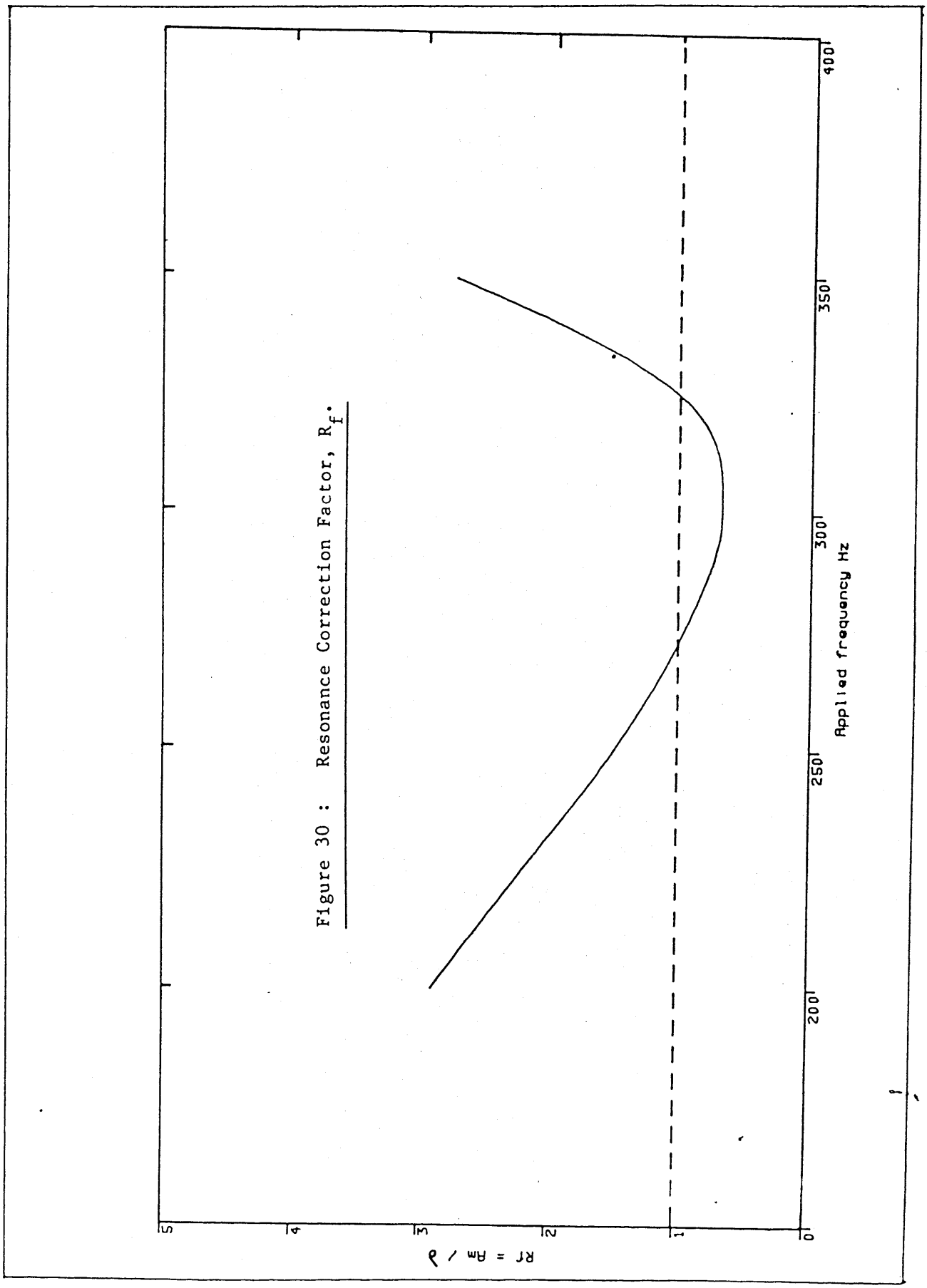

Figure 30 : Resonance Correction Factor, R_f.

TABLE 16

Experimental Data For Resonance Correction Factor
At Different Applied Frequencies.

S.No	Applied Frequency (Hz)	Applied Amplitude δ (mm)	Measured Amplitude Am (mm)	Ratio $\frac{Am}{\delta}$
1.	200	0.018	0.05230	2.906
2.	275	0.012	0.01156	0.964
3.	300	0.150	0.10222	0.681
4.	350	0.015	0.04147	2.758

the jet radius in a shorter time when 200 Hz frequency is applied than in the case of 300 Hz frequency.

The graph in Figure 30 can be used to determine the value of actual amplitude (Ac) of the composite wave at any frequency. Referring to Rayleigh's equation

$$L = -\frac{U_n}{B} \ln \frac{a_n}{Ac} \qquad [R13]$$

Therefore Ac from Figure 30 will be equal to $\delta.Rf$ and equation R13 can be written as ;

$$L = -\frac{U_n}{B} \ln \frac{a_n}{\delta\, Rf} \qquad [R14]$$

This equation indicates that a plot of jet length vs $\ln -\frac{a_n}{\delta\, Rf}$ should give a straight line relationship. The family of curves obtained at various frequencies (shown in Figures 27,28,29) should yield one straight line. The results from Tables 13,14,15 are ploted in figure 31,32,33 (Tables 17,18,19) and show the expected configuration (i.e straight line).

Figure 31 : Plot of predicted jet breakup length
Nozzle velocity - 562 mm / sec
Nozzle diameter - 0.61 mm.
System - Water /Decane

— - predicted jet length.
o - 200 Hz.
◂ - 275 Hz.
+ - 300 Hz.
* - 350 Hz.

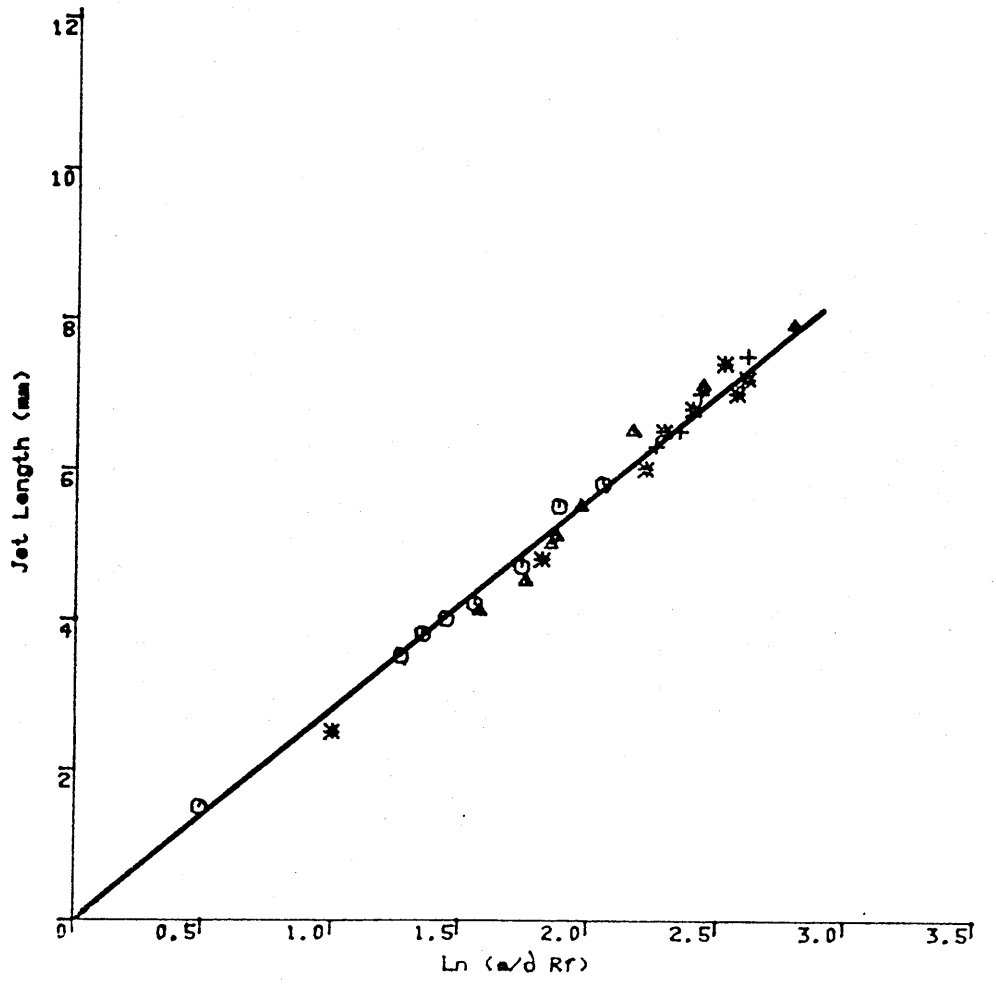

Figure 32 : Plot of predicted jet breakup length.
Nozzle velocity - 510 mm /sec.
Nozzle diameter - 0.61 mm.
System - Water / Decane.

— - Predicted jet length.
o - 200 Hz.
◂ - 275 Hz.
\+ - 300 Hz.
* - 350 Hz.

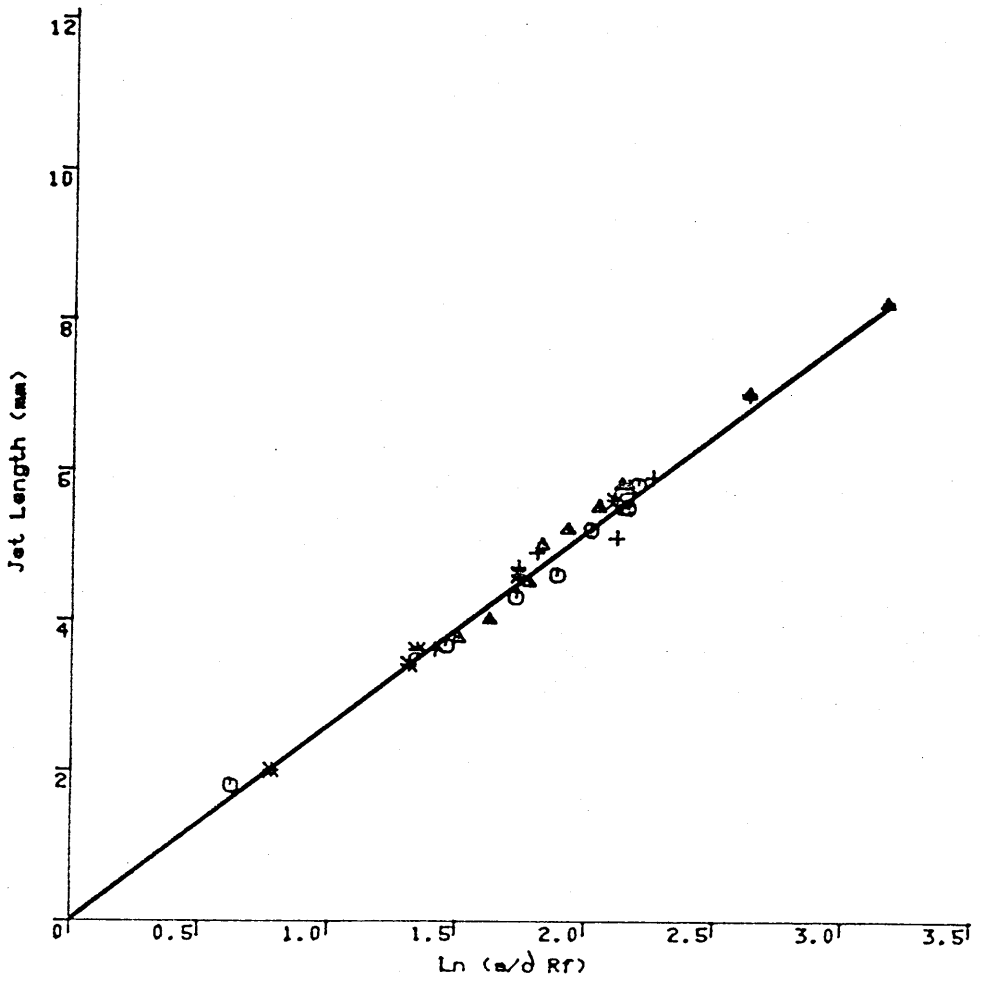

Figure 33 : Plot of predicted jet breakup length.
Nozzle velocity - 464 mm /sec.
Nozzle diameter - 0.61 mm.
System - Water / Decane

— - Predicted jet length
o - 200 Hz.
◂ - 275 Hz.
+ - 300 Hz.
✱ - 350 Hz.

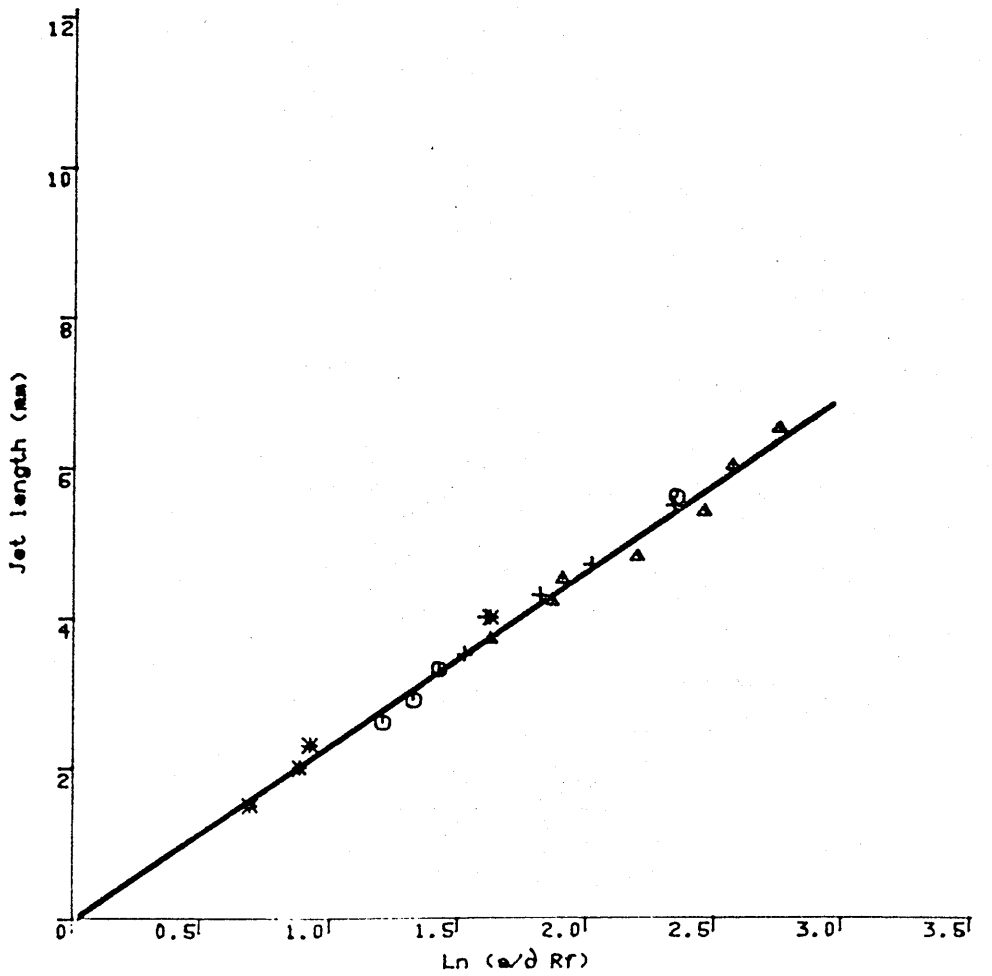

TABLE 17

Experimetal And Predicted Jet Break-up length In Low Flowrate Region

Jet velocity - 562 mm/sec.
Nozzle diameter - 0.61 mm.
System - Water/Decane

Serial No.	Applied Frequency (Hz)	Actual Amplitude (mm)	Experimental Jetlength (mm)	Predicted Jetlength (mm)
1.	200	0.0039	5.80	5.80
2.	200	0.0468	5.50	5.31
3.	200	0.0539	4.70	4.91
4.	200	0.0647	4.20	4.39
5.	200	0.0719	4.00	4.08
6.	200	0.0791	3.80	3.82
7.	200	0.0861	3.50	3.58
8.	200	0.1870	1.50	1.38
9.	275	0.0188	7.90	7.89
10.	275	0.0266	7.10	6.89
11.	275	0.0351	6.50	6.13
12.	275	0.0455	5.50	5.39
13.	275	0.0467	5.10	5.30
14.	275	0.0481	5.00	5.24
15.	275	0.0530	4.50	4.94
16.	275	0.0632	4.10	4.45
17.	300	0.0225	7.50	7.37
18.	300	0.0271	7.00	6.86
19.	300	0.0293	6.50	6.64
20.	300	0.0319	6.30	6.38
21.	350	0.0223	7.20	7.37
22.	350	0.0234	7.00	7.09
23.	350	0.0246	7.40	7.12
24.	350	0.0279	6.80	6.78
25.	350	0.0312	6.50	6.47
26.	350	0.0333	6.00	6.27
27.	350	0.0490	4.80	5.16
28.	350	0.1160	2.50	2.83

TABLE 18

Experimetal And Predicted Jet Break-up length In Low Flowrate Region

Jet velocity - 510 mm/sec.
Nozzle diameter - 0.61 mm.
System - Water/Decane

Serial No.	Applied Frequency (Hz)	Actual Amplitude (mm)	Experimental Jetlength (mm)	Predicted jetlength (mm)
1.	200	0.0341	5.80	5.64
2.	200	0.0354	5.50	5.53
3.	200	0.0361	5.50	5.49
4.	200	0.0372	5.20	5.17
5.	200	0.0464	4.60	4.84
6.	200	0.0545	4.30	4.43
7.	200	0.0706	3.65	3.73
8	200	0.1647	1.80	1.58
9.	275	0.0131	8.20	8.10
10.	275	0.0222	7.00	6.74
11.	275	0.0361	5.80	5.49
12.	275	0.0303	5.50	5.25
13.	275	0.0447	5.20	4.94
14.	275	0.0492	5.00	4.69
15.	275	0.0522	4.50	4.54
16.	275	0.0606	4.00	4.16
17.	275	0.0656	3.75	3.86
18.	300	0.0220	7.00	6.74
19.	300	0.0319	5.90	5.79
20.	300	0.0347	5.70	5.59
21.	300	0.0363	5.50	5.48
22.	300	0.0368	5.10	5.43
23.	300	0.0496	4.90	4.64
24.	300	0.0538	4.70	4.45
25.	300	0.0745	3.60	3.63
26.	350	0.0365	5.60	5.40
27.	350	0.0543	4.60	4.44
28.	350	0.0801	3.60	3.44
29.	350	0.0825	3.40	3.36
30.	350	0.1395	2.00	2.01

TABLE 19

Experimetal And Predicted Jet Break-up length In Low Flowrate Region

Jet velocity - 464 mm/sec.
Nozzle diameter - 0.61 mm.
System - Water/Decane

Serial No.	Applied Frequency (Hz)	Actual Amplitude (mm)	Experimental Jetlength (mm)	Predicted Jetlength (mm)
1.	200	0.0286	5.60	5.40
2.	200	0.0737	3.30	3.31
3.	200	0.0818	2.90	3.08
4.	200	0.0844	2.60	2.80
5.	275	0.0196	6.50	6.39
6.	275	0.0235	6.00	5.97
7.	275	0.0262	5.40	5.71
8.	275	0.0338	4.80	5.13
9.	275	0.0456	4.50	4.43
10.	275	0.0472	4.20	4.34
11.	275	0.0606	3.70	3.78
12.	300	0.0295	5.50	5.43
13.	300	0.0408	4.70	4.69
14.	300	0.0495	4.30	4.22
15.	300	0.0610	4.00	3.73
16.	300	0.0662	3.50	3.54
17.	350	0.0606	4.00	3.75
18.	350	0.1215	2.30	2.14
19.	350	0.1269	2.00	2.04
20.	350	0.1524	1.50	1.61

4.3.2 EFFECT OF FREQUENCY ON DROP SIZE

Disintegration of laminar liquid jet under the influence of the applied vibration for the production of monosize droplets showed a considerable change in drop diameter at various frequencies. The experimental results for the nozzle of 0.61 mm diameter in the continuous phase of viscosity 1.25 cp, are given in Table 20 The velocity of the dispersed phase was kept constant(564 mm/sec). As the frequency of the applied vibration was varied from 200 to 300 Hz drop diameter changes. This is quite consistent with the work of most previous workers(33,35) who have suggested that number of drops are equal to the applied frequency. As the flow rate of the dispersed phase was kept cosntant therefore it is obvious that with the increase of number of drops per unit time , the size of drop will decrease, as shown in plate 6.

4.3.3 EFFECT OF AMPLITUDE ON DROP DIAMETER

In the disintegration of a laminar liquid jet with applied vibration it was found that there is a lower critical value of applied amplitude after which monosized drops are produced in a single stream . When value of applied amplitude was increased it was found that there is an upper critical limit above which the jet breaks-up into two streams of monosize droplets and both of these streams increasingly diverge with any increase in the applied amplitude as shown in plate 7.

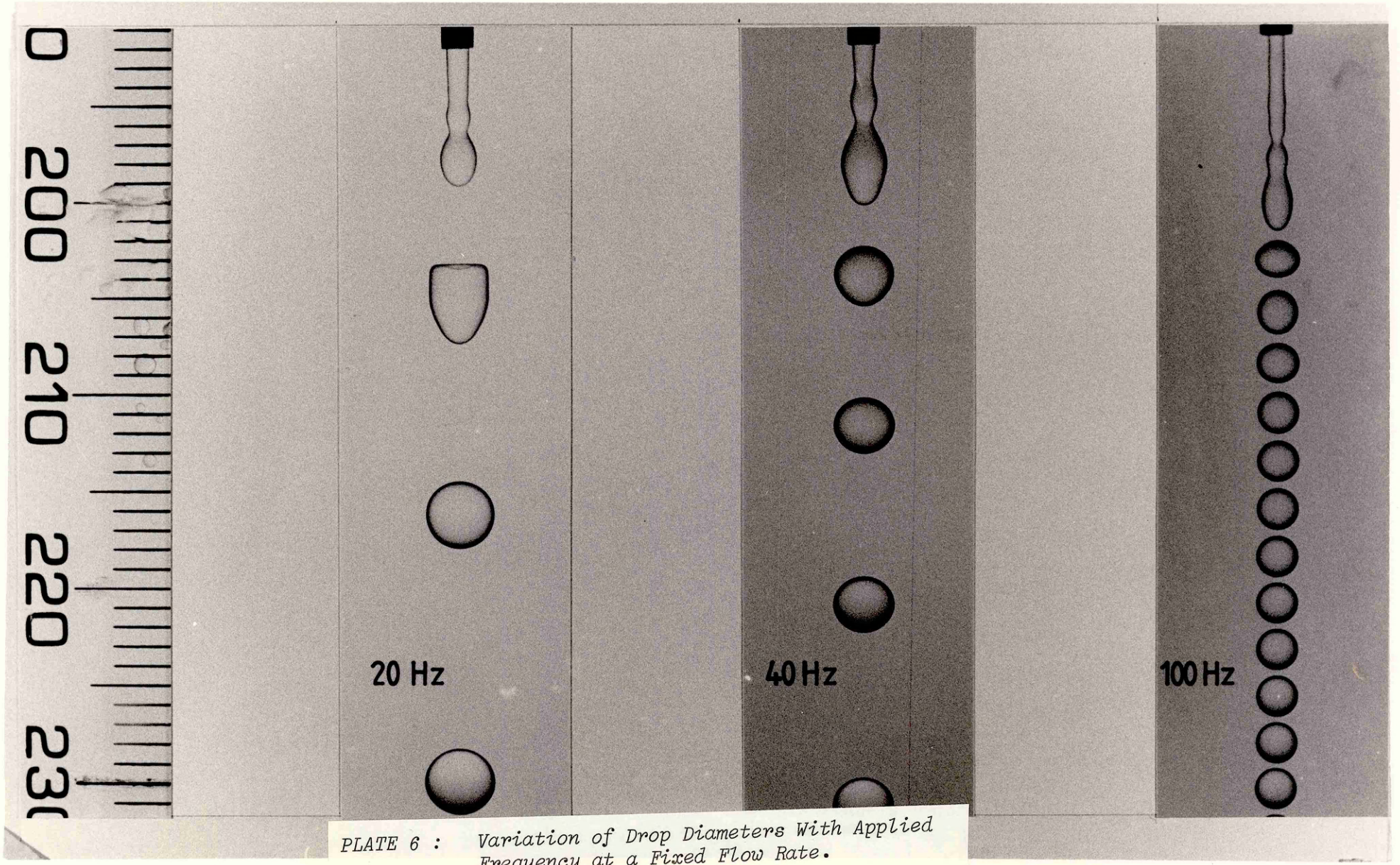

PLATE 6 : *Variation of Drop Diameters With Applied Frequency at a Fixed Flow Rate.*

Nozzle Diameter - *0.61 mm*
Flow rate - *0.50 cc / sec.*
Sustem - *Water / Decane*

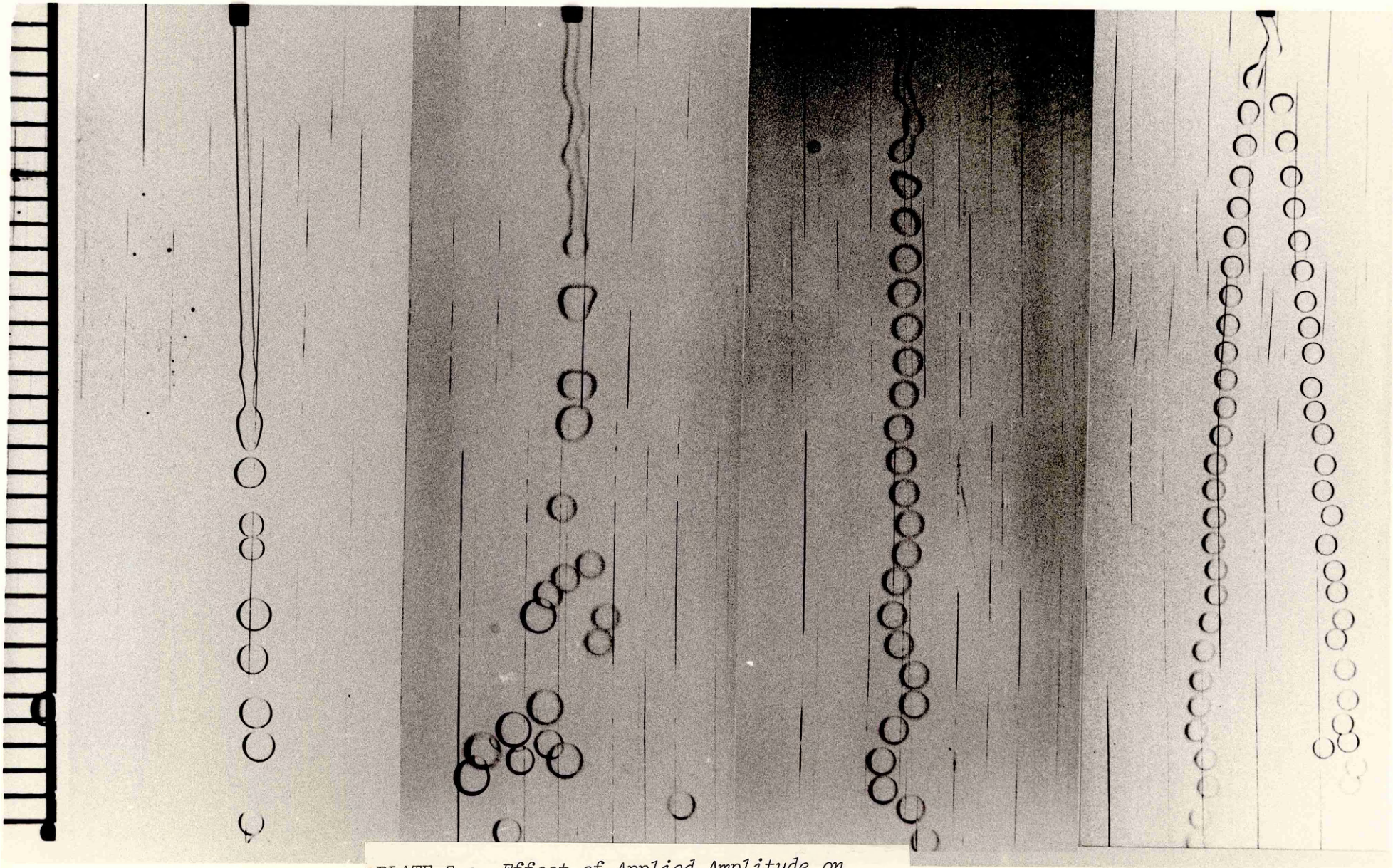

PLATE 7 : *Effect of Applied Amplitude on Liquid Jet Break-up Length.*
Nozzle dia - 0.61 mm
System - Water / Decane

TABLE - 20

Variation of the drop size with externally applied frequency.

Flow rate - 0.5 cm^3/sec.
Nozzle diameter - 0.61 mm.
System - Water / Decane

Serial No.	Applied frequency (Hz)	Drop formation time (sec)	Drop frequency No. of drops / sec.	Drop diameter (cm)
1.	20	0.476	20.97	0.3571
2.	40	0.0244	40.95	0.2857
3.	100	0.1029	97.18	0.2141

5.0 CONCLUSIONS AND RECOMMENDATIONS FOR FUTURE WORK

5.1 CONCLUSIONS

1. In the disintegration of laminar liquid jets under the influence of an applied vibration, the growth rate of the composite wave is independent of the frequency of the applied vibration.

2. Rayleigh's equation can be modified to predict the jet break-up length, if frequency and the amplitude of the applied vibration are known.

3. At low flow rates one natural wave is predominant in the disintegration of a laminar liquid jet.

4. At a constant flow rate the number of monosize drops are equal to the frequency of the applied vibration and the size of the drops changes with any change in the applied frequency.

5.2 RECOMMENDATIONS FOR FUTURE WORK

1. Disintegration of laminar liquid jets for the production of the monosize droplets should be applied in an investigation of mass and heat transfer characteristics in liquid-liquid contactors.

2. For a commercial application the mutual interaction of more than one jet should be investigated.

3. Deflection of electrically charged drops should be investigated to separate a single drop from a main stream after regular intervals. This technique should be applied to study heat and mass transfer of a single drop.

LECTURES, COURSES AND SYMPOSIA ATTENDED

1. M.Sc Module on 'Liquid-Liquid Equilibria'
   By Dr. D W Pritchard
   Department of Chemical Engineering
   Teesside Polytechnic
   22 February to 31 March 1982.

2. Computer,Chemical Engineering and Fluid Separation Proceses
   Annual General Meeting
   Institution of Chemical Engineers
   5 to 7 April 1982

3. M.Sc Module on 'Liquid-Liquid Extraction'
   By Dr.M M Anwar
   Department of Chemical Engineering
   Teesside Polytechnic
   12 May to 7 July 1982

4. Drop Behaviour in Agitated Liquid-Liquid Dispersions
   By Dr.V Rod
   Special Lecture, Department of Chemical Engineering
   Teesside Polytechnic
   24 May 1982

5. M.Sc Module on 'Distillation'
   By Dr.D W Pritchard
   Department of Chemical Engineering
   Teesside Polytechnic
   7 June to 28 June 1982

6. The Formation of Liquid-Liquid dispersions
   Chemical and Engineering Aspects
   Society of Chemistry and Industry
   22 February 1982

7. Process Engineering Aspects of Immobilised Cell Systems
   Institute of Chemical Engineering
   At UMIST, Manchester.
   28 /29 March 1984

NOMENCLATURE

a - Jet radius, cm.

a_j - Jet radius at break-up, cm.

a_n - Nozzle radius, cm

A_1, A_2 - Constants in general instability derivation.

B_1, B_2 - constants in general instability derivation.

A_c - Actual amplitude of the disturbance, cm.

A_m - Measured amplitude of the disturbance, cm.

d_j - Jet diameter, cm.

d_n - Nozzle diameter, cm.

d_d - Drop diameter, cm.

$f_{(max)}$ - frequency for maximum instability, sec^{-1}

Fr - Froude number, $U_n^2 / d_n g$

g - Accelaration due to gravity, 980.8 cm/sec^2.

i - square root of -1

ln(ka) - Modified bessel function of first kind n^{th} order.

$\acute{ln}$(ka) - Derivative of ln(ka).

k - Wave number of the jet surface disturbance, $2\pi / \lambda$, cm^{-1}.

ka - Dimensionless wave number $2\pi a / \lambda$.

$ka_{(max)}$ - Dimensionless wave number at maximum instabilty.

$Kn(ka)$- Modified Bessel function of second kind of n^{th} order.

$Kn'(ka)$- Derivative of $Kn(ka)$.

L - Liquid jet break-up length, cm.

n - Circumferencial wave number $2\pi/\lambda$, cm^{-1}.

Oh - Ohnesorge number.

Po - Surface potential energy, ergs/cm.

Q - Volumetric flow rate through nozzle, cm^3/sec.

r - Radial distance, Cm.

Re - Reynold number.

R_f - resonance correction factor, A_c/A_m.

t - Time , Sec.

U_A - Ave. jet velocity, cm/sec.

U_g - Ave. gross velocity of continuous phase from jet surface,cm/sec

U_I - Interfacial velocity, cm/sec.

U_j - Jetting velocity, cm/sec.

U_n - Ave. nozzle velocity, cm/sec.

V_f - volume of drop , cm^3.

We - Weber number.

z - distance from nozzle tip, cm.

NOMENCLATURE Greek letters

B - Growth rate , sec^{-1}.

$B_{(max)}$ - Growth rate of disturbance at maximum instabilty, sec^{-1}.

∂ - Applied amplitude of the vibration, cm.

∂_o - Initial amplitude of the natural disturbance, cm.

θ - Angular distance, radians.

λ - Wave length of disturbance, cm.

$\lambda_{(max)}$ - Wave length of fastest growing disturbance, cm.

μ_c - viscosity of continuous phase.

μ_d - viscosity of dispersed phase.

v - Kinematic viscosity, μ/ρ cm^2/sec

π - 3.1416

ρ_c - Density of continuous phase.

ρ_d - Density of dispersed phase.

σ - Interfacial tension.

ϕ_1, ϕ_2 - Functions defined by equation 11.

ψ_1, ψ_2 - Stokes stream function satisfying various equations.

BIBLIOGRAPHY

1. Savart,F. Ann.Chem.Phys A-93 , 373 , 1917.
2. Plateau,M. Statique des Liquides, Paris 1873.
3. Rayleigh,J S W. Proc. Lond. Math Soc. 10 , 4 , 1878.
4. Rayleigh,J S W. Proc. Roy. Soc. 29 , 71 , 1879.
5. Rayleigh,J S W. Phil. Mog. 34 , 145 , 1892.
6. Rayleigh,J S W. Phil. Mag. 24 , 177 , 1892.
7. Weber,C. Z. Angew. Math. Mech. 11 , 136 , 1931.
8. Tomotika,S. Proc. Roy. Soc. A150 , 322 , 1935.
9. Christiansen,R M. Ph.D Thesis , University of Pennys , USA 1955
10. Middleman, S. Chem. Eng.Sci. 20 , 1037 , 1965.
11. Goren, S. J.Colloid. Sci. 19 , 81 , 1964.
12. Taylor, G I. A.R.C. Research Item No 19
13. Ranz,W E and Dreier,W M. Ind. Eng. Chem. Fund. 3 , 53 , 1964.
14. Levich,V G. 'Physicochemical Hydrodynemics' Prentice-Hall 1962.
15. Debye,P. and Daen,J. Phys. Fluids 2 , 416 , 1956.
16. Meister,B J. and Scheele,G F. A I Ch E J 13 , 682 , 1967.
17. Das,T K. Ph.D Thesis , Bradford 1980.
18. Smith,S W J. and Moss,H. Proc.Roy.Soc. A93 , 373 , 1917.
19. Tyler,E. and Richardson,E G. Proc. Roy. Soc. 37 , 297 , 1925.
20. De Juhuzz,K G., Zahn,O.F and Schweitzer,P.H
State Bull No 40 , 24 , 1932.
21. Tyler,E.and Watkin,F. Phill Mag 14 , 849 , 1932.
22. Ohnesorge, G. Z. Angew.Math Mech. 16 , 355 , 1936.
23. Merrington,A C. and Richardson,E G. Proc.Roy.Soc. 59 , 1 , 1947.
24. Fujinawa,K., Mruyama,T and Nakaike, Y. kagaku kikai 21 , 194 , 1957.

25. Anwar,M M. Bright, A. Das, T K. and Wilkinson, W L. Trans I ChemE 60 , 306 , 1982.

26. Craine,L E. Birch,S. and Mc Cormack Brit.J. Appl.Phys. 15,743,1964.

27. ibid ibid 16,395,1965.

28. Donnelly,R J and Glaberson,W. Proc.Roy.Soc. A290 , 547 , 1966.

29. Haelein, A. N A C A Tech.Memo No.659 , 1932.

30. Yuen,M C. J Fluid.Mech. 33 , 151 , 1968.

31. Goedde,E F. and Yuen,M C. J Fluid Mech 40 , 4945 , 1970.

32. Wang,D P. J. Fluid Mech. 34 , 299 , 1968.

33. Wissema,J G. and Davies,G.A. Can. J Chem.Eng. 47 , 530 , 1969.

34. Rutland,D F. and Jameson,G J. J.Fluid Mech. 46 , 267 , 1971.

35. Rajgopalan,R.,Tien,C. and Suramanyam Can. J. Chem. Eng. 50,410,1972.

36. Rajgopalan,R. and Tien,C Can. J. Chem. Eng. 51 , 272 , 1973.

37. Schneider,J M. and Hendricks C D. Rev. Sci. Inst 35 , 1349 , 1964.

38. Dabora E K. Rev. Sci. Inst. 38 , 502 , 1967.

39. Nelder, J A and Mead, R. Computer Journal 7 , 308 , 1664

40. Spendley, W. Hexr ,G R and Hinsworth, F R. Journal of Math 4 , 441 , 1962.

```
C
C           PROGRAM TO CORRELATE DATA FOR POLYNOMIAL
C
C
C
C      * * * * * * P R O G R A M  F L E X I P L E X * * * * * *
C
C
C
C      NX        TOTAL NUMBER OF INDEPENDENT VARAIBLES
C      NC        TOTAL NUMBER OF EQUALITY CONSTRAINTS
C      NIC       TOTAL NUMBER OF INEQUALITY CONSTRAINTS
C      SIZE      EDGE LENGHT OF THE INITIAL POLYHEDRON
C      CONVER    CONVERGENCE CRITERION FOR TERMINATION OF THE SEARCH
C      AIFA      THE REFLECTION COEFFICIENT
C      BETA      THE CONTRACTION COEFFICIENT
C      GAMA      THE EXPANSION COEFFICIENT
C      X(I)      THE ASSUMED VECTOR TO INITIATE THE SEARCH
C      FDIFER    THE TOLERANCE CRITERION FOR CONSTRAINT VIOLATION
C      ICONT     A COUNTER TO RECORD STAGE COMPUTATIONS
C      NCONT     A COUNTER TO PRINT INFORMATION EVERY (NX+1) STAGE
C      LOW       AN INDEX TO IDENTIFY INFORMATION RELATED TO THE LOWEST
C                VALUE OF OBJ. FUNCTION IN MOST RECENT POLYHEDRON
C      LHIGH     AN INDEX TO IDENTIFY INFORMATION RELATED TO LARGEST VALU
C                OF OBJ. FUNCTION IN MOST RECENT POLYHEDRON
C      LSEC      AN INDEX TO IDENTIFY INFORMATION RELATED TO THE SECOND
C      LARGEST VALUE OF OBJ. FUNCTION IN MOST RECENT POLYHEDRON
C
C                              ****************
C
      DIMENSION X(50),X1(50,50),X2(50,50),R(100),SUM(50),F(50),SR(50),
     1 ROLD(100), H(50)
      DIMENSION EXPX4(105)
      COMMON/A1/NX,NC,NIC,STEP,AIFA,BETA,GAMA,IN,INF,FDIFER,SEQL,K1,K2,
     1K3,K4,K5,K6,K7,K8,K9,X,X1,X2,R,SUM,F,SR,ROLD,SCALE,FOLD,SIZE
      COMMON/A2/LFEAS,I5,I6,I7,I8,I9,R1A,R2A,R3A
      COMMON/A3/WIL(105),HAL(105),MNDP,ZZB(105,7),ZZA(105,7)
C      PROBLM IDENTIFICATION HEADER IS READ IN AFTER THIS CARD
C     READ (5,759)
C     PARAMETERS FOR THE  PROBLM ARE READ IN AFTER THIS CARD
      READ (5,*) NX,NC,NIC,SIZE,CONVER,ISTAGE
       WRITE (6,*) NX,NC,NIC,SIZE
      READ (5,*) (X(I),I=1,NX)
      ALFA = 1.
      BETA = 0.5
      GAMA = 2.
      MZCONT=0
C     PERMANENT DATA FOR THE  PROBLM SHOULD BE READ IN AFTER THIS CARD
      CALL PROBLM(4)
C  10 CALL SECOND(TIME)
   10 CONTINUE
C     TEMPORARY DATA FOR THE  PROBLM, SUCH AS VARIABLE COEFFICIENTS OR
C     NEW PARAMETERS SHOULD BE READ IN AFTER THIS CARD
      STEP = SIZE
C     THE ASSUMED INITIAL VECTOR IS READ IN AFTER THIS CARD
C     READ (5,2) (X(I), I = 1, NX)
C     IF(EOF,10)9999,11
   11 WRITE (6,106)
C     WRITE (6,759)
      WRITE (6,756) NX,NC,NIC,SIZE,CONVER,TIME
```

```
      ETA = (STEP1 + (XNX - 1.)*STEP2)/(XNX + 1.)
      DO 4 J = 1, NX
      X(J) = X(J) - ETA
    4 CONTINUE
      CALL START
      DO 9 I = 1, N1
      DO 9 J = 1, NX
      X2(I,J) = X1(I,J)
    9 CONTINUE
      DO 5 I = 1, N1
      IN = I
      DO 6 J = 1,NX
    6 X(J) = X2(I,J)
      CALL SUMR
      SR(I) = SQRT(SEQL)
      IF(SR(I).LT.FDIFER) GO TO 8
      CALL FEASBL
      IF(FOLD.LT.1.0E-09) GO TO 80
    8 CALL  PROBIM(3)
      F(I) = R(K9)
    5 CONTINUE
 1000 STEP = 0.05*FDIFER
      ICONT = ICONT + 1
C   SELECT LARGEST VALUE OF OBJECTIVE FUNCTION FROM POLYHEDRON VERTICES
      FH = F(1)
      LHIGH = 1
      DO 16 I = 2, N1
      IF(F(I).LT.FH) GO TO 16
      FH = F(I)
      LHIGH = I
   16 CONTINUE
C    SELECT MINIMUM VALUE OF OBJECTIVE FUNCTION FROM POLYHEDRON VERTICES
   41 FL = F(1)
      LOW = 1
      DO 17 I = 2, N1
      IF(FL.LT.F(I)) GO TO 17
      FL = F(I)
      LOW = I
   17 CONTINUE
      DO 86 J = 1, NX
   86 X(J) = X2(LOW,J)
      IN = LOW
      CALL SUMR
      SR(LOW) = SQRT(SEQL)
      IF(SR(LOW).LT.FDIFER) GO TO 87
      INF = LOW
      CALL FEASBL
      IF(FOLD.LT.1.0E-09) GO TO 80
      CALL  PROBIM(3)
      F(LOW) = R(K9)
      GO TO 41
   87 CONTINUE
C     FIND CENTROID OF POINTS WITH I DIFFERENT THAN LHIGH
      DO 19 J = 1, NX
      SUM2 = 0.
      DO 20 I = 1,N1
   20 SUM2 = SUM2 + X2(I,J)
   19 X2(N2,J) = 1./XN*(SUM2-X2(LHIGH,J))
      SUM2 = 0.
      DO 36 I = 1, N1
```

```
      DO 36 I = 1, NX
      SUM2 = SUM2 + (X2(I,J) - X2(N2,J))**2
   36 CONTINUE
      FDIFER = (NC + 1)/XN1*SQRT(SUM2)
      IF(FDIFER.LT.FOLD) GO TO 98
      FDIFER = FOLD
      GO TO 198
   98 FOLD = FDIFER
  198 CONTINUE
      FTER = F(LOW)
  137 NCONT = NCONT + 1
      IF(NCONT.LT.4*N1) GO TO 37
      IF(ICONT.LT.1500) GO TO 337
      FOLD = 0.5*FOLD
  337 NCONT = 0
      PRINT 35
      PRINT 758, ICONT, FDIFER
      CALL WRITEX
      IF(ABS(PREVSQ-R(K9)).LT.0.1) GOTO 9999
      PREVSQ=R(K9)
      MZCONT=MZCONT+1
      IF(MZCONT.GT.ISTAGE) GOTO 9999
   37 IF(FDIFER.LT.CONVER) GO TO 81
C  SELECT SECOND LARGEST VALUE OF OBJECTIVE FUNCTION
      IF(LHIGH.EQ.1) GO TO 43
      FS = F(1)
      LSEC = 1
      GO TO 44
   43 FS = F(2)
      LSEC = 2
   44 DO 18 I = 1, N1
      IF(LHIGH.EQ.I) GOTO 18
      IF(F(I).LT.FS) GO TO 18
      FS = F(I)
      LSEC = I
   18 CONTINUE
C     REFLECT HIGH POINT THROUGH CENTROID
      DO 61 J = 1, NX
      X2(N3,J) = X2(N2,J) + ALFA*(X2(N2,J) - X2(LHIGH,J))
   61 X(J) = X2(N3,J)
      IN = N3
      CALL SUMR
      SR(N3) = SQRT(SEQL)
   89 IF(SR(N3).LT.FDIFER) GO TO 82
      CALL FEASBL
      IF(FOLD.LT.1.0E-09) GO TO 80
   82 CALL  PROBLM(3)
      F(N3) = R(K9)
      IF(F(N3).LT.F(LOW)) GO TO 84
      IF(F(N3).LT.F(LSEC)) GO TO 92
      GO TO 60
   92 DO 93 J = 1, NX
   93 X2(LHIGH,J) = X2(N3,J)
      SR(LHIGH) = SR(N3)
      F(LHIGH) = F(N3)
      GO TO 1000
C    EXPAND VECTOR OF SEARCH ALONG DIRECTION THROUGH CENTROID AND
C     REFLECTED VECTOR
   84 DO 23 J = 1, NX
      X2(N4,J) = X2(N3,J) + GAMA*(X2(N3,J) - X2(N2,J))
```

```
   23 X(J) = X2(N4,J)
      IN = N4
      CALL SUMR
      SR(N4) = SQRT(SEQL)
      IF(SR(N4).LT.FDIFER) GO TO 25
      INF = N4
      CALL FEASBL
      IF(FOLD.LT.1.0E-09) GO TO 80
   25 CALL  PROBLM(3)
      F(N4) = R(K9)
      IF(F(LOW).LT.F(N4)) GO TO 92
      DO 26 J = 1, NX
   26 X2(LHIGH,J) = X2(N4,J)
      F(LHIGH) = F(N4)
      SR(LHIGH) = SR(N4)
      GO TO 1000
   60 IF(F(N3).GT.F(LHIGH)) GO TO 64
      DO 65 J = 1, NX
   65 X2(LHIGH,J) = X2(N3,J)
   64 DO 66 J = 1, NX
      X2(N4,J) = BETA*X2(LHIGH,J) + (1. - BETA)*X2(N2,J)
   66 X(J) = X2(N4,J)
      IN = N4
      CALL SUMR
      SR(N4) = SQRT(SEQL)
      IF(SR(N4).LT.FDIFER) GO TO 67
      INF = N4
      CALL FEASBL
      IF(FOLD.LT.1.0E-09) GO TO 80
   67 CALL  PROBLM(3)
      F(N4) = R(K9)
      IF  (LHIGH.GT.F(N4)) GO TO 68
      DO 69 J = 1, NX
      DO 69 I = 1, N1
   69 X2(I,J) = 0.5*(X2(I,J) + X2(LOW,J))
      DO 70 I = 1,N1
      DO 71 J = 1, NX
   71 X(J) = X2(I,J)
      IN = I
      CALL SUMR
      SR(I) = SQRT(SEQL)
      IF(SR(I).LT.FDIFER) GO TO 72
      INF = I
      CALL FEASBL
      IF(FOLD.LT.1.0E-09) GO TO 80
   72 CALL  PROBLM(3)
   70 F(I) = R(K9)
      GO TO 1000
   68 DO 73 J = 1, NX
   73 X2(LHIGH,J) = X2(N4,J)
      SR(LHIGH) = SR(N4)
      F(LHIGH) = F(N4)
      GO TO 1000
   81 PRINT 760,ICONT, FDIFER
      CALL WRITEX
C     CALL SECOND(TIME)
      PRINT 755, TIME
      PRINT 761
      GO TO 10
   80 PRINT 760, ICONT, FDIFER
```

```
      CALL WRITEX
      PRINT 762
      GO TO 10
    1 FORMAT(3I5,F10.5,E10.5)
    2 FORMAT(8F10.5)
   35 FORMAT(/,40X,' * * * * * * * * * * * * * * * * * * * * * *
  106 FORMAT(1H1,//)
  115 FORMAT(//,  ' THE STARTING VECTOR SELECTED BY USER IS ')
  116 FORMAT(8E16.6)
  755 FORMAT(//, ' THE COMPUTATION TIME IN SECONDS =',E12.5 )
  756 FORMAT(//,10X,' NUMBER OF INDEPENDENT VARIABLES           ',I5,/,'
     1,' NUMBER OF EQUALITY CONSTRAINTS            ',I5,/,10X,40H NUMBE
     2F INEQUALITY CONSTRAINTS            ,I5/,10X,40H SIZE OF INITIAL P
     3HEDRUN                    ,E12.5/,10X,40H THE DESIRED CONVERGENCE IS
     4            ,E12.5/,10X,40H THE COMPUTATION TIME IN SECONDS
     5,E12.5)
  757 FORMAT(//,71H THE INITIAL X VECTOR DOES NOT SATISFY THE INITIAL
     1LERANCE CRITERION )
  758 FORMAT( /,10X,27H STAGE CALCULATION NUMBER = I5, 20X, 27H THE TO
     2RANCE CRITERION = E14.6)
C 759 FORMAT(80H
C    1                                    )
  760 FORMAT(//, 39H TOTAL NUMBER OF STAGES CALCULATIONS = I5, 10X, 25
     1THE CONVERGENCE LIMIT = E14.6)
  761 FORMAT(//,50X,25H THESE ARE FINAL ANSWERS )
  762 FORMAT(//,50X,29H THESE ARE NOT FINAL ANSWERS )
  763 FORMAT(//,10X,40H THE INITIAL TOLERANCE CRITERION IS       E12.5,/
     110X,40H THE SUM OF VIOLATED CONSTRAINTS IS       E12.5)
  764 FORMAT(//,70H THE VECTOR FOUND BY PROGRAM WHICH SATISFIES THE IN
     1IAL TOLERANCE IS )
  765 FORMAT(/, 31H SUM OF VIOLATED CONSTRAINTS = E17.7)
 9999 CONTINUE
C
C
C
C
C
      DO 9998 I=1,MNDP
      WRITE (6,*) WII(I),HAL(I)
 9998 CONTINUE
      V1=3.E-5
C     CALL P101(ZZB,X,MNDP,EXPX4,V1)
C     CALL PLOT(ZZB,EXPX4,MNDP)
C
C
C
      STOP
      END
      SUBROUTINE FEASBI
C
      DIMENSION X(50),X1(50,50),X2(50,50),R(100),SUM(50),F(50),SR(50),
     1ROLD(100), R1(100), R2(100),R3(100), FIG(10), H(50)
  100 FORMAT(8E16.6)
      COMMON/A1/NX,NC,NIC,STEP,DUM1,DUM2,DUM3,IN,INF,FDIFER,SPCL,K1,K2,
     1K3,K4,K5,K6,K7,K8,K9,X,X1,X2,R,SUM,F,SR,ROLD,SCALE,FOLD,SIZE
      COMMON/A2/LFEAS,I5,I6,I7,I8,I9,R1A,R2A,R3A
      COMMON/A3/WII(105),HAL(105),MNDP,ZZB(105,7),ZZA(105,7)
      RETURN
      END
      SUBROUTINE START
```

```
      DIMENSION A(50,50)
      DIMENSION X(50),X1(50,50),X2(50,50),R(100),SUM(50),F(50),SR(50)
     1 ROID(100)
      COMMON/A1/NX,NC,NIC,STEP,ALFA,BETA,GAMA,IN,INF,FDIFER,SEQL,K1,K
     1K3,K4,K5,K6,K7,K8,K9,X,X1,X2,R,SUM,F,SR,ROID,SCALE,FOLD,SIZE
      COMMON/A2/LFEAS,L5,L6,L7,L8,L9,R1A,R2A,R3A
      COMMON/A3/WIL(105),HAL(105),MNDP,ZZB(105,7),ZZA(105,7)
      VN = NX
      STEP1 = STEP/(VN*SQRT(2. ))*(SQRT(VN + 1.) + VN - 1.)
      STEP2= STEP/(VN*SQRT(2.))*(SQRT(VN + 1.) - 1.)
      DO 1 J = 1, NX
    1 A(1,J) = 0.
      DO 2 I = 2, K1
      DO 4 J = 1, NX
    4 A(I,J) = STEP2
      L = I - 1
      A(I,L) = STEP1
    2 CONTINUE
      DO 3 I = 1, K1
      DO 3 J = 1, NX
    3 X1(I,J) = X(J) + A(I,J)
      RETURN
      END
      SUBROUTINE WRITEX
      DIMENSION X(50),X1(50,50),X2(50,50),R(100),SUM(50),F(50),SR(50),
     1ROLD(100)
      COMMON/A1/NX,NC,NIC,STEP,ALFA,BETA,GAMA,IN,INF,FDIFER,SEQL,K1,K2
     1K3,K4,K5,K6,K7,K8,K9,X,X1,X2, R,SUM,F,SR,ROLD,SCALE,FOLD,SIZE
      COMMON/A2/LFEAS,L5,L6,L7,L8,L9,R1A,R2A,R3A
      COMMON/A3/WIL(105),HAL(105),MNDP,ZZB(105,7),ZZA(105,7)
      CALL  PROBLM(3)
      PRINT 1, R(K9)
    1 FORMAT(/, 28H OBJECTIVE FUNCTION VALUE = E17.7)
      PRINT 2, (X(J), J = 1, NX)
    2  FORMAT(/,  ' THE INDEPENDENT VECTORS ARE' /(6E17.7))
      IF( NC.EQ.0) GO TO 6
      CALL  PROBLM(1)
      PRINT 3, (R(J), J = 1, NC)
    3 FORMAT(/, 36H THE EQUALITY CONSTRAINT VALUES ARE /(6E17.7))
    6 IF (NIC.EQ.0) GO TO 5
CZM     CALL  PROBLM(2)
CZM     PRINT  4 , (R(J), J = K7,K6)
CZM   4 FORMAT(/, 34H THE INEQUALITY CONSTRAINT VALUES /(6E17.7))
    5 RETURN
      END
      SUBROUTINE SUMR
C
C*****THIS SUBROUTINE COMPUTES THE SUM OF THE SQUARE VALUES OF THE
C     VIOLATED CONSTRAINTS IN ORDER TO BE COMPARED WITH THE TOLERANCE
C     CRITERION
C
      DIMENSION X(50),X1(50,50),X2(50,50),R(100),SUM(50),F(50),SR(50),
     1ROLD(100)
      COMMON/A1/NX,NC,NIC,STEP,ALFA,BETA,GAMA,IN,INF,FDIFER,SEQL,K1,K2
     1K3,K4,K5,K6,K7,K8,K9,X,X1,X2,R,SUM,F,SR,ROLD,SCALE,FOLD,SIZE
      COMMON/A2/LFEAS,L5,L6,L7,L8,L9,R1A,R2A,R3A
      COMMON/A3/WIL(105),HAL(105),MNDP,ZZB(105,7),ZZA(105,7)
      SUM(IN) = 0.
      CALL  PROBLM(2)
      SEQL = 0.
```

```
      IF(NIC.EQ.0) GO TO 4
      DO 1 J = K7, K8
      IF(R(J).GE.0.) GO TO 1
      SEQL = SEQL + R(J)*R(J)
    1 CONTINUE
    4 IF(NC.EQ.0) GO TO 3
      CALL  PROBIM(1)
      DO 2 J = 1, NC
    2 SEQL = SEQL + R(J)*R(J)
    3 SUM(IN) = SEQL
    5 RETURN
      END
C
C
C
      SUBROUTINE PROBIM(INQ)
      DIMENSION X(50),X1(50,50),X2(50,50),R(100),SUM(50),F(50),SR(50)
     1 ROLD(100)
      DIMENSION FVECC(105)
      COMMON/A1/NX,NC,NIC,STEP,ALFA,BETA,GAMA,IN,INF,FDIFER,SEQL,K1,K2
     1K3,K4,K5,K6,K7,K8,K9,X,X1,X2,R,SUM,F,SR,ROLD,SCALE,FOLD,SIZE
      COMMON/A2/LFEAS,L5,L6,L7,L8,L9,R1A,R2A,R3A
      COMMON/A3/WIL(105),HAL(105),MNDP,ZZB(105,7),ZZA(105,7)
C
      GOTO (1,2,3,4),INQ
C
    4 READ (5,*) MNDP,NCOL
      READ (5,*) ((ZZA(I,J),J=1,NCOL),I=1,MNDP)
      DO 50 I=1,MNDP
      DO 50 J=1,NCOL
   50 ZZB(I,J)=ZZA(I,J)
      GOTO 5
C
C
    1 GOTO 5
C
C
  2         GOTO 5
C   2 DO 40  I=1,NX
C     J=NX+I
CC    R(J)=10.-X(I)
C  40 R(I)=X(I)-1.0E-2
C     I=NX+NX+1
C     GOTO 5
C
C
    3 CONTINUE
      DO 60 I=1,MNDP
      CALL FUNI(I,FF)
      FVECC(I)=FF
   60 CONTINUE
      FC=0.
      DO 70 I=1,MNDP
   70 FC=FC+FVECC(I)*FVECC(I)
C     WRITE (6,*) FC
      CONTINUE
      J=NIC+1
      R(J)=FC
    5 RETURN
      END
```

```
C
      SUBROUTINE FUNI(I,FF)
      DIMENSION X(50),X1(50,50),X2(50,50),R(100),SUM(50),F(50),SR(50)
     1 ROLD(100)
      COMMON/A1/NX,NC,NIC,STEP,ALFA,BETA,GAMA,IN,INF,FDIFER,SEQL,K1,K2
     1K3,K4,K5,K6,K7,K8,K9,X,X1,X2,R,SUM,F,SR,ROLD,SCALE,FOLD,SIZE
      COMMON/A2/LFEAS,I5,I6,I7,I8,I9,R1A,R2A,R3A
      COMMON/A3/WIL(105),HAL(105),MNDP,ZZR(105,7),ZZA(105,7)
C
C     *************** DEFINE PROBLEM HERE *********
       POI=X(1)*ZZA(I,6)+X(2)*ZZA(I,6)**2+X(3)
      WIL(I)=EXP(ZZA(I,1)*(ZZA(I,3)/ZZA(I,2)))
      HAL(I)=ZZA(I,4)/(ZZA(I,5)*POI)
       WIL(I)=1./WIL(I)
       HAL(I)=1./HAL(I)
      FF=WIL(I)-HAL(I)
      RETURN
      END
```